Position Paper 26

Marine geohazards

Safeguarding society and the Blue Economy from a hidden threat

European MARINE BOARD
Advancing Seas & Ocean Science

www.marineboard.eu

European Marine Board IVZW

The European Marine Board provides a pan-European platform for its member organizations to develop common priorities, to advance marine research, and to bridge the gap between science and policy in order to meet future marine science challenges and opportunities.

The European Marine Board is an independent and self-sustaining science policy interface organization that currently represents 35 Member Organizations from 18 European countries. It was established in 1995 to facilitate enhanced cooperation between European marine science organizations towards the development of a common vision on the strategic research priorities for marine science in Europe. The EMB promotes and supports knowledge transfer for improved leadership in European marine research. Its membership includes major national marine or oceanographic institutes, research funding agencies and national consortia of universities with a strong marine research focus. Adopting a strategic role, the European Marine Board serves its member organizations by providing a forum within which marine research policy advice is developed and conveyed to national agencies and to the European Commission, with the objective of promoting the need for, and quality of, European marine research.

www.marineboard.eu

European Marine Board Member Organizations

Marine geohazards

Safeguarding society and the Blue Economy from a hidden threat

European Marine Board IVZW – Position Paper 26

This Position Paper is a result of the work of the European Marine Board Expert Working Group on Marine Geohazards. See Annex 1 for the list and affiliations of the Working Group members.

Working Group Chairs

Heidrun Kopp, Francesco Latino Chiocci

Contributing Authors

Christian Berndt, Namık Çağatay, Teresa Ferreira, Juana Fortes, Eulàlia Gràcia, Alba González Vega, Achim Kopf, Mathilde B. Sørensen, Nabil Sultan, Isobel Yeo

Series Editor

Sheila JJ Heymans

Publication Editors

Ángel Muñiz Piniella, Paula Kellett, Rebecca van den Brand, Britt Alexander, Ana Rodríguez Perez, Jana Van Elslander, Sheila J. J. Heymans

External Reviewers

David Coetzee, Sarah-Jayne McCurrach, Dimitris Sakellariou

Internal Review Process

The content of this Position Paper has been subject to internal review, editorial support and approval by the European Marine Board Member Organizations.

Suggested reference

Kopp, H., Chiocci, F. L., Berndt, C., Çağatay, M. N., Ferreira, T., Fortes, C. J. E. M., Gràcia, E., González Vega, A., Kopf, A. J., Sørensen, M. B., Sultan, N., Yeo, I. A. (2021) Marine geohazards: Safeguarding society and the Blue Economy from a hidden threat. Muñiz Piniella, A., Kellett, P., van den Brand, R., Alexander, B., Rodríguez Perez, A., Van Elslander, J., Heymans, J. J., [Eds.] Position Paper 26 of the European Marine Board, Ostend, Belgium. 100 pages.
ISSN: 2593-5232. ISBN: 9789464206111 DOI: 10.5281/zenodo.5591938

www.marineboard.eu
info@marineboard.eu

Design

Zoeck

We acknowledge the work of Amber Moreels, Amber Devreker, Ellis Deleeck and Margaux Vandevelde, from the Artevelde University of Applied Sciences, in designing and creating the infographics used in this document. Additional scientific input was kindly provided by Gemma Ercilla and David Casas (CSIC-ICM), Daniele Casalbore (University of Rome "Sapienza") and Paolo Tommasi (CNR-IGAG).

November 2021

Foreword

In September 2021, the eruption of the Cumbre Vieja volcano on La Palma in the Canary Islands made global headlines. Images of lava flowing down the mountain and people losing everything they own encapsulated our feeling of powerlessness when facing such a geological catastrophe. This caused me to recall other paroxysmal explosive eruptions in history which led to huge loss of life and major geopolitical changes (e.g. Santorini, Vesuvius, Tambora, Krakatau) and the impact of tsunamis such as those in Indonesia and Japan, in 2004 and 2011 respectively. We should also not forget the largest underwater eruption ever recorded and evidenced, which took place in 2019 giving birth to a massive new volcano near Mayotte and leading to a 15 cm subsidence of the island. In Europe, geological hazards (such as volcanoes and tsunamis) are a fact of life and will occur in the future without warning. At present, there is limited awareness of the geological hazards present in European seas, such as groundwater seepage or submarine landslides. Threats to society from marine geohazards include harm to people and property, the devastation and disappearance of valuable land near the shoreline, and the destruction of seafloor installations (e.g. communication cables, pipelines).

Europe is looking at the opportunities provided by our coasts to achieve the ambitious objectives of the European Green Deal. However, with an increasing number of human activities conducted in the marine environment and the increasing human population on European coasts, society will be more exposed and vulnerable to marine geohazards. Our only option is therefore to increase our knowledge of marine geohazards and hence to inform measures to reduce our exposure and vulnerability to these events. We want a safe Ocean where lives and livelihoods are protected from Ocean-related hazards. This is one of the societal outcomes that the United Nations Decade of Ocean Science for Sustainable Development (2021 – 2030) strives towards.

The topic of marine geohazards has been discussed at the European Marine Board (EMB) since 2015, including a dedicated Open Session at the EMB Autumn Plenary Meeting in Trieste, Italy, in 2018. Marine geohazards was selected as a new activity at the EMB Spring Plenary Meeting in Paris, France, in 2019. The aim is to direct political attention to the topic at European and international level by highlighting the impacts on society and the Blue Economy. In February 2020 the EMB Working Group on 'Marine Geohazards' kicked-off with a meeting in Rome, Italy. Working online during the COVID-19 pandemic, this Position Paper is the primary output of this group. It aims to inform changes in management practices and policies that protect the population and economic activities at sea, while also highlighting the need for increased knowledge on processes, triggers and precursors of marine geohazards.

On behalf of the European Marine Board, I would like to thank the members of the EMB 'Marine Geohazards' Working Group, the external reviewers, and additional contributors (Annex I and II) for delivering such a comprehensive Position Paper during such a difficult time. My thanks also go to the EMB Secretariat, for their work in coordinating the Working Group and the synthesis and publication of this document, namely Ángel Muñiz Piniella, Paula Kellett, Rebecca van den Brand, Britt Alexander, Ana Rodríguez Perez, Jana Van Elslander and Sheila Heymans. Finally, I would like to thank Amber Moreels, Amber Devreker, Ellis Deleeck and Margaux Vandevelde (students from the Artevelde University of Applied Sciences in Belgium) for designing and creating the infographics used in this document to illustrate these complex issues in a simple way.

Gilles Lericolais
Chair, European Marine Board IVZW
November 2021

Table of Contents

Executive Summary

Marine geohazards pose a significant threat to the European coastal population and to the development of the Blue Economy. This Position Paper discusses the type (Chapter 2), distribution (Chapter 3) and impact (Chapter 4) of marine geohazards on the European coastal regions and the Blue Economy, as well as what and how novel scientific approaches may broaden our understanding of their trigger mechanisms and drive a risk-mitigating European policy (Chapter 5). This document focuses on short-onset geological hazards and does not deal with long-term processes such as coastal erosion, land subsidence, intrusion of salt water in coastal aquifers; or with hazards associated by atmospheric disturbances such as storm surges and meteo-tsunamis. This document is primarily aimed at local, regional, national and European institutions in charge of managing risk assessments & mitigation, land and sea management, funding research, monitoring and infrastructures, and public awareness of hazards. In addition, this document may also be relevant to the scientific community interested in, or exploring this subject, and to stakeholders outside Europe, in light of the United Nations Decade of Ocean Science for Sustainable Development (2021-2030).

Large but (luckily) infrequent events attract most public attention and media coverage (such as tsunamis and volcanic eruptions), and prompt changes in policies for reducing future risks. However, for the management of the marine and coastal areas, smaller but more frequent events that produce localized, though severe disasters, should also be considered, especially in regions with high density populations, living or working near the coast and regions, hosting substantial infrastructure or serving as tourist destinations. The only hazards that can be defined with confidence in the European seas are those related to volcanic eruptions, earthquakes and earthquake-generated tsunamis, as those are the only hazards that have adequate instrumental data. More detailed studies are required to undertake a comparable census and understanding of landslides, fluid escape features and migrating bedform fields. In addition, engineering projects may generate human-induced geohazards such as landslides and related tsunamis. Often cascading or cumulative events may worsen the impact of a single event, demonstrating the need to move towards a multi-hazard approach.

The increasing population density on European shores implies higher risks resulting from marine geohazards. Today, our society is more dependent on critical infrastructure such as ports, roads and telecommunication cables. While the industry understands the widespread presence and relevance of marine geohazards, the general public, policy makers and public authorities remain largely unaware of these hazards. Increasing our knowledge of geohazard triggers and processes is needed to raise the general awareness and to implement specific legislation, framing marine geohazards into pro-active action that would mitigate the risk.

Considering that geological hazards are unavoidable and will certainly continue to occur in the future, mitigation measures (for risk reduction) should therefore be focused on decreasing the risk (exposure and vulnerability) and increasing resilience. These measures should be based on the scientific knowledge of events that occurred in the past, their triggering mechanisms and the propagation of their consequences. To achieve this, we recommend to:

- Include marine geohazards as natural hazards in all policies relating to risk mitigation and land management, at European, regional, national and local levels.
- Consider marine geohazards in local, national and EU marine and maritime legislation such as the EU Marine Spatial Planning Directive, and legislation pertaining to Integrated Coastal Zone Management, and that pertain to the safe development of the Sustainable Blue Economy.
- Require that public authorities use all seafloor infrastructure installations for environmental and geohazards monitoring.
- Develop probabilistic scenarios of marine geohazard risks for all major coastal settlements and industrial infrastructures.
- Establish a stakeholder forum to identify knowledge gaps and technological needs. This could be achieved through the development of specific EU research programs on marine geohazards.
- Set up a field laboratory for marine geohazards at a focus site in Europe to concentrate research, facilities and *in situ* modelling.
- Promote a common standard for marine geohazard interpretation and mapping to ensure the safe development of the Blue Economy.
- Combine long-term *in situ* monitoring with geohazard studies in the surrounding region to identify long-range signals.
- Support technological advancement in order to improve the detection capability and availability of sensors.
- Create holistic databases of raw data and homogeneous interpretations and make them available to the scientific community to apply advanced techniques in support of marine geohazard studies.

1

Introduction
A hidden threat to Europe?

Credit: Gürsu Yaman

Nearly half of Europe's population lives in coastal regions (Figure 1.1.) and this number is increasing (Hugo, 2011; Margaras, 2019). The high population density along our coasts and the expected growth of complex critical infrastructure and Ocean services in coastal regions lead to mounting levels of exposure and vulnerability to marine geohazards. Underlying drivers including rapid urbanization, complex supply chains, and increase in communication and navigation infrastructure, and the effects of climate change on geological conditions further raise the level of risk to communities and the Blue Economy.

The Blue Economy accounted for 1.5% of the European economy and 2.2% of employment in 2018 (European Commission, 2020; Scholaert *et al.*, 2020). These figures are expected to increase in the near future due to the expansion of coastal settlements and infrastructure, growth in shipping industry for transportation of goods and people, the increased production of renewable energy from wind, tides and waves, and the ongoing exploitation of marine resources (raw minerals, aggregates, fish processing and aquaculture) (OECD, 2016). To guarantee safe and sustainable growth of the Blue Economy, the assessment of marine geological hazards (or geohazards) is needed; yet to date this is not included in the marine-related directives and initiatives such as the Maritime Spatial Planning (MSP) Directive, Integrated Coastal Zone Management (ICZM), or the Marine Strategy Framework Directive (MSFD).

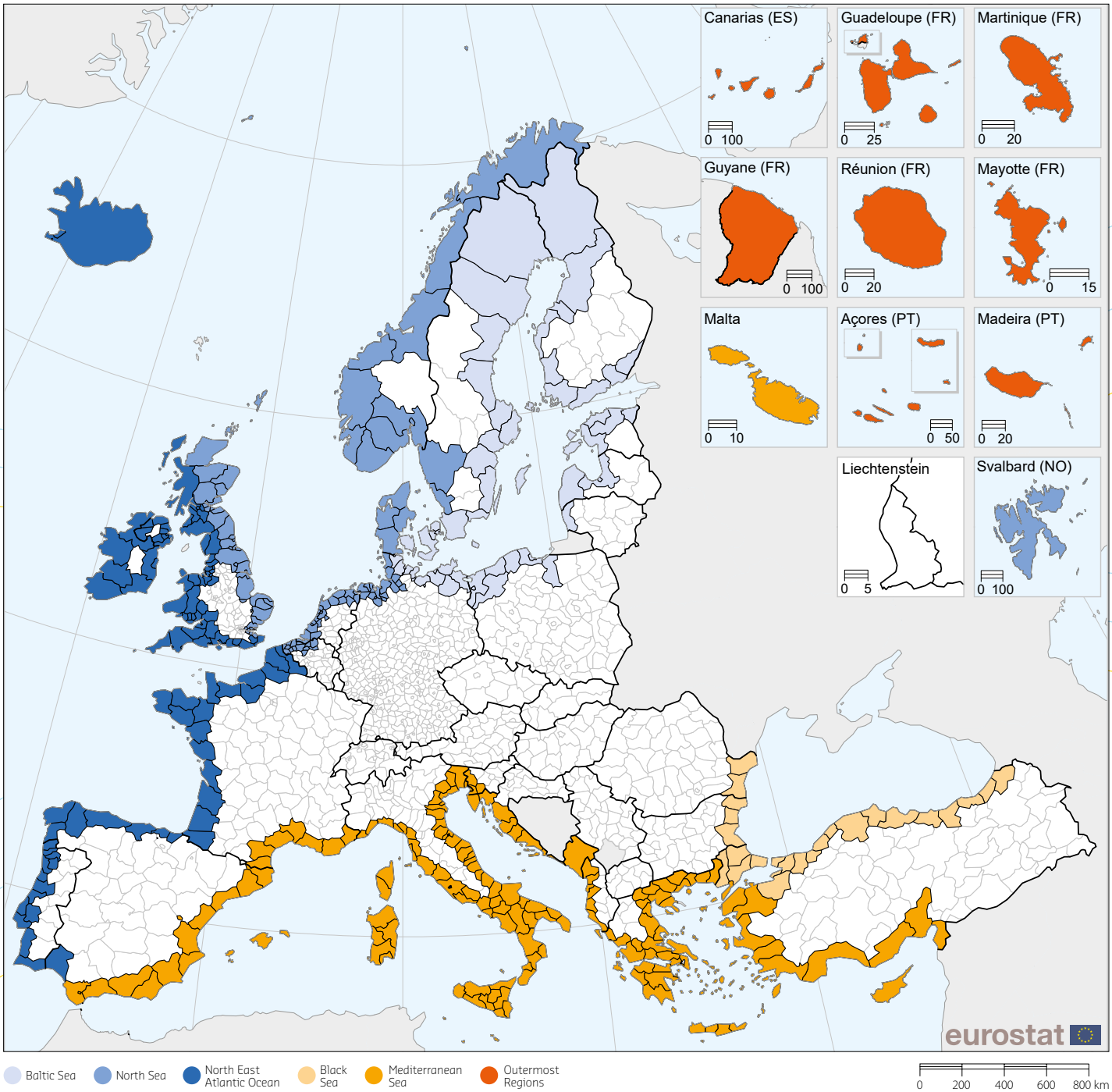

Figure 1.1. Coastal regions in Europe based on the nomenclature of territorial units for statistics (NUTS) 2021. We acknowledge that the French outermost region of Saint-Martin is not shown on the image. Administrative boundaries: © EuroGeo graphics © UN-FAO © Turkstat. Cartography: Eurostat – GISCO, 02/2021

Marine geohazards related to seafloor processes include earthquakes (the most destructive earthquakes that have affected humanity have occurred at sea), landslides, volcanic eruptions and the tsunamis associated with these. Marine geohazards can also include rapid changes on the seafloor such as migrating bedforms, seabed liquefaction and gas migration that can lead to local overpressure in sediments and potential underwater landslides (see Chapter 2 for more information). To date, most of the geohazard features that occur on the seafloor are unknown, ill-characterized, and difficult to monitor (with present-day technology).

Hazards are intimately linked to **risk** (Figure 1.2.). A risk is the probability of an event causing potential loss of life, injury, or destruction or damage of assets, which could occur to a system, society or a community within a specific period of time. A risk is therefore determined as the product of three factors: the **hazard**, i.e. the probability that a given event will occur in a given time; the **exposure**, i.e. the human lives and the amount and value of the items exposed to the hazardous event; and the **vulnerability**, i.e. the amount of damage that the event will cause to the exposed items. The tsunami risk is, for instance, the product of the likelihood that a tsunami occurs (H), the number of people and amount of property and systems that are present on the coast affected by the tsunami and subject to potential losses (E) and the damage they will suffer by that event (V):

$$R = (H \times E \times V)$$

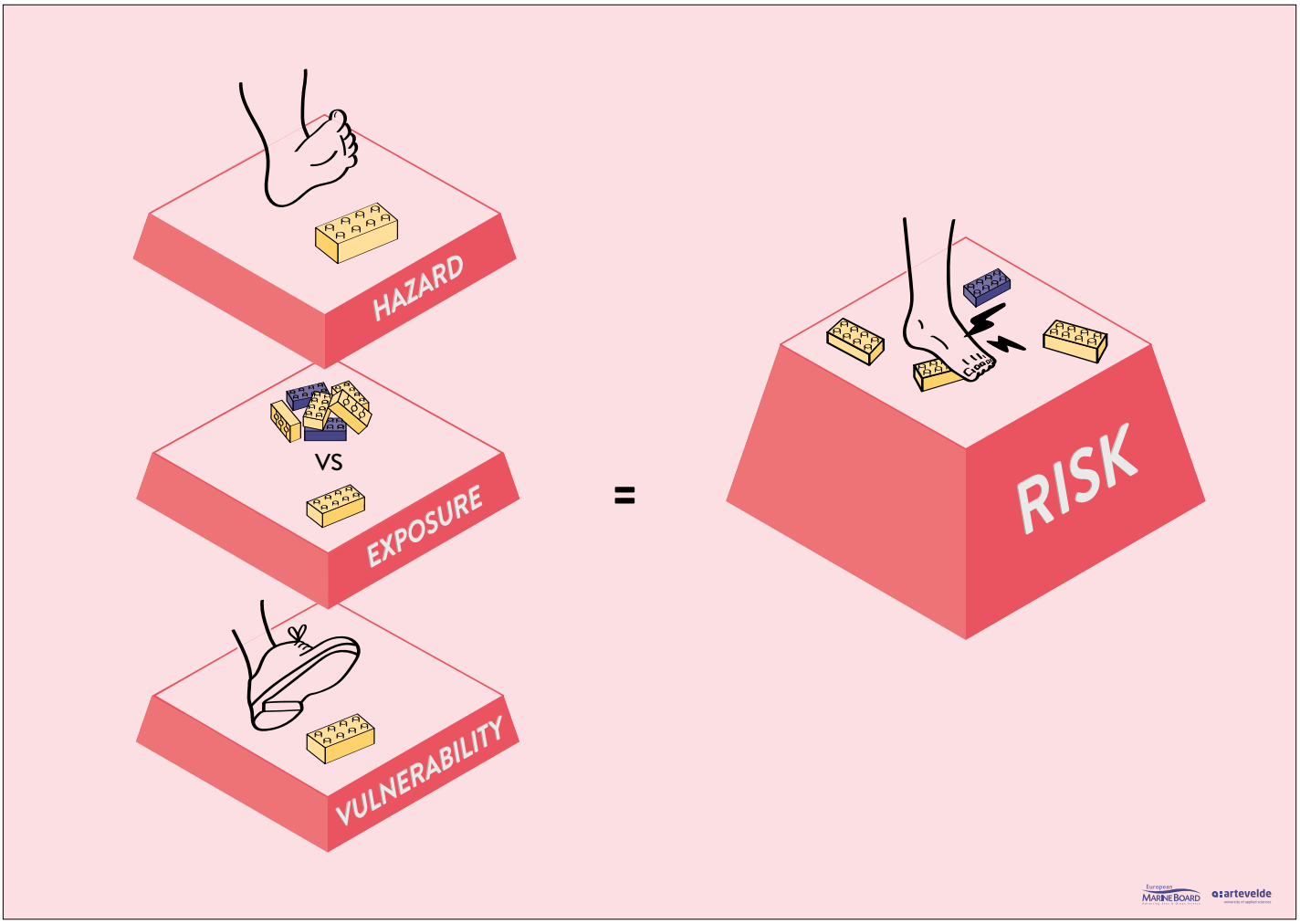

Figure 1.2. Infographic illustrating the difference between hazard and risk. The risk of stepping on a toy brick (the disaster) is dependent on the probability of stepping on a toy brick (hazard), if you walk where there are a lot of bricks on the floor or just a few (exposure) and whether you are wearing shoes or are barefoot (vulnerability).

In this formula, if one factor is zero, the risk is also zero. For instance, there is no risk if a tsunami occurs on an unpopulated desert coast (E=0), or in an area where there will be no damage because of tsunami-resistant construction (e.g. well above sea level) and because early-warning and safety procedures are fully effective (V=0).

Marine geohazards will result either in dangerous or catastrophic events with the associated risk to life, infrastructure and the environment involving several nations (in this report referred to as “intensive risk”) or in smaller events that are widespread and pervasive in certain areas and threaten regional marine and coastal communities and infrastructure (referred to as 'extensive risk') (see Box 1). The United Nations Office for Disaster Risk Reduction (UNDRR) define **intensive risk** as a disaster risk associated with low-probability, high-impact events, whereas **extensive risk** is a disaster risk associated with high-probability, lower-impact events.

BOX 1: A SMALL LANDSLIDE CAN BE AS DANGEROUS AS A LARGE ONE

A hazard, an important factor driving risk, can be seen as the product of the frequency (recurrence in time) of a given phenomenon and the magnitude (severity and extension of effects).

$$\textit{Hazard} = \textit{Frequency} \times \textit{Magnitude}$$

Therefore, frequent, local-scale events can lead to the same risk level as an extremely large but rare event. The figure below exemplifies that the risk of an Ocean-scale tsunami such as the one caused by the gigantic Storegga slide off Norway (Kvalstad *et al.,* 2005) can be similar to large but local tsunamis caused by submarine landslides or rockfalls in the fjords that propagate only in the surroundings. In the figure, inspired by Casalbore *et al.,* (2011) several landslide-generated tsunami events covered in this document are compared in terms of magnitude and frequency, and the hazard level depends on the magnitude of the event and the recurrence time (or probability of occurrence).

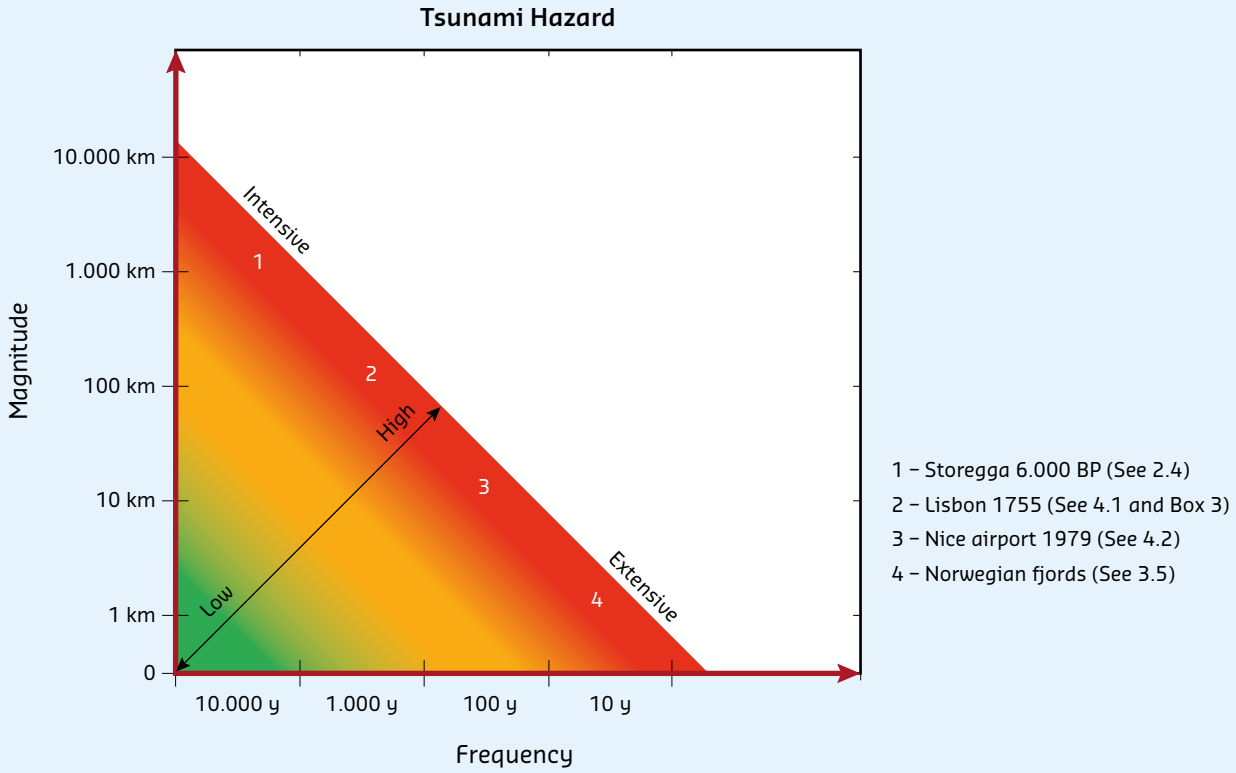

High-probability, low-impact, local, extensive risk events are much more frequent than low-probability, high impact, intensive risk events. However, they attract much less attention and media coverage, despite the fact that in the last 50 years in Europe, local events alone have caused collapses in harbours and airports (Gioia Tauro 1977, Nice 1979), wide-spread cable breaks (Algeria 2003), local but often deadly tsunamis (Nice 1979, Finneidfjord 1996, Stromboli 2002), and volcanic crises (Eyjafjallajökull, Iceland 2010, El Hierro 2011-2012, La Palma 2021). These events cause significant costs for response and recovery. Therefore, risk reducing incentives and initiatives should focus both on high probability, low consequence events, balanced with low probability, high consequence events.

The relevance of this extensive risk, i.e. risk due to events that are frequent even if not high-impact, should not be underestimated. For instance, small submarine landslides or fluids escaping from the sediment can break underwater cables or damage pipelines, oil rigs or harbours, representing a significant threat to the Blue Economy, considering the large amount of infrastructure that is already installed on the seafloor. From an economic and environmental point of view, such events should be considered when planning coastal settlements, seafloor activities and infrastructure.

Risk mitigation is the reduction of risk exposure and/or the adverse effects of risk. Mitigation is therefore the denominator of the risk equation:

$$R = \frac{H \times E \times V}{M}$$

For most risk related to geological processes, prevention or lowering of the hazard is unlikely as it is impossible to avoid natural phenomena. Risk mitigation should therefore focus on the reduction of exposure and vulnerability to hazard phenomena through the assessment of: 1) the likelihood of a geohazard event occurring, 2) the definition of its location, size and character, and 3) the primary and secondary effects it will cause (e.g. earthquake –> tsunami). Such a geohazard assessment would lead to informed decisions regarding the location of settlements and key infrastructure, it would also facilitate the use of early-warning systems to alert authorities and the population of an incoming event, and it would promote procedures and engineering prevention measures that would reduce damage. In addition, the concept of risk tolerance should be considered when investigating possible trade-offs in decision-making related to risk assessment. Risk tolerance is the willingness of an institution(s) or communities to take a risk(s). Well defined risk tolerance criteria brings rigour across the (geo)hazard risk assessment and management when deciding, officially, what is tolerable, intolerable or can be accepted. It is often seen as a requirement to ensure robust implementation of appropriate risk reduction/resilience measures.

Consequently, scientific knowledge of magnitude, spatial and temporal scales of marine geohazards is a prerequisite for the assessment and mitigation of the risk to communities, critical infrastructure and the environment (Ercilla *et al.,* 2021). Recent analysis of disaster loss databases from the Centre for Research on the Epidemiology of Disasters (CRED) and the United Nations data between 1998 and 2017 showed that the majority of human fatalities resulting from natural hazards were due to high-impact, sudden-onset, geological events, including earthquakes, tsunamis and mass movements (CRED & UNISDR, 2018). Geological events accounted for only 9% of total disasters in the past 20 years, but for 59% of all disaster-related deaths, making them by far the deadliest type of disaster (Mizutori & Guha-Sapi, 2020).

During the last two decades, marine geohazards have drawn more attention, as there is a substantial increase in the awareness of dangers associated with large-scale disasters. Single extreme events like the 2004 Indian Ocean earthquake and tsunami, or the 2011 Tohoku-Oki earthquake and tsunami in Japan caused a large number of casualties and heavy economic losses. The global reverberations of the related disaster impact document the tight socio-economic interconnections of societies across political boundaries and continents. Cascading or cumulative events, such as the 2011 Tohoku-Oki earthquake and tsunami affecting the Fukushima-Daiichi power plant in Japan may strongly amplify damage, resulting in significant direct and indirect economic losses. Similar large catastrophic high-impact events have occurred in Europe in the past, such as the 1755 Lisbon earthquake and tsunami and the 1908 Messina earthquake and tsunami event. However most Europeans do not perceive that there is a threat of comparable destructive events occurring again, and hence there is little awareness that a future hazard will impact our European coasts.

Insight into the mechanisms and characteristics that underlie hazardous events is critical to fully understand their hazard potential and related disaster risk (Ercilla *et al.,* 2021) and to design a safe operating space for human activities and infrastructure. It requires understanding the triggers, how these geological hazards progress in time and space, and what their impacts are on the shoreline (including possible cascading effects) (Urlaub *et al.,* 2018). These events represent fundamental geological processes, which cannot be controlled or re-directed and are thus independent of anthropogenic factors. Consequently, accurate disaster risk assessment and mapping for individual processes and regions is critically important for risk governance and mitigation at the national and local levels. Regulatory agencies need this information for contingency planning and geohazard management, as well as capacity assessment, business continuity and development of offshore infrastructure and resources. Disaster risk information is critical for risk reduction strategies and policies to minimize the potential damage that could be created in the case of a natural or a human-induced geohazard.

This Position Paper discusses the type (Chapter 2), distribution (Chapter 3) and impact (Chapter 4) of marine geohazards on the European Blue Economy and coastal regions, as well as what and how novel scientific approaches may broaden our understanding of their trigger mechanisms and drive a risk-mitigating European policy (Chapter 5). In addition to natural hazards, the impact of human activities on marine geohazards and of changing Ocean conditions due to climate change are evaluated.

2021 2030 United Nations Decade of Ocean Science for Sustainable Development

This Position Paper and its recommendations support the UN Decade of Ocean Science for Sustainable Development (Ocean Decade) in a number of ways.

The Position Paper highlights knowledge to support Societal Outcome 4 *(A predicted Ocean where society understands and can respond to changing ocean conditions*) by providing recommendations on how to better model the potential impact of marine geohazards that could be quantified using hazard maps or risk models to set up early warning and rapid response systems. It also provides input to Outcome 5 *(A safe Ocean where life and livelihoods are protected from ocean-related hazards)* by providing recommendations that aim to increase the science needed to understand processes, triggers and precursors of marine geohazards and avoid disasters and losses at the Blue Economy sectors. The Position Paper also provides recommendations to Societal Outcome 7 *(An inspiring and engaging Ocean where society understands and values the Ocean in relation to human wellbeing and sustainable development)* on how to increase awareness of marine geohazards among public authorities, in order to prevent heavy impacts on coastal societies

Regarding the Ocean Decade Challenges, this document addresses Challenge 4 *(Generate knowledge, support innovation, and develop solutions for equitable and sustainable development of the ocean economy under changing environmental, social and climate conditions)* by discussing how to enhance scientific research on marine geohazards at all levels and create partnerships with industry to increase our knowledge of the Ocean. This document also addresses Challenge 6 *(Enhance multi-hazard early warning services for all geophysical, ecological, biological, weather, climate and anthropogenic related ocean and coastal hazards, and mainstream community preparedness and resilience)* by presenting how to increase awareness of marine geohazards among public authorities, and to frame marine geohazards in administrative management rules. Finally, to address Challenge 7 *(Ensure a sustainable Ocean observing system across all Ocean basins that delivers accessible, timely, and actionable data and information to all users*), this document makes recommendations to promote a census of geohazard features in European seas, to integrate deep sea monitoring infrastructures with seafloor mapping and geohazard research, and take advantage from data mining, virtual access and artificial intelligence.

2

What is a marine geohazard?

Marine geohazards are generated from diverse geological conditions, ranging from broad-scale to local scale. At any time, they may develop into a situation that poses a direct threat and disaster risk to coastal communities and the Blue Economy. While the pre-conditions usually form over geological times, the onset of the hazard can be very sudden and infrequent, and hence difficult to predict – they virtually come 'out of the blue'. The focus of this document is on geohazards that originate from submarine or deep geological regions relevant for European coastal regions, sea basins and outermost regions. It excludes littoral hazards with slow onset-times such as coastal erosion, seawater intrusion, or coastal subsidence; and hazards associated by atmospheric disturbances such as storm surges and meteo-tsunamis.

2.1 Earthquakes

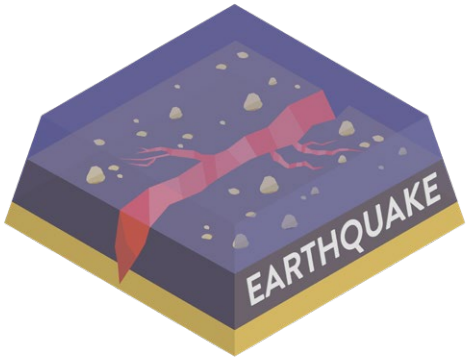

An earthquake manifests in the sudden movement of the Earth's surface, resulting from an abrupt release of energy by the rupture of faults in the crust and upper mantle of the Earth. This is among the most damaging of geohazards, frequently causing devastating loss of lives, assets and infrastructure, especially in densely populated areas. Since 1998, earthquakes have caused a higher number of deaths than all other geophysical (e.g. mass movement, volcanic activity) and hydro-meteorological hazards (e.g. floods, storms, extreme temperatures) combined (CRED & UNISDR, 2018).

Earthquakes with epicentres at sea are usually difficult to locate precisely because of the inadequate or distant location of seismic networks, which are mainly located onshore. However, if the subsurface rupture reaches the seafloor, as is the case for faults causing large earthquakes, the seafloor sediment offers a unique opportunity to depict and quantify fault direction, dimension and movement through time. These are the parameters needed for seismic hazard assessment and for the design of anti-seismic infrastructures. Recent technological advances, such as monitoring the seafloor deformation prior to earthquakes, offer the opportunity to measure the current stress build-up along a fault prior to rupture induced by an earthquake (Lange *et al.,* 2019).

The magnitude of an earthquake is the amount of energy released, and although the Richter scale (M_L) is most well-known, it is not commonly used anymore, as the Moment Magnitude (M_w) is more accurate, especially for larger events. The Moment Magnitude (M_w) is an exponencial scale, without a theoritical upper limit (in practice, an earthquake larger that M_w 10 cannot happen as no fault long enough to generate such a magnitude is known to exist, and if it did, it would extend around most of the planet). The greatest submarine earthquakes (M_w>8) occur along destructive tectonic plate boundaries, referred to as subduction zones (e.g. Sallarès & Ranero, 2019) where one tectonic plate is thrust underneath another. Recent examples are the Sumatra-Andaman (Indonesia, 2004) and Tohoku-Oki (Japan, 2011) earthquakes (both M_w>9), which both ruptured undersea faults and triggered destructive tsunamis. Indirect earthquake effects also include submarine mass movements that may cause extensive cable breaks (see Section 2.8 on Cascading and/or cumulative events). In Europe, the largest and most destructive subduction zone earthquake with M_w>8 occurred in 365 AD offshore of Crete Island (Shaw *et al.,* 2008). It led offshore of Crete to an instantaneous uplift of Western Crete by more than 6 m and triggered a catastrophic tsunami that impacted nearly all coastal areas around the East Mediterranean Sea.

2.2 Volcanoes

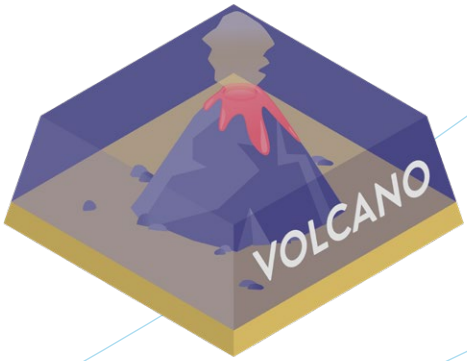

Volcanoes may form at, or near, the margins of tectonic plates where magma reaches the surface, or over hot spots, i.e. over deep magma sources located in the lower Earth mantle. In the Ocean, volcanoes may be completely submerged, or grow large enough to form islands or coastal volcanoes, many of which have been inhabited since prehistory to benefit from the fertile soils.

Santorini Island in the Aegean Sea (Figure 2.1.), is a good example of a large, inhabited caldera volcano. It has a population of >15,000 people, and 500,000 visitors during the summer months. The island took its present shape in the Bronze Age when a super-eruption created the caldera and caused a tsunami that contributed to the end of the Minoan civilization (3000-1100 BCE).

Figure 2.1. **Top:** Santorini Island is the rim of a large caldera left after the gigantic 'Minoan'super-eruption in the Bronze Age. A new volcano, Nea Kameni, is forming at the centre of the caldera and emerged from the sea in the 18th century.

Bottom: The fresh lava flows of Nea Kameni in the foreground and the highly touristic slopes of Santorini Island in the background.

Volcanic eruptions imply expulsion of lava which is at about 1,000°C. The eruptive style (explosive, such as 1980 eruption of Mount St. Helens, vs. effusive, such as the regular rivers of lava in Hawaii) is due to the sudden decompression of gasses dissolved in the magma, and sometimes due to the violent interaction with water (phreatomagmatic eruptions). The explosivity is therefore primarily controlled by the depth of the water, as water pressure can suppress the rate of gas expansion. Phreatomagmatic eruptions occur when the vent is in shallow water. The huge amount of volcaniclastic sediment often causes the emergence of new land, such as occurred at Ferdinandea Island in the Sicily Channel in the early 19th century, Capelinhos in the Azores Islands in the late 1950s, and Surtsey in Iceland in the late 1960s. Typically, eruptions deeper than 300 m will rarely break the water surface, but their products can still pose hazards. Massive emission of fluids from the seafloor may dramatically decrease water density and thus buoyancy causing the sinking of vessels, as probably occurred in 1944 in the Caribbean Sea with 67 casualties[1], and in the sinking of the Japanese research vessel in 1932, causing 31 casualties (Nakano *et al.,* 1954).

Both during and outside of periods of activity, the over-steepened flanks of volcanic edifices can be prone to large landslides or collapses that can trigger tsunamis, such as the 2018 flank collapse of Anak Krakatoa, Indonesia (Figure 2.2), while seafloor activity can damage cables, affecting communications (Favali *et al.,* 2006).

[1] https://uwiseismic.com/volcanoes/kick-em-jenny/kej-hazards/

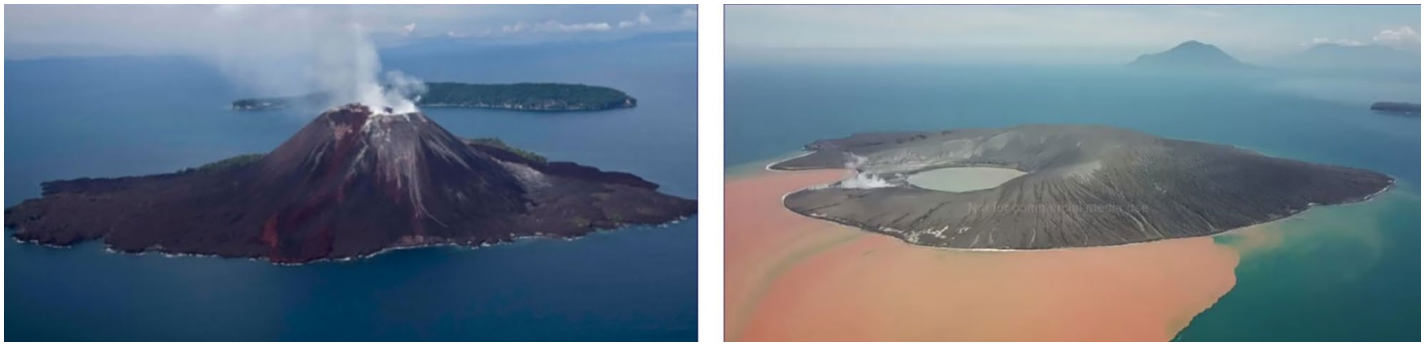

A: Anak Krakatoa **before** eruption

B: Anak Krakatoa **after** eruption

Figure 2.2. Photographs showing the Anak Krakatoa volcano before **(A)** and after **(B)** the 22 December 2018 eruption.

While many volcanic islands are densely inhabited and/or tourist destinations (e.g. Mediterranean islands, Canary and Azores Islands, Mayotte, Caribbean and Polynesia), the locations of submarine vents remain largely unknown and completely unmonitored. Volcanic activity poses obvious threats to life and property, but other economic impacts should not be discounted either. Both nearshore and deep ocean volcanic eruptions can generate large rafts of floating volcanic rock (lava balloons or pumice), as occurred in El Hierro in 2011 and in Pantelleria in 1891. These may remain buoyant for any time between days to years, and can be dispersed by Ocean currents and winds. These pumice rafts can be transboundary volcanic hazards that are able to damage vessels and inundate harbours and fisheries. Volcanoes may also produce vast ash plumes that can ground planes, as was the case in the 2010 Eyjafjallajökull volcano, which is estimated to have cost the aviation industry US$250 million per day (Gudmundsson *et al.,* 2010).

2.3 Tsunamis

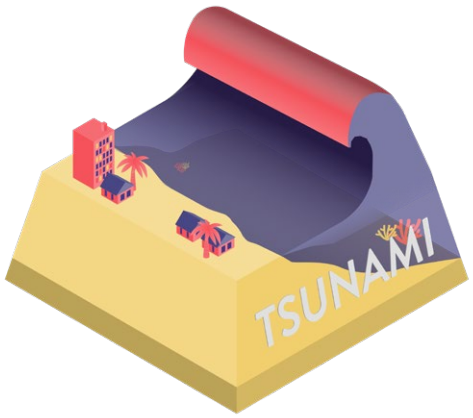

A tsunami is a succession of waves of extremely long wavelength generated by a powerful, underwater disturbance that causes a sudden displacement of a large volume of water from the sea floor. Unlike wind waves that only move the surface of the ocean, tsunami waves move the whole column of water from sea floor to the surface. Tsunamis may be triggered by earthquakes, volcanic eruptions, submarine landslides, and by onshore landslides in which large volumes of debris fall into the water (USGS, 2006). Very low-probability meteorite impacts could potentially also generate a tsunami. The waves travel away from the area of origin and can be extremely damaging when they reach the shore.

If a tsunami-causing disturbance (i.e. earthquake or volcano) occurs close to the coastline, the resulting tsunami can reach coastal communities within minutes. The height of a tsunami wave in the deep Ocean is typically a few decimetres, and the distance between wave crests can be up to 100 km. The speed at which the tsunami travels decreases as water depth decreases. In open water, where the water depth reaches 4-5 kilometres, tsunami speeds can be more than 700 kilometres per hour. As tsunamis reach shallow water around islands or on a continental shelf, the speed decreases but the height of the waves increases manifold. Depending on the seafloor morphology, wave heights may reach more than 20 m. The great distance between wave crests prevents tsunamis from dissipating energy as breaking surf; instead, tsunamis cause water levels to rise rapidly along coastlines much like very strong and fast-moving tides (i.e. strong surges and rapid changes in sea level). Much of the damage inflicted by tsunamis is caused by strong currents and floating debris. Tsunamis travel much further inland than normal storm waves[2].

One of the most well-known examples is the 2004 Indian Ocean tsunami triggered by the Sumatra-Andaman earthquake, which killed 283,000 people in coastal areas in 13 countries around the Indian Ocean. A few years later, in 2011, a catastrophic tsunami produced by the Tohoku-Oki earthquake (Lay *et al.,* 2005), hit the north-eastern coast of Japan causing more than 18,000 deaths and extensive damage to houses and industrial facilities, including the Fukushima Daiichi nuclear power plant (Goto *et al.,* 2015). This event and its consequences are further discussed in Section 2.8 (Cascading and/or cumulative events).

Landslide-generated tsunamis also threaten European coasts. They can range in size from the gigantic Storegga tsunami (see Section 2.4), to local tsunamis such as in Stromboli in 2002 (Chiocci *et al.,* 2008) where a submarine landslide caused waves up to 10 m high (Figure 2.3.). Stromboli, located in the Eolian archipelago, is a crowded tourist destination during the summer season. In 1977 in Gioia Tauro (Italy) and in 1979 in Nice (France) small submarine landslides, caused by engineering work for harbour or port construction at the heads of submarine canyons, caused tsunamis that destroyed the infrastructure and in the case of Nice, caused several casualties. See Section 2.7 Human induced and technological Hazards for more details.

[2] https://www.usgs.gov/special-topic/water-science-school/science/tsunamis-and-tsunami-hazards?qt-science_center_objects=0#qt-science_center_objects

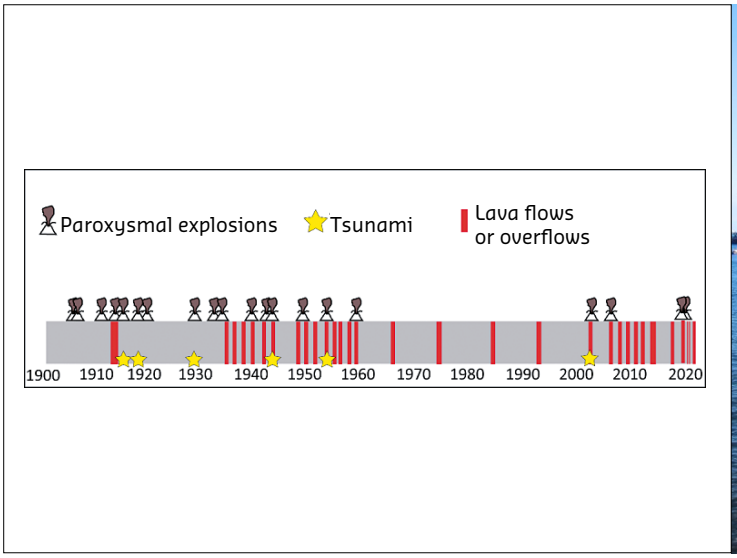

Credit: courtesy of F. Di Traglia, Florence University

Credit: Marcus Andersson (CC BY-SA 2.0)

Figure 2.3. **Left:** recurrence time of volcanic eruption and tsunamis at Stromboli in the last 120 years.
Right: Tourists on a beach in Stromboli. If a similar tsunami that occurred on 30 Dec. 2002 would occur in the summer, it would cause a real disaster.

2.4 Submarine mass movements

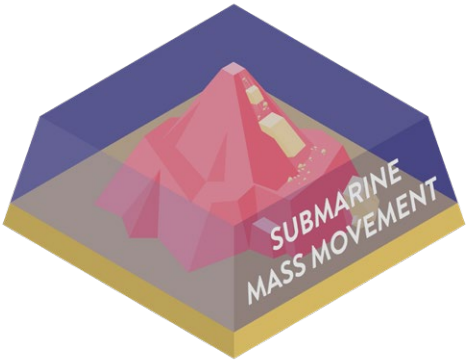

Submarine slopes are generally prone to fail with destructive consequences. Their intrinsic instability is due to the fact that the seafloor is usually made up of unconsolidated soft-sediment which is saturated by water, and often develops overpressure between grains. Furthermore, the typical lithological, morphological and stratigraphic homogeneity of the seafloor over large areas means that failure can create large mass movements, which easily propagate over extremely broad regions. Seafloor surveys have shown that such mass movements can involve several thousand cubic kilometres of material, i.e. be several orders of magnitude larger than any mass movement on land (Urgeles & Camerlenghi, 2013). Landslides also have a major impact on the global sediment flux from land to sea (Korup, 2012). One of the largest and best studied events is the Storegga slide (Figure 2.4.), which occurred in offshore Norway some 8,200 years ago, affecting an area the size of Hungary and mobilizing 3,000 km³ of sediment (Bondevik *et al.*, 2005). For comparison, the largest known subaerial landslide (Mount St. Helens, 1980) involved less than 3 km³ of sediment.

There are numerous causes of submarine mass movements including erosion, rapid sediment deposition, groundwater activity in coastal aquifers, deep fluids (e.g. from mineral dehydration and serpentinization), earthquake loading; seafloor loading by cyclones, storm waves or tidal pumping, volcanic eruptions, rapid sea level

Credit: Britt Lonneville - VLIZ

Figure 2.4. The Storegga slide occurred some 8,200 years ago offshore of Norway, involved about 3000 km³ of sediments (Kvalstad *et al.*, 2005) and affected an area the size of Hungary (both areas are outlined in red). Sources: EMODnet Bathymetry Consortium (2020): EMODnet Digital Bathymetry (DTM) . Storegga slide: Norges geologiske undersøkelse: Marine landformer (accessed on 2021-04-28).

[3] https://doi.org/10.12770/bb6a87dd-e579-4036-abe1-e649cea9881a

change, gas generated by microbial decay of organic matter, gas hydrate decomposition processes, or anthropogenic activity such as coastal infrastructure development, land reclamation, etc. (see Section 2.7).

In coastal waters, submarine landslides occur commonly on soft, unconsolidated sediments, in areas where deltaic, glacial or volcaniclastic deposits have rapidly accumulated, or at the head of submarine canyons. Despite their usually small size, shallow water landslides are extremely dangerous when they occur in areas with dense infrastructure (i.e. industrial and public facilities, cables, pipelines, rigs). They have the greatest potential to cause tsunamis and their retrogressive evolution may affect the coastline, as occurred in Finneidfjord, Nice, or Stromboli (Longva *et al.,* 2003; Dan *et al.,* 2007; Chiocci *et al.,* 2008). They therefore represent a very high 'extensive' risk (see Box 1). In most cases, coupled factors and processes give rise to unpredictable failure events, such as the combined lateral tectonic faulting and coastal landslides following the M_w 7.6 Izmit earthquake in 1999 (Altınok *et al.,* 2001), the M_w 6.8 Boumerdès earthquake in 2003, which struck the coast of Algeria (Meghraoui *et al.,* 2004), the M_w 7.8 Amorgos earthquake in 1956 in the South Aegean Sea (Okal *et al.,* 2009) and the M_w 7.0 Haiti earthquake in 2010 (Hornbach *et al.,* 2010).

In deep-water, landslides may affect astonishingly large areas and the role of marine gas hydrates in slope stability is still a matter of scientific debate. Gas hydrates are ice-like crystals of water and gas molecules that solidify at low temperature and under high pressure. They are commonly found on continental margins (i.e. deeper than several hundreds of metres). When gas hydrates dissociate (if temperature rises, pressure decreases or salinity increases) they can destabilize the submarine slope. In the Black Sea for instance, salinity changes caused by the reconnection of the Black Sea with the Mediterranean Sea ~9000 years ago could have caused extensive gas hydrate dissociation, and hence submarine landslides (Riboulot *et al.,* 2018). The role and process of global warming in hydrate dissociation is also a question of scientific debate (Kvenvolden, 1988; Kretschmer *et al.,* 2015).

2.5 Fluid activity and its manifestations

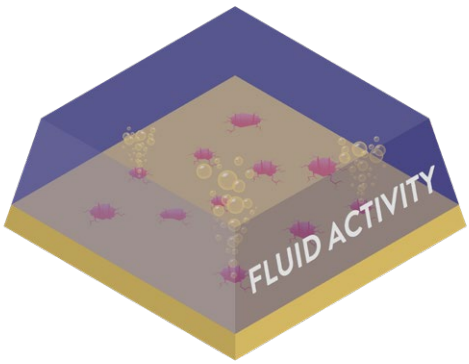

Fluid flow through marine sediment is a common process that occurs when the water from the underlying sediment is expelled, as the sediments are buried, or due to biogeochemical processes, hydrothermal activity, or the migration of deep-seated fluid from the bedrock and Earth's crust. Generally, fluid accumulates under the sediment when there are rapid sedimentation events. Initial porosity, i.e. fluid content between grains, may be as high as 80% in clay, and with stress from overlying sediment, the pore fluid is expelled. Organic matter decay, mineral transformation and diagenesis will add significant amounts of secondary fluids, both water and gases.

If the fluid can escape along faults and fractures, or through the pores of the sediment, it seeps into the Ocean (see Figure 2.5.) where it may fuel unique seafloor ecosystems. If the flow to the seafloor is hampered by barely permeable sediment, the fluids are trapped and significant overpressure builds up. If that pressure exceeds the strength of the sediment, the seafloor stability may be weakened, causing failure and submarine landslides.

The role of fluid migration and overpressure build-up were in fact hypothesized as driving or concurring factors for many submarine landslides, such as the 'small' 1979 Nice landslide (groundwater seepage) to the 'very large' Storegga slide (methane hydrate dissociation). In addition, continuous circulation of fresh water may alter clay-rich sediment by leaching chemical compounds. This may reduce the cohesion of the deposits and favour instability and liquefaction as occurs in many Norwegian fjords.

In regions with significant fluid seepage, craters known as pockmarks (Figure 2.6.) are created by gravitational collapse of a seafloor that used to overlie the fluid reservoir. These pockmarks can range from several metres to hundreds of metres in diameter, and from decimetres to few tens of metres in depth (Hovland *et al.,* 2002).

Similarly, fast release of over-pressured material may generate mud volcanoes. In contrast to pockmarks, mud volcanoes are complex systems that manifest as cone- or shield-shaped mounds, emerging from the seafloor (Figure 2.6.). They may reach up to several kilometres in diameter and up to a few hundred metres in height (Kopf, 2002). Mud volcanoes are considered the most effective means of solid and fluid release from deeper sediments to the surface, with the most violent, rapid examples termed diatremes (Brown, 1990). In shallow water, gas eruption from mud volcanoes may threaten navigation (Casalbore *et al.,* 2020).

Regardless of the size, the genesis and positioning, fluid release from the seafloor may represent a geohazard, either directly to seafloor infrastructure or drilling operations, or indirectly due to a loss in density and hence buoyancy that may jeopardize vessels, rigs and floating infrastructure above.

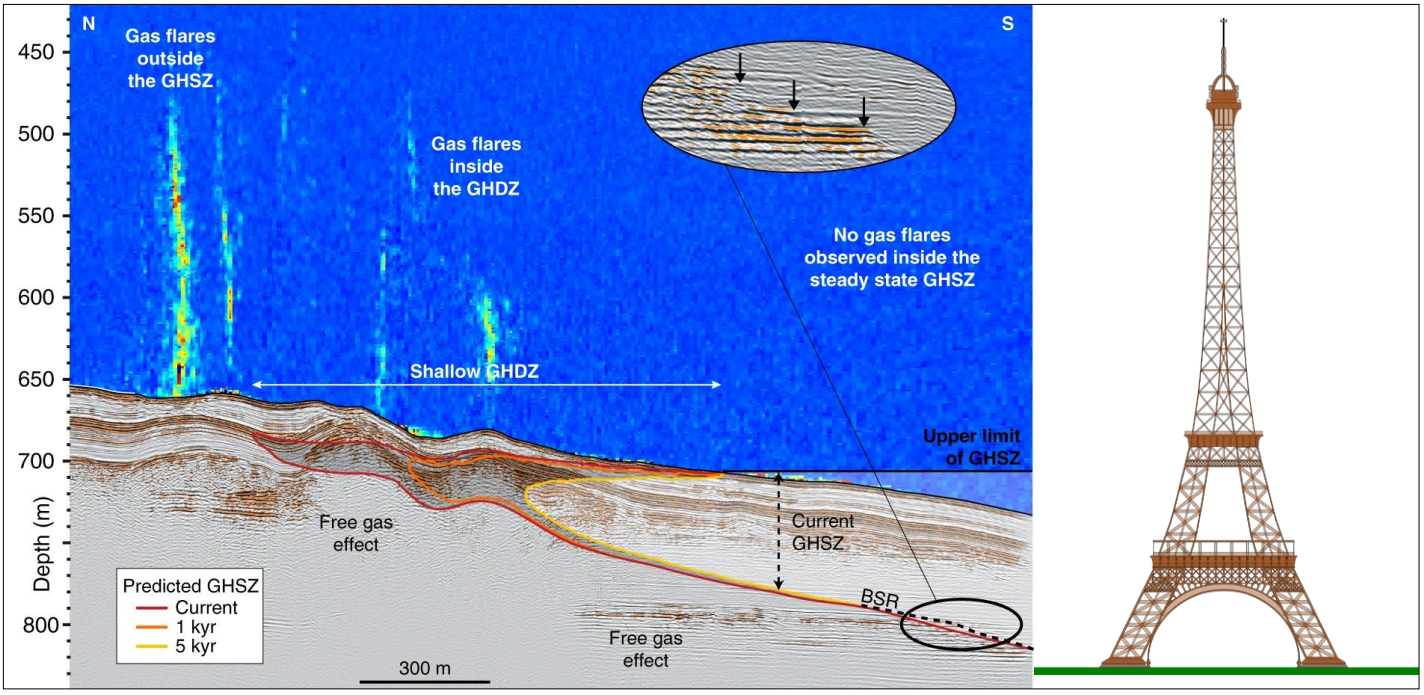

Credit: Modified from Riboulot *et al.*, (2018) (CC BY 4.0)

Figure 2.5. Geophysically detected gas plumes (flares) in the Black Sea. Note that these gas flares are comparable to the height of the Eiffel Tower in Paris, France. In the right part of the seismic profile a low-permeability Gas Hydrate Stability Zone (GHSZ) occurs while to the left a GHSZ does not exist and gas is able to migrate into the water column.

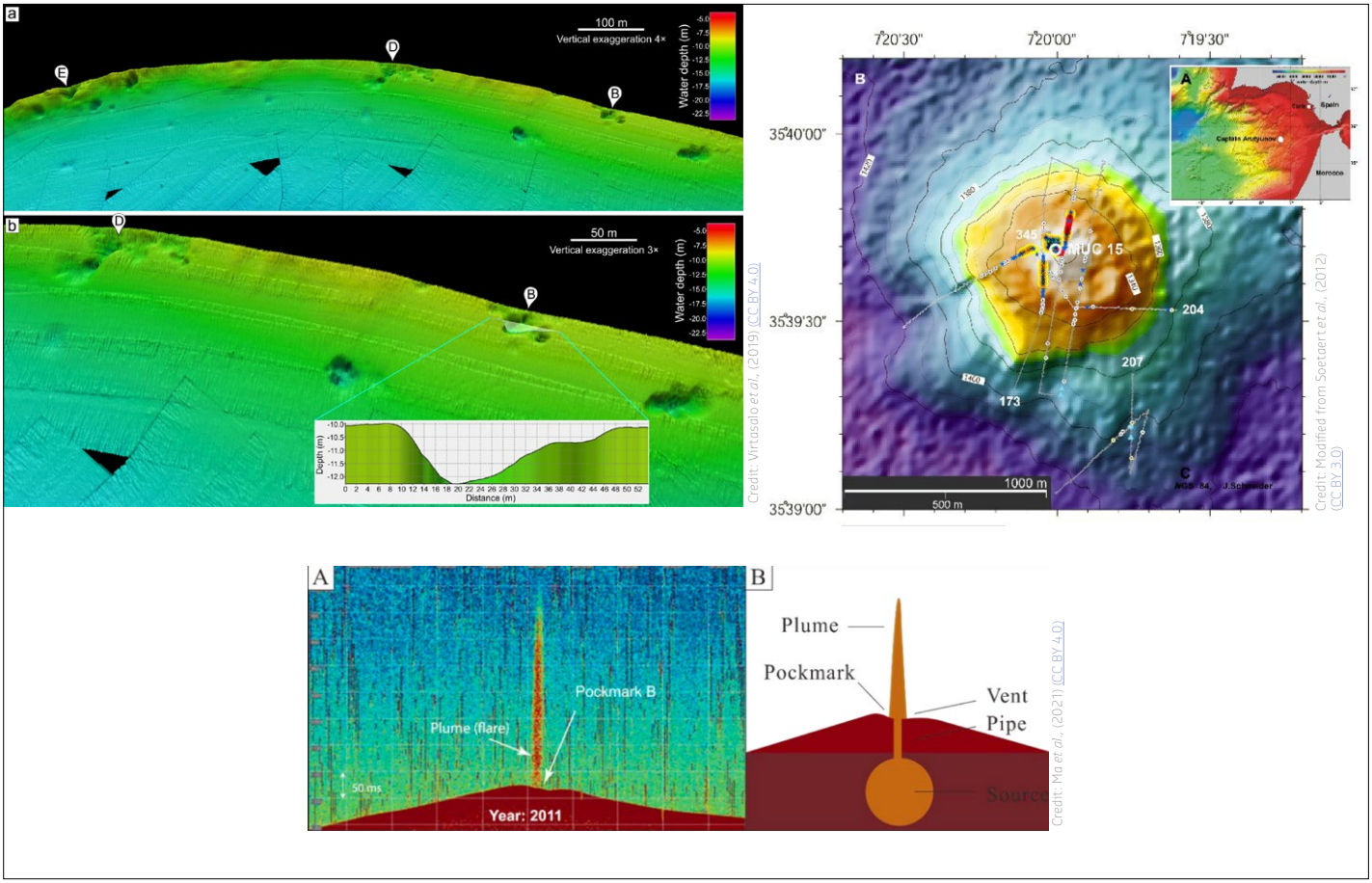

Credit: Virtasalo *et al.*, (2019) (CC BY 4.0)

Credit: Modified from Soetaert *et al.*, (2012) (CC BY 3.0)

Credit: Ma *et al.*, (2021) (CC BY 4.0)

Figure 2.6. **Top left:** Multibeam bathymetric images of pockmarks South of Finland. Inset below shows a depth profile over pockmark B.

Top right: Location and bathymetric map of the mud volcano Captain Arutyunov in the Gulf of Cadiz.

Bottom: Seafloor morphology and flare in the water column above **(A)** indicating active venting in the Vestnesa Ridge (Svalbard continental margin) and a descriptive mechanism of seepage **(B)**.

2.6 Migrating bedforms

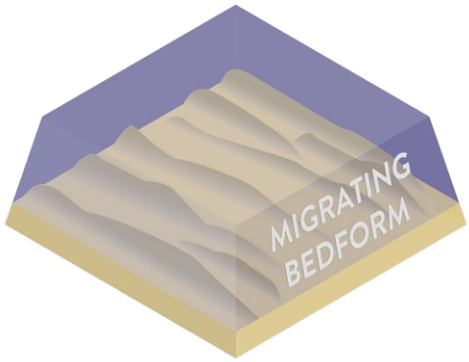

In areas with a strong tidal regime and loose sediment, bottom currents produce sand waves, i.e. migrating bedforms similar in shape and dimensions to desert dunes. They can also occur in straits and seaways where currents are forced to accelerate. In submarine canyons and channels, sediment flows produced by gravity generate bedforms called cyclic steps and antidunes, that migrate upstream causing erosion to the canyon heads. Migrating bedforms may harm critical seafloor infrastructure, such as submarine cables and pipelines (e.g. Barrie *et al.,* 2005; Cecchini *et al.,* 2011) (Figure 2.7.).

Seaways connecting islands to coasts or running parallel to the shore usually host a large number of cables and pipelines that may be threatened by the migrating bedform fields. This is common in the Mediterranean Sea (Bosporus-, Messina-, Bonifacio- and Gibraltar Straits) and in the Atlantic Ocean (English Channel, Danish Strait). Submarine canyons with cyclic steps are present on almost all European continental slopes and such features represent a geohazard for the submarine cables that have to pass through them.

2.7 Human induced and technological hazards

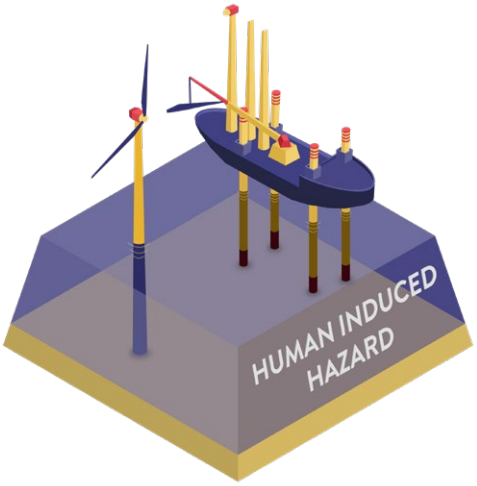

In densely populated European coastal areas, human activities such as construction of large coastal infrastructures, water pumping and creation of dams can lead to subsidence, landslides and erosion along the coasts and offshore. The ill-judged effect of natural phenomena and hazards in combination with an inauspicious location is responsible for most of the damage produced to seafloor infrastructures and coastal settlements. However, there are instances where human activity directly enhanced the marine geohazard, causing events that would not have occurred naturally.

Underwater canyons are characterized by natural coastward migration of their head, occurring when the erosion reduces the slope and the weight of the rock mass overcomes the resistance of the rock mass itself. If the seafloor immediately above the canyon head is loaded with engineering structures, the collapse of the structure will be more likely to occur. Examples include the tsunami-forming landslides that occurred in 1977 at the Gioia Tauro port in Italy (Colantoni *et al.,* 1992) and in 1979 at the Nice harbour in France (Ioualalen *et al.,* 2010). Other human activities that may trigger natural marine geohazards are fracking, i.e the injection of

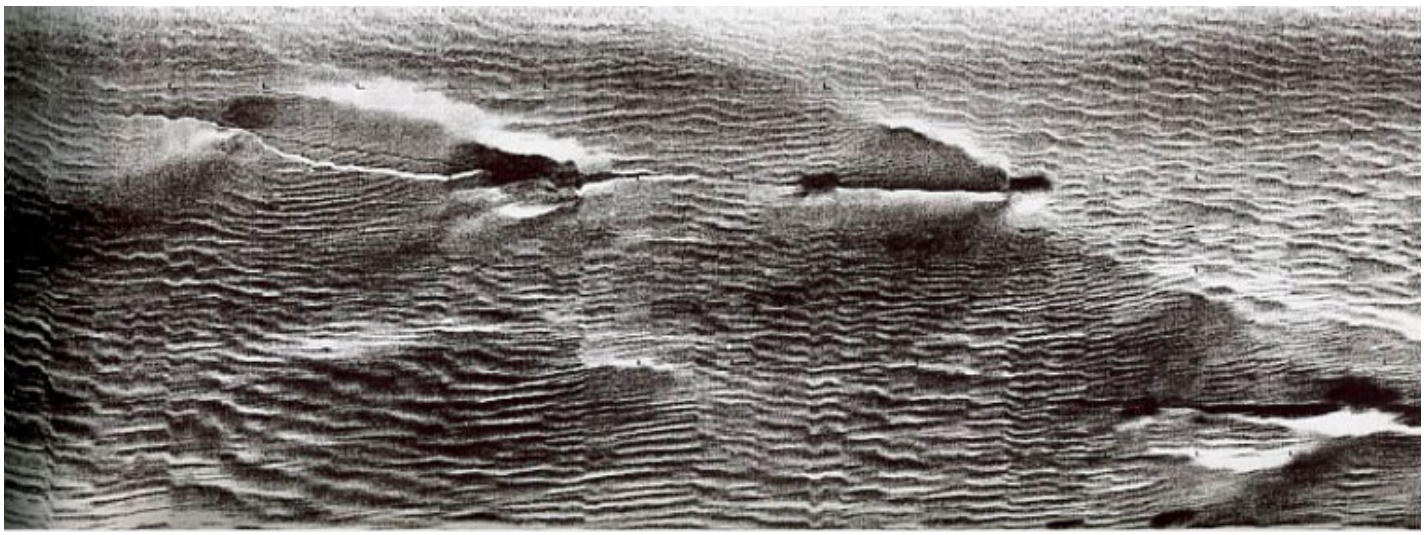

Credit: F. L. Chiocci

Figure 2.7. Side scan sonar image of the seafloor north of the Messina Strait. A free span of a liquefied natural gas (LNG) pipeline can be seen between sand wave crests in the upper left. To the right, the pipeline is buried in the sand. The damage to such seafloor infrastructures may cause an economic loss and create a risk for maritime traffic (loss of buoyancy) and environment.

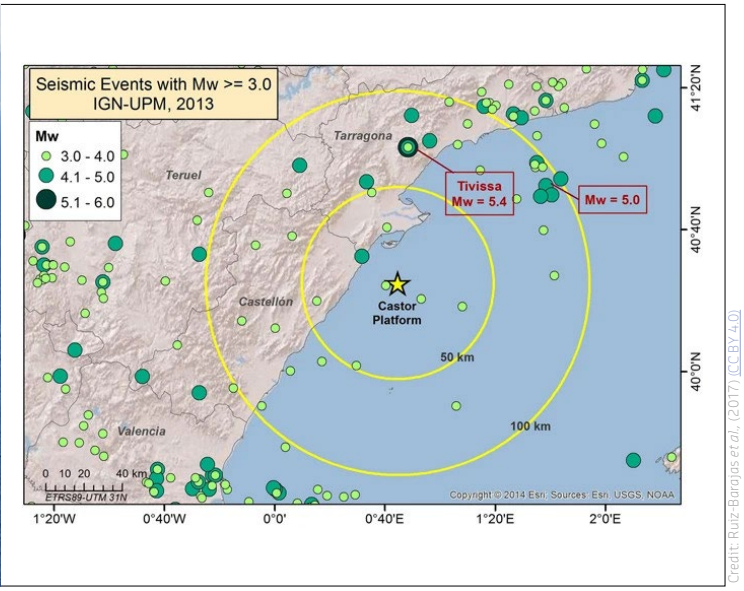

Figure 2.8. **Left:** The marine platform *'Castor'* in the Mediterranean Sea, aimed to inject large quantities of gas in the subsurface, to create one of the largest strategic hydrocarbon reservoirs in Spain. The project started in April 2012 and caused the appearance of seismic activity in the surrounding area.

Right: Instrumental seismicity induced in the area around the Castor platform (yellow star) by the injection of gas. The project was abandoned in 2013 due to increased levels of induced seismicity, culminating in up to 1,000 earthquakes up to magnitude M_w 4.2 over a period of 40 days (Cesca *et al.,* 2014; Ruiz-Barajas *et al.,* 2017). The estimated economic loss was >€4 Billion.

fluids into sub-seafloors to recover hydrocarbons or storage gas (Vilarrasa *et al.,* 2021) and possibly CO_2 sequestration (see Figure 2.8.). Another trigger for marine geohazards is the large outbursts caused by drilling operations, such as the blowout that caused an explosion on the rig 'Deepwater Horizon' in 2010 in the Gulf of Mexico (USA), producing one of the largest ecological disasters to date[4].

2.8 Cascading and/or cumulative events

Cascades and cumulative events are multi-hazard chains where one hazard event triggers a process that leads to other phenomena, resulting in additional and often greater impacts and consequences (e.g. additive or multiplying impacts) that significantly increase fatalities and damage. Cascading hazards can be natural (for example, earthquake-tsunami-fire) or exacerbated by human-made hazards (see Box 2). For a cumulative hazard, the impact multiplies and thus significantly magnifies (Daniell *et al.,* 2017; Cutter, 2018).

The flooding and subsequent meltdown of the Fukushima Daiichi nuclear power plant in northern Japan is a good example of a cumulative event (Figure 2.9.). The power plant was hit by a 14-15 m high tsunami generated by an earthquake, which swept over the plant's seawall and flooded the lower grounds of the reactor buildings with seawater, causing a failure of the emergency generators (Hasegawa *et al.,* 2016). The cascade of events resulted in nuclear meltdown, hydrogen explosions and radioactive contamination, including the release of contaminated water into the Pacific Ocean (Lipscy *et al.,* 2013).

Cumulative effects occur under a wide set of different phenomena, where the occurrence of the initial triggering event entails a number of (often interacting) secondary events (see Box 2). An earthquake for instance may cause structural collapse of buildings due to ground motion, but may also interrupt supply routes (freeways, harbours), generate a tsunami, provoke subaerial and submarine landslides (some tsunami forming or tsunamigenic), cause land subsidence that favours coastal inundation, produce dispersion of pollutants (including e.g. nuclear waste in 2011), or damage emergency infrastructures. This is evident for low-probability high-impact events, as many of the most devastating examples recently have all crossed the sea-land boundary, with destructive effects demonstrating their potential to cause humanitarian crises.

Cascading effects commonly occur in coastal towns when buildings suffering from structural damage inflicted by earthquake-shaking are subsequently exposed to a tsunami, as happened in Messina in 1908 and in Lisbon in 1755. In Lisbon, the cascade effect also included an extensive fire.

[4] https://www.epa.gov/enforcement/deepwater-horizon-bp-gulf-mexico-oil-spill

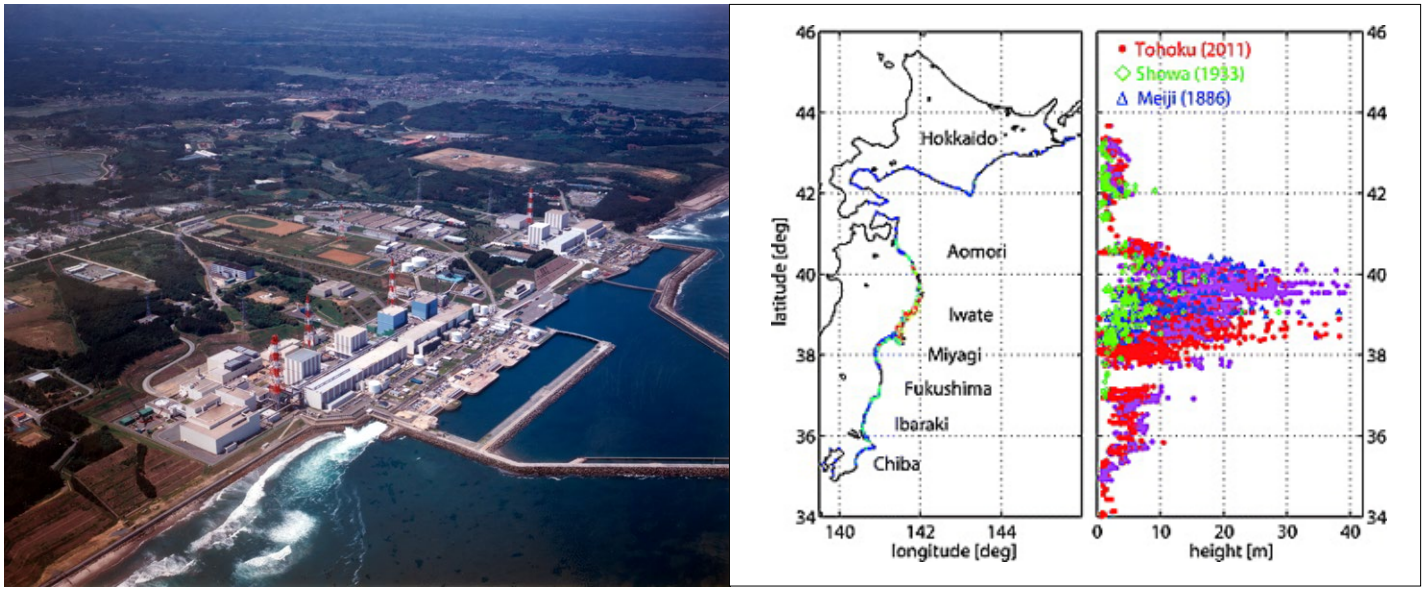

Credit: Tokyo Electric Power Co., TEPCO (CC BY-SA 2.0)

Credit: Mori *et al.* (2011)

Figure 2.9. **Left:** The Fukushima Daiichi Nuclear Power Plant was flooded by 14-15 m tsunami waves generated by a M_w 9.0 earthquake in 2011. As a consequence, three of the 11 reactors lost the ability to maintain proper reactor cooling causing a release of radioactive material and the evacuation of ca. 100,000 people. It took weeks to stabilize the reactors.

Right: The run-up of the 2011 tsunami after the earthquake along the Japanese coast, compared to two previous events in 1886 and 1933.

BOX 2: A TIME BOMB OUT-OF-THE-BLUE

The risk level of high-probability low-impact events may increase by an order of magnitude if cascading events are taken into consideration. For instance, if seismically active regions with high mountain ranges close to the coast (e.g. Alboran Sea, Ligurian Sea, Calabria region, Eastern Sicily, Aegean Sea) experience large earthquakes, a collapse of transport infrastructure can be expected either due to ground shaking, landslides or tsunamis. In such a scenario, population rescue, evacuation and emergency response will mainly rely on immediate airborne intervention, followed by ship-transported aid reaching the area through entry-points, usually ports and harbours. If these infrastructures are damaged by even small submarine landslides or seafloor failures (triggered by the earthquake), even a relatively minor initial geohazard would have catastrophic consequences.

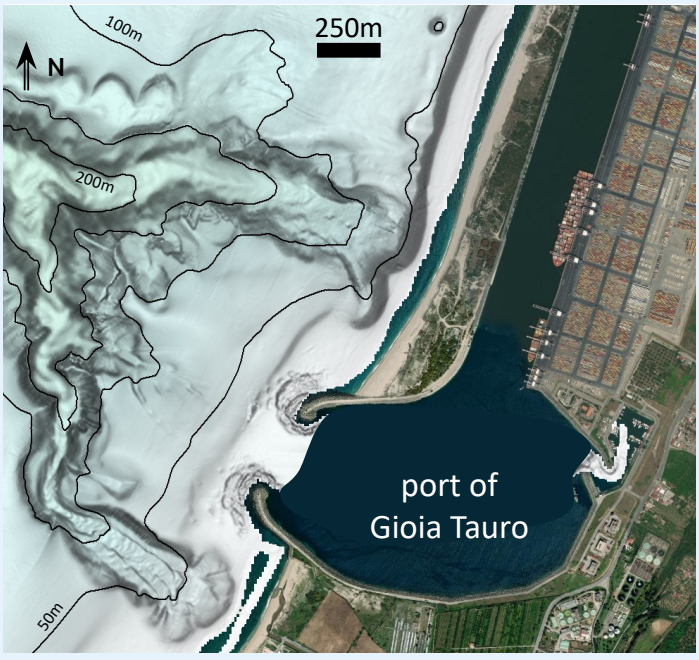

Credit: F. L. Chiocci. Map Data: © 2018 Google

A good example is the Gioia Tauro port in southern Calabria, one of the most seismically active regions of the Mediterranean Sea. The Gioia Tauro port is one of the main hubs for container ships in the Mediterranean Sea and potentially the main entry point for large ships that would need to convey aid to the Calabria region in case of a natural disaster. The port is located at the head of the Gioia Tauro canyon, which is located very near to the shore, and in very shallow water (see Figure 2.10.). During its construction in 1977, its external pier collapsed and was partially destroyed because of a submarine landslide and the waves this caused (Colantoni *et al.*, 1992). The port is still at risk to collapse because erosive evolution at the canyon head is still ongoing. Therefore, if a large earthquake were to strike here, ground shaking could trigger a submarine landslide, which could directly or indirectly (e.g. with tsunami waves as in 1977) affect the port and prevent its use as an entry point for large rescue vessels and facilities.

Figure 2.10. Multibeam bathymetry offshore Gioia Tauro port. Gioia Tauro is one of the main container ports of the Mediterranean and a possible entry point for emergency rescue vessels in case of a natural disaster in Calabria.

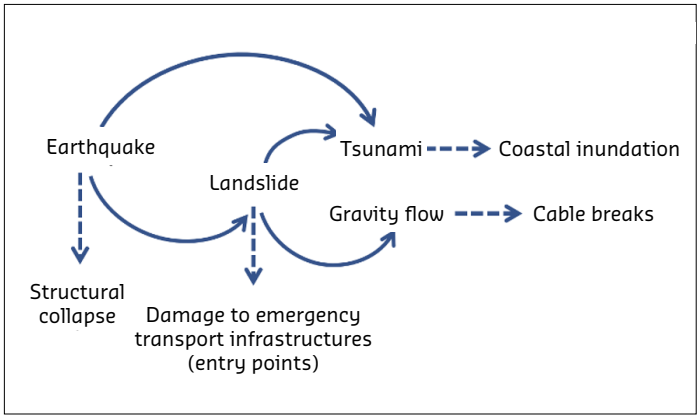

Figure 2.11. Conceptual sketch of a cumulative event. The cascading geohazard may strongly amplify damage and economic loss.

A classic cascading event for marine geohazards is the earthquake that generates a submarine landslide, which in turn causes a tsunami and turbidity currents (gravity flows) with cable breaks occurring hours or days after the initial event (Figure 2.11.).

There is increasing evidence that many tsunamis associated with earthquakes were not caused by the earthquake itself but rather were triggered by landslides caused by the earthquake (Tappin, 2017). Such phenomena may explain discrepancies between modelled arrival times and run-up of waves compared to measurements from the 2011 Tohoku and 1908 Messina cases (Satake *et al.,* 2007; Pino *et al.,* 2009; Suzuki *et al.,* 2012).

The cascading hazard risk rises exponentially with the increasing use of the seafloor for engineering infrastructure (cables, pipelines, energy plants, aquaculture farms and others). For instance, 10 hours after the Messina earthquake in 1908, a cable connecting Malta to Greece was broken 190 km south of the epicentre by a turbidity current (Ryan & Heezen, 1965). In Newfoundland (Canada), cable breaks caused by an earthquake-generated landslide in 1928 was the first *in situ* evidence that sparked the evaluation of gravity flow dynamics at sea (Heezen & Ewing, 1952). Finally, in 2003, a M_w 6.8 earthquake triggered a large turbidity current that caused 29 submarine cable breaks along a 150 km long span of the Algerian margin (Cattaneo *et al.,* 2012) (Figure 2.12.).

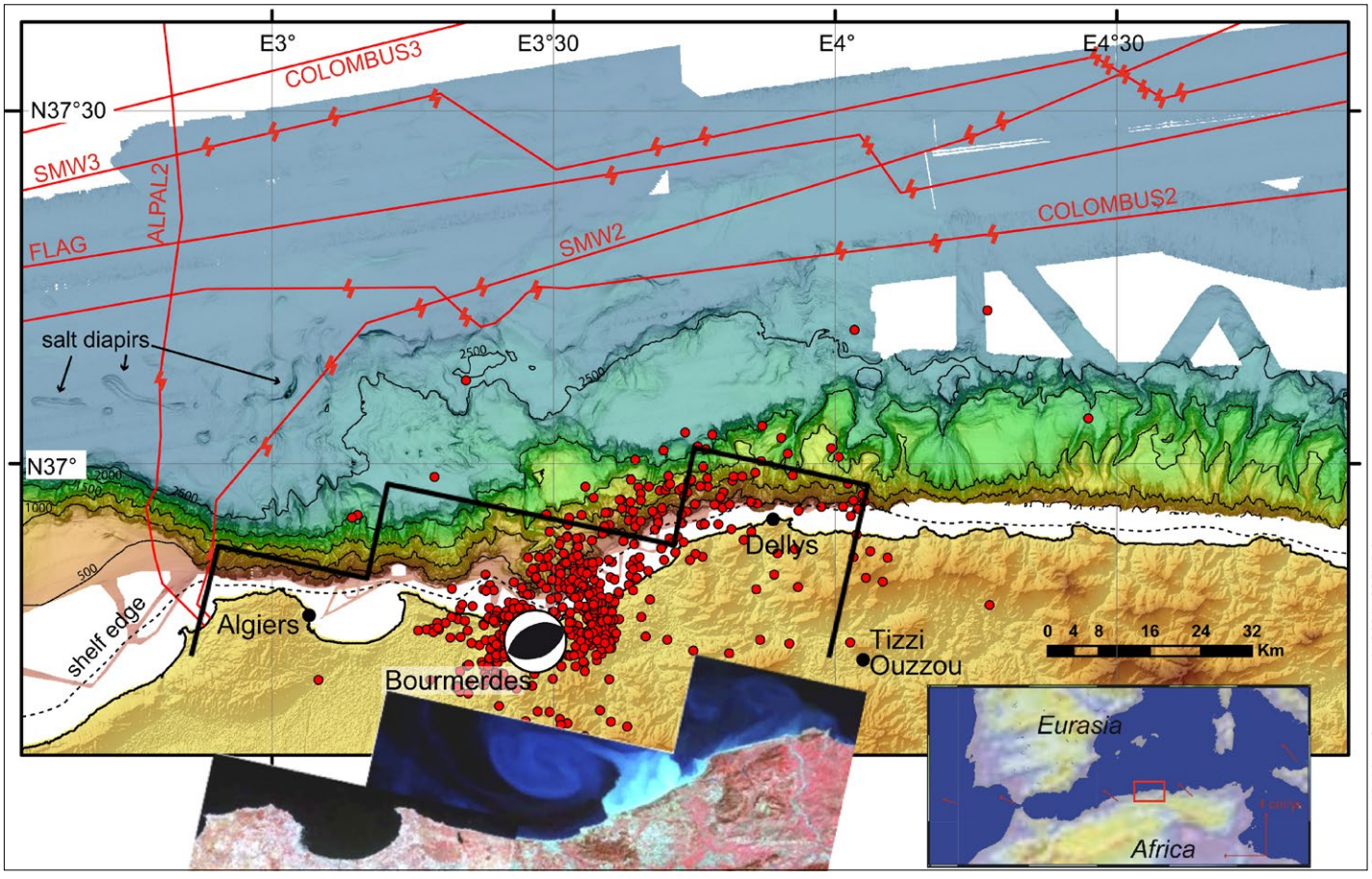

Credit: Modified from Cattaneo *et al.*, (2021) CC BY 3.0

Figure 2.12. The Boumerdès earthquake (M_w 6.8) occurred on 21 May 2003, about 60 km east of Algiers (northern Algeria). This earthquake was the strongest to hit Algeria in more than 20 years. The multiple cable breaks (indicated by the red lightning signs in the figure) were caused by gravity flows due to submarine landslides induced by the seismic event, creating a risk for maritime traffic (loss of buoyancy) and environment.

In order to decrease their risk to society, we must embrace a multi-hazard risk assessment approach instead of treating marine geohazards independently, with separate monitoring and assessment of the effects on infrastructure affected by each individual hazard. This can be achieved by multi-hazard, scenario-based assessments and subsequent planning. The transition from a single to a cascading hazard significantly increases the complexity of the process, requiring a shift from a 'hazard-centred' perspective to a 'territorial-centred' perspective (Gasparini & Garcia-Aristizabal, 2014), and requires us to take into account the specific conditions the geographical region (Ercilla *et al.*, 2021).

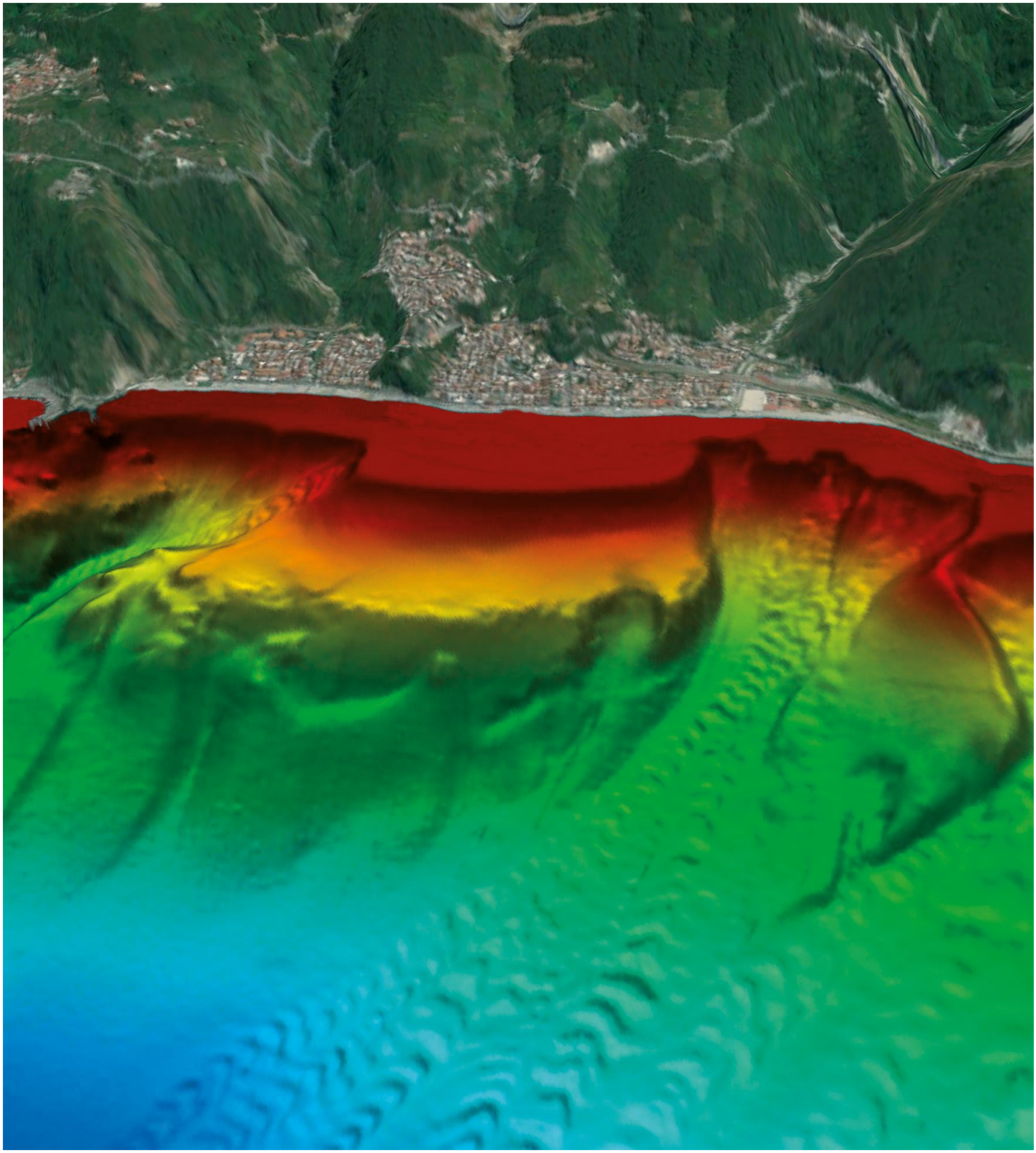

Credit: F. L. Chiocci. Map data ©2018 Google

3

Where do marine geohazards occur in European Seas?

Credits: Gaby Al Aour

3.1 Plate tectonics in Europe

Plate tectonics is the overarching process leading to geohazard formation and distribution. The Earth's outermost shell, the lithosphere, is divided into tectonic plates that move continuously on geological timescales. The boundaries of the plates (Figure 3.1.), may be constructive (also called divergent, where tectonic plates move away from each other), destructive (or convergent, where tectonic plates converge, with one driven beneath the other in a process called subduction), or conservative (along transform boundaries, where tectonic plates move past each other). The Eurasian plate, which contains Europe, experiences a variety of different conditions at its margins, many of which are associated with marine geohazards (Figure 3.2.), but also give rise to the diversity of landscapes on- and offshore.

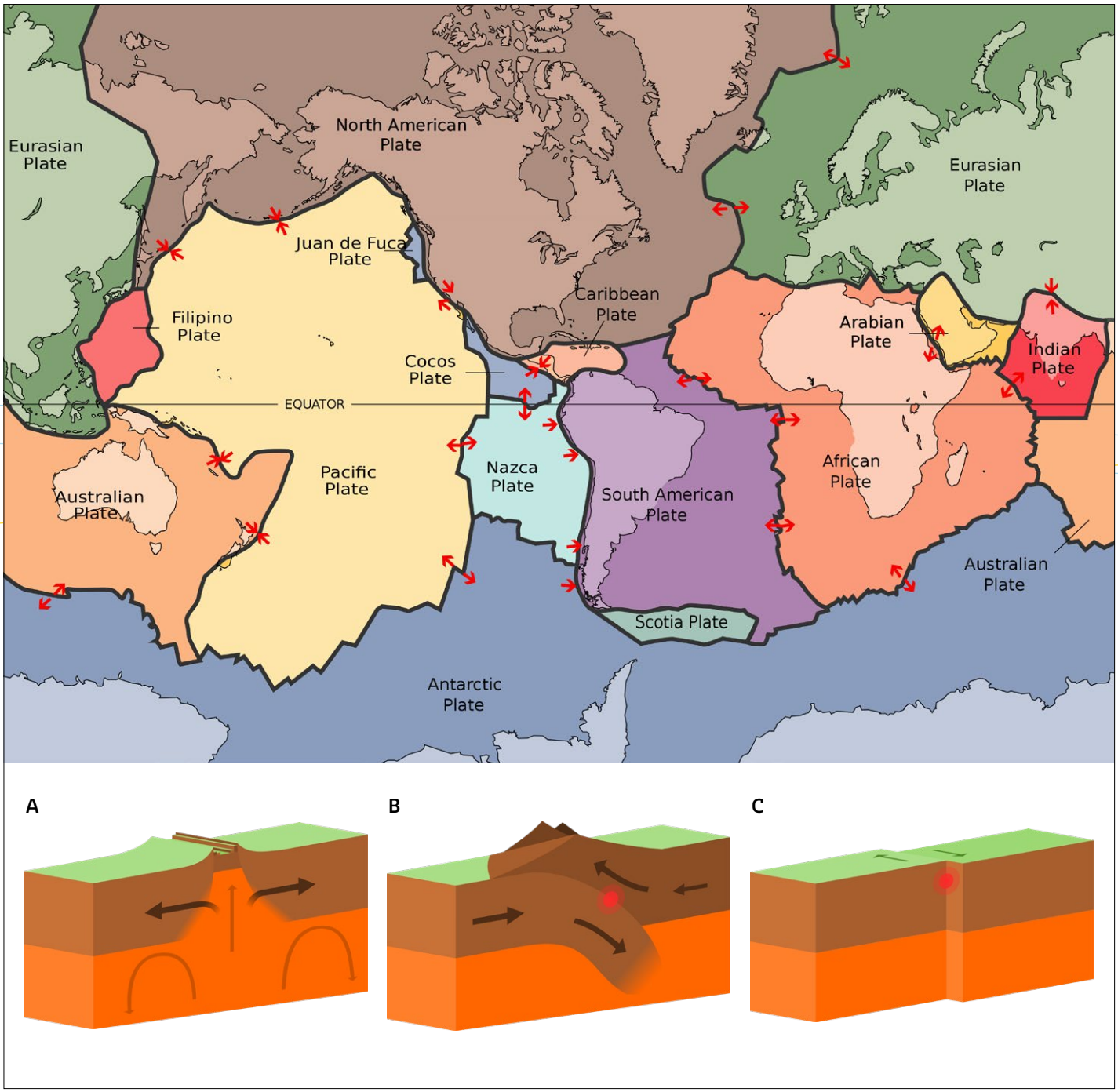

Credit: Scott Nash, via Wikimedia Commons (public domain)

Credit: Adam Jones, via Wikimedia Commons (CC BY 4.0)

Figure 3.1. Sketches of the tectonic plates on Earth and of the three types of plate boundaries, i.e. **A.**constructive (divergent), **B.** destructive (convergent) and **C.** conservative (transcurrent).

Constructive plate boundaries are found on both the western (Mid-Atlantic Ridge) and northern (Gakkel Ridge in the Arctic Ocean) edges of the Eurasian plate, while the southern boundary is a much more complicated mixture of conservative and destructive plate boundaries. Both constructive and destructive plate boundaries are associated with high volcanic and earthquake activity. The destructive boundary with the African plate has caused repeated large earthquakes in the Mediterranean Sea, which have been reported in ancient Egyptian sources, Greek and Roman myths, and the Hebrew Bible (Guidoboni *et al.*, 1994). In some areas, the intersection of the constructive plate margin with a region where the higher mantle is melting (e.g. the Azores Islands and Iceland) may produce larger volcanoes than those typically expected for a constructive margin. Any of these processes may result in slopes or landforms that are unstable and prone to landslides.

This chapter provides an overview of the distribution of marine geohazards in European seas. We acknowledge that all nine outermost regions[5] of the European Union are not equally described in this section. Even though the events highlighted in this chapter have occurred in the past there is currently no way to predict using the available technology when similar events will occur in the future.

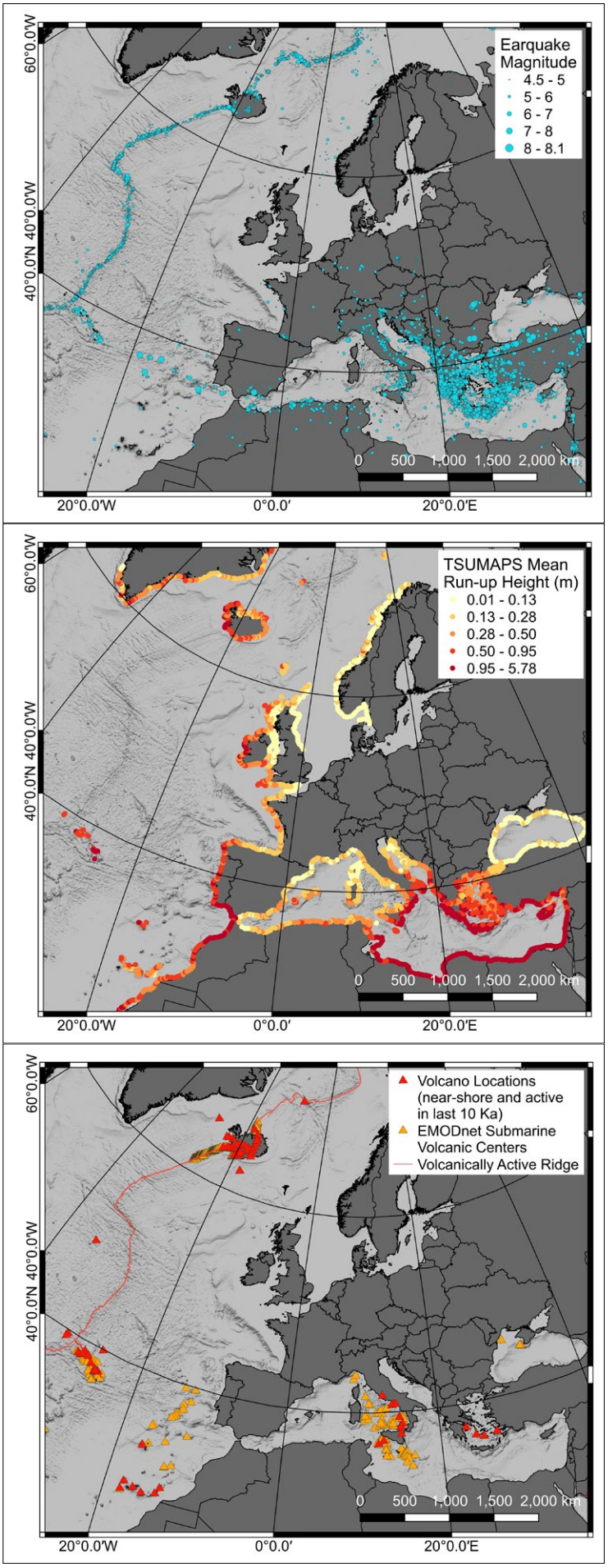

Figure 3.2. Locations of some of the main marine geohazards in Europe and European Seas since 1900.

Top: Earthquakes with epicentes M_w >4.5. Data accessed and downloaded in February 2021 from the United Stated Geological Survey Earthquake Catalogue.

Middle: Tsunami hazards from seismically induced tsunamis. The mean run-up height (m) predicted by the Probabilistic TSUnami Hazard MAPS for the NEAM Region (TSUMAPS-NEAM) Tsunami Hazard Model 2018 for European Coastlines described in Basili *et al.*, (2021). Data provided by Roberto Basili, INGV. Tsunamis induced by landslides are not considered.

Bottom: Location of mapped submarine, island and nearshore volcanoes (red when active). Other volcanic sites that were active less recently or lie too far from shorelines to represent a marine hazard are excluded. Volcanoes occur with a similar density to that mapped north and south of Iceland along the lengths of active volcanic ridges. Volcano data sources include submarine volcanoes (at 1:100,000 and 1:250,000 scale), made available by EMODnet Geology. Data collected by Silvana D'Angelo (Italian Institute for Environmental Protection and Research, ISPRA), accessed and downloaded in February 2021. Data on the periods of activity for the majority of the volcanoes are not available. Other volcano locations (reduced to those only active in the last 10 thousand years) were taken from Global GIS: volcanoes of the world; volcano basic data from the American Geological Institute retrieved in February 2021. Ridges from Bird, (2003) are manually edited to remove all but active volcanic ridges. Other marine geohazards such as submarine landslides, active faults, gas seepages, and migrating bedforms are not shown because no standard mapping of these features exists for all European Seas.

Credit: Isobel Yeo

[5] French Guiana, Guadeloupe, Martinique, Mayotte, Reunion Island and Saint-Martin (France), Azores and Madeira (Portugal), and the Canary Islands (Spain)

3.2 Atlantic Ocean

The Mid-Atlantic ridge is a constructive plate boundary, where the Eurasian and North American plates move away from each other and new seafloor grows (Figure 3.3.). Here volcanic eruptions and volcanoes are formed as the result of decompression melting and brittle stretching between the plates. These volcanoes and associated earthquakes tend to be relatively small and pose little hazard to people, although lava flows and fracturing could potentially damage trans-Atlantic deep-sea cables. Exceptions exist where volcanoes are associated with anomalously high levels of mantle melting (called 'hot spots'), for example Iceland and the Azores Islands. Hot spots may also produce volcanoes away from plate margins, as with the Canary Islands. Increased eruption frequency and regular eruptions in the same place can build large volcanoes, which may break the sea surface to form islands. These eruptions tend to be more explosive than those in deep water. This can also happen on volcanoes topped by lakes or ice, as was the case of the Eyjafjallajökull eruption in Iceland in 2010, which halted air traffic over northern and central Europe and caused significant economic losses.

The most recent submarine eruption in Europe occurred in 2011-2012 offshore of El Hierro in the Canary Islands. This eruption lasted five months and produced floating debris, also called lava balloons i.e. crust of solidified lava surrounding a large cavity, floating on the sea surface after rising from a submarine volcanic eruption (Figure 3.4.). This floating debris disrupted the local fishery and caused alarm in the population (Gómez-Letona *et al.*, 2018). This phenomenon had already been observed in 1892 after the eruption of Pantelleria in the Sicily Channel as recorded in books from the period (Ricco, 1892).

Many island-forming (or insular) volcanoes grow in height because of eruptive activity. Their flanks become steep-sided and unstable (see Figure 2.2.). Sector collapses of volcanoes create large landslides that can produce tsunamis, which can travel for thousands of kilometres across the Ocean. The volcanic islands in the Atlantic are home to millions of people and are some of the continent's most popular holiday destinations for European and global tourists.

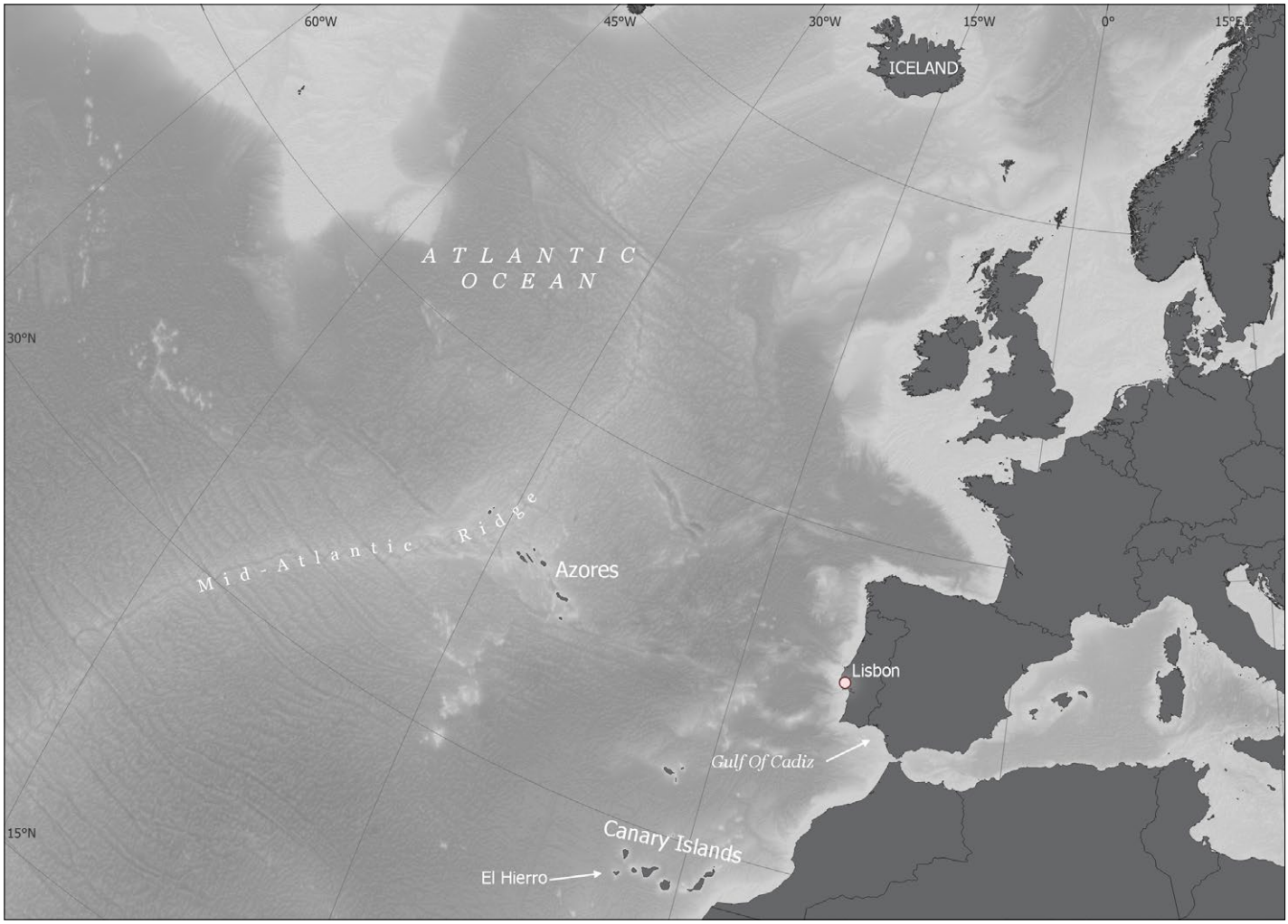

Figure 3.3. Map of the North East Atlantic indicating places highlighted in this document. The Mid-Atlantic Ridge is a constructive plate boundary separating the Eurasian and North-American plates where new seafloor is formed at a rate of 2.5 cm/yr. This process, known as seafloor spreading, is associated with small magnitude earthquakes and volcanism, which may pose a hazard to trans-Atlantic deep-sea cables. Sources: GEBCO Compilation Group (2019) GEBCO 2019 Grid (doi:10.5285/836f016a-33be-6ddc-e053-6c86abc0788e). IHO-IOC GEBCO Gazetteer of Undersea Feature Names, www.gebco.net. https://www.geonames.org/

Figure 3.4. Lava balloons floating on the sea surface during the 2011 eruption of El Hierro, Canary Islands.

Non-volcanic hazards in the Atlantic include the potential for large earthquakes along the boundary between the Eurasia and African plates, which historically have had the potential to cause tsunamis. The plate boundary runs through the Gulf of Cadiz. The offshore boundary of the Gulf of Cadiz is seismically active, with several faults which are possibly able to generate great magnitude earthquakes (see Box 3) such as the 1755 Lisbon earthquake and tsunami (M_w 8.5-9) (Figure 3.5.) (Gràcia *et al.,* 2003; Gutscher *et al.,* 2006; Zitellini *et al.,* 2020), and the 1969 Horseshoe earthquake (M_w 7.8-8) (Fukao, 1973).

Seafloor surface ruptures and submarine landslides provide further evidence of the tectonic activity in the Gulf of Cadiz and the overall compressive regime generates widespread mud volcanism and fluid venting (Pinheiro *et al.,* 2003) with over forty active mud volcanoes at water depths between 200 m and 4000 m.

BOX 3: WHAT WOULD HAPPEN IF THE 1755 EARTHQUAKE WOULD OCCUR TODAY?

Using the Lisbon tsunami of 1755 as a reference, it is possible to make an approximate calculation of the consequences of an equivalent tsunami occurring today. In 1755, the total number of victims would have reached 45,000 in the different countries facing the Gulf of Cadiz (Figure 3.5.) but also in Brazil and North America, although accurate records do not exist. In Spain, the recorded amount of fatalities along the coast was 1,214 people, out of a total population of 9 – 10 million inhabitants. Given that the population has grown 5 times (20 times in coastal areas), if a similar event occurred today, the number of deaths would be between 5,000 and 24,000 people, and 60,000 people if seasonal tourists are considered. These numbers represent the estimated deaths of Spain alone, and exclude the fatalities in Portugal (records estimate 10,000 victims in Lisbon only in 1755) and other countries that would be affected by the tsunami.

The damage due to the event in Spain was approximately 70 million Reals in 1755, estimated today as an equivalent to €700 million. However, since 1755, the infrastructure in and around the coastal populations and beyond has increased exponentially, therefore the financial cost would be exponentially higher.

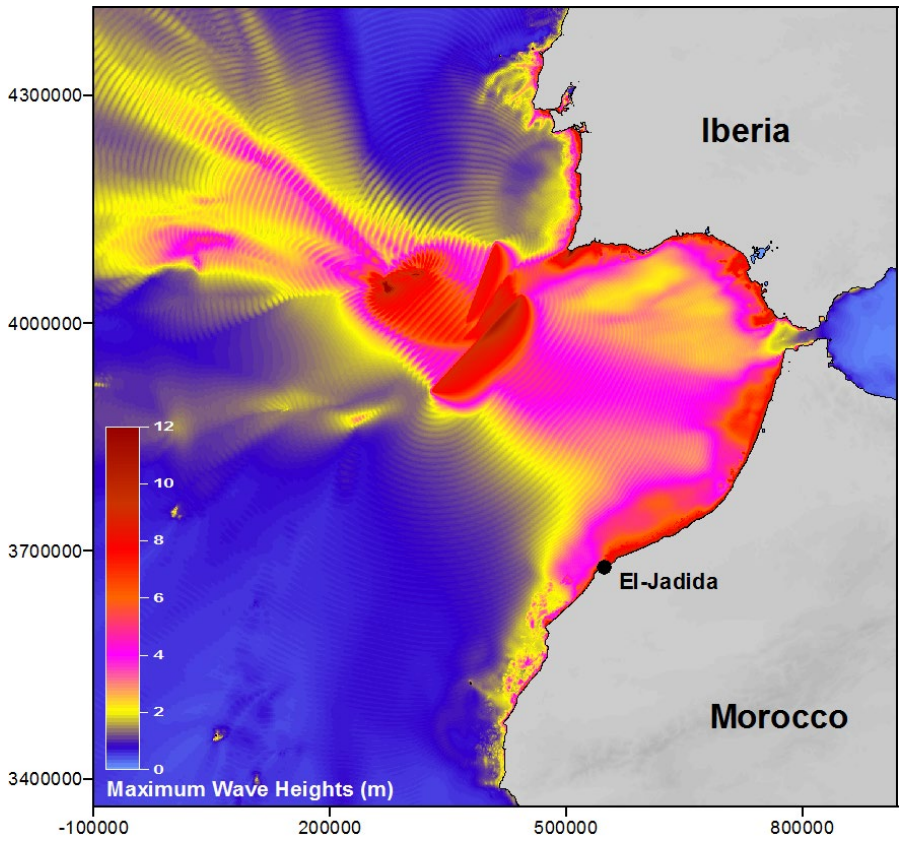

Figure 3.5. Maximum wave heights modelled for the 1755 Lisbon earthquake. Note the shoaling effect of tsunami waves that increase in height when they reach the coast. Despite being named after Lisbon, the city that was hit hardest, the earthquake and tsunami occurred roughly 400 km to the south and also affected many towns in Iberia and Morocco.

3.3 The Mediterranean Sea

The Mediterranean Sea, located at the African-Eurasian plate boundary, is subject to strong earthquakes because of its active geology (mainly in Algeria, Italy, Greece and Turkey), while two of the five largest volcanic eruptions ever recorded on Earth (Campi Flegrei 40,000 and Santorini 1600 BCE) occurred in the Tyrrhenian and Aegean Sea. The Mediterranean seafloor is characterised by countless mass movement processes, including submarine landslides, debris avalanches and large turbidity flows. Steep continental slopes fed by mountain-supplied rivers are prone to seabed instability and, because of high sedimentation rates and the retrogressive evolution of the canyon heads that often reach the coast, small landslides are ubiquitous (de Lange *et al.,* 2011).

3.3.1 The Western Mediterranean

The Western Mediterranean (Figure 3.6.) stretches from the Straits of Gibraltar to the Italian Peninsula and is defined by a string of semi-enclosed sub-basins, including the Alboran, the Algerian, the Liguro-Provençal and the Tyrrhenian Basin and the Sicily Channel, connecting to the Eastern Mediterranean. Between these basins, there are a series of large and small islands, such as Corsica and Sardinia, Sicily, the Balearic Islands, and the Tyrrhenian archipelagos. The Western Mediterranean is seismically active and dominated by an elaborate pattern of tectonic fault systems and shear zones. Repeated large- to moderate-size earthquakes pose a severe hazard to the region and seismic activity is commonly associated with tsunami generation.

The Alboran Sea forms the westernmost part of the Mediterranean between the Iberian Peninsula and the African coast and connects to the Atlantic through the Straits of Gibraltar. The region has witnessed a series of seismic events up to M_w 7.1 that have caused thousands of casualties and have made hundreds of thousands of people homeless. Off Morocco, earthquakes occurred in 1994 (M_w 6.2), 2004 (M_w 6.0) and 2016 (M_w 6.4) (Gómez de la Peña *et al.,* 2018; Spakman *et al.,* 2018) on the Al-Idrissi Fault System (Gràcia *et al.,* 2019), which is growing through propagation and linking between individual fault segments. Further to the east, earthquakes have occurred over the last decades along the African-Eurasian plate boundary in the Algerian Basin. The 1980 El Asnam (M_w 7.1) earthquake caused between 2,600 and 5,000 casualties (Philip & Meghraoui, 1983). In 2003, the Boumerdès (M_w 6.8) earthquake resulted in 2,266 deaths and 10,000 injured, leaving approximately 200,000 homeless (Meghraoui *et al.,* 2004). Deepwater submarine landslides along the Algerian margin are also associated with highly liquefiable sandy/silty sediments that cause landslides on very gentle slopes not exceeding 4 degrees (see Figure 2.12.).

Submarine mass movements are a significant geohazard in the Western Mediterranean, due either to seismicity (Galindo-Zaldivar *et al.,* 2018) (Figure 3.7.), groundwater charging, high sediment accumulation or anthropogenic modification of the seafloor. For instance, the Tyrrhenian Sea and the Ligurian Sea, with their narrow continental shelves and steep slopes, have experienced human-induced submarine mass movement, that involved a cascade of events resulting in the generation of a tsunami (Colantoni *et al.,* 1992; Sahal & Lemahieu, 2011). Prehistorically, large-volume

Figure 3.6. Map of the Western Mediterranean indicating places highlighted in this document Sources: GEBCO Compilation Group (2019) GEBCO 2019 Grid (doi:10.5285/836f016a-33be-6ddc-e053-6c86abc0788e). IHO-IOC GEBCO Gazetteer of Undersea Feature Names, www.gebco.net. https://www.geonames.org/.

debris flows and turbidite events were triggered by catastrophic slope failures that resulted in the transport of enormous volumes of sediment (~500 km³) from the continental margins to the deep sea (Rothwell *et al.,* 1998). One example is the BIG'95 event on the Iberian margin, which occurred 11,500 years ago, covering an area of 2,200 km² (roughly the size of Luxembourg), with 26 km³ of debris. Megaturbidite events are triggered by seismic activity or may result from gas hydrate release (Nisbet, 1992) and pose a severe hazard to offshore infrastructure. Countless small submarine landslides occur in the most active parts of the Western Mediterranean Sea (see Figure 5.1.).

Hazardous active volcanoes in the Western Mediterranean include Mount Etna (the largest and most active volcano on the European mainland), Vesuvius, Ischia and Campi Flegrei in the Gulf of Naples, Stromboli and Vulcano in the Aeolian Islands, and the Pantelleria Island and Ferdinandea volcano. These rank amongst the world's most active volcanoes and are in a state of almost constant activity. Mount Etna (Figure 3.8.) and Vesuvius were designated as Decade Volcanoes by the United Nations[6], worthy of close study in light of their potentially large, destructive eruptions and proximity to densely populated areas. In addition to eruptions, volcano flank failure or collapse triggering catastrophic tsunamis in Ocean island volcanoes or flanks near the shoreline also pose potential hazards (Urlaub *et al.,* 2018). Such collapses have been seen in Ischia (Chiocci & De Alteriis, 2006) and Stromboli (Tibaldi, 2001). At Mount Etna, continuous onshore GPS measurements since the early 1980s have shown large-scale seaward motion at an average rate of 3-5 cm/year. Recent seafloor geodetic observations confirm similar motions on the submerged offshore flank of Mount Etna (Urlaub *et al.,* 2018).

In the Tyrrhenian Sea, large submarine volcanoes such as the Marsili Seamount, which is as high as the Mount Etna volcano, is active with eruptions dating back only a few thousands of years (Iezzia *et al.,* 2014). Possible flank collapses of Marsili volcano would generate tsunamis affecting the whole southern Tyrrhenian Sea (Teresita *et al.,* 2019).

3.3.2 The Eastern Mediterranean

The Eastern Mediterranean stretches from the Italian Peninsula to the Levant in the east. The destructive plate boundary between Eurasia and Africa runs along the Calabrian, Hellenic and Cyprus arcs as well as the Herodotus Basin, the Nile delta and the Levant Basin (Figure 3.9), where the plate subdivides into smaller fragments (Anatolian plate and Arabian plate). The main marine seismogenic zones in the Eastern Mediterranean are the Calabrian, Hellenic and Cyprus arcs and the North Anatolian Fault, all of which are recurrent sources of tsunamis.

The Hellenic Arc creates large earthquakes commonly associated with large tsunamis. The largest known earthquake (M_w 8.3) in

[6] http://www.un.org/ga/search/view_doc.asp?symbol=A/RES/44/236

the Mediterranean Sea occurred in 365 CE with its epicentre located offshore from western Crete (Papazachos *et al.,* 2000). This earthquake generated a tsunami that was most destructive along the coast of western Crete and in the Nile delta in Egypt (Tinti *et al.,* 2005). This tsunami created giant turbidity currents and deposited a well-recognizable sediment unit throughout the Mediterranean Sea (Polonia *et al.,* 2016). The second largest earthquake (M_w 8) and a tsunami occurred in 1303 in the Hellenic Arc. It caused widespread damage along south-eastern Crete, southern Rhodes, western Cyprus, southern Syria, northern Israel, and the Nile delta region (e.g. Guidoboni & Comastri, 2005).

Seismogenic fault zones between the Eurasian and African plates that create a sharp boundary between the deep Oceanic crust of the eastern Mediterranean and the shallow continental crust of the Sicily Channel, have been identified in the Ionian Sea and adjacent margins, including the Malta Escarpment. All these faults have the potential to generate large earthquakes and associated tsunamis (Tselentis *et al.,* 2010; Polonia *et al.,* 2011), as documented by the 1908 (M_w 7.1) Messina earthquake and tsunami, which left >80,000 dead in the region surrounding the Messina Strait that separates Sicily from the Italian mainland (Calabria, see Section 4.1.2 for more details). The Calabrian Arc is also known for its vigorous fluid activity, documented in mud volcanoes, pockmarks and active gas-seepage sites (Papatheodorou *et al.,* 1993).

Calculations have shown that a tsunami with a maximum amplitude of up to a few metres can be expected in the Adriatic Sea, despite its overall shallow water depth (typically less than 400 m) (Paulatto *et al.,* 2007). This concurs with a number of historical events in the region, mostly generated by moderate-sized earthquakes (M_w ≤7). The coasts enclosing the Adriatic Sea host numerous tourist destinations and are home to millions of people.

Further east in the Levant Basin, earthquakes generated along the Cyprus Arc and submarine landslides from the Nile delta front pose significant geohazards. The rate of seismicity here is lower, possibly because the plate moves faster (McClusky *et al.,* 2003). Historically, fifteen known strong destructive earthquakes have hit Cyprus (Papazachos & Papaioannou, 1999), with the most recent being the 1996 (M_w 6.8) Paphos earthquake (Wdowinski *et al.,* 2006). Large earthquakes in the Cyprus Arc and along the Dead Sea Transform Fault have the potential to trigger submarine landslides especially from the Nile delta.

The major geohazards in the northern Aegean Sea and the Sea of Marmara originate from the activity of the North Anatolian Fault: the major boundary between the Eurasian and Anatolian-Aegean plates. In the Sea of Marmara, the North Anatolian Fault creates recurrent, devastating earthquakes of M_w >7 every ~250 years in an extremely densely populated area. Historically, 55 major earthquakes and 30 tsunamis have occurred in the last 2,000 years (Yalçıner *et al.,* 2002) with the 1999 Izmit earthquake (M_w 7.6) causing 2.5 m high tsunami waves in the gulf and more than ~18,000 casualties. In 1509, the Little Apocalypse, a M_w 7.2 earthquake, was associated with >6 m high tsunami waves, and caused widespread damage in Istanbul and the surrounding Marmara region (Guidoboni *et al.,* 1994; Ambraseys, 2002).

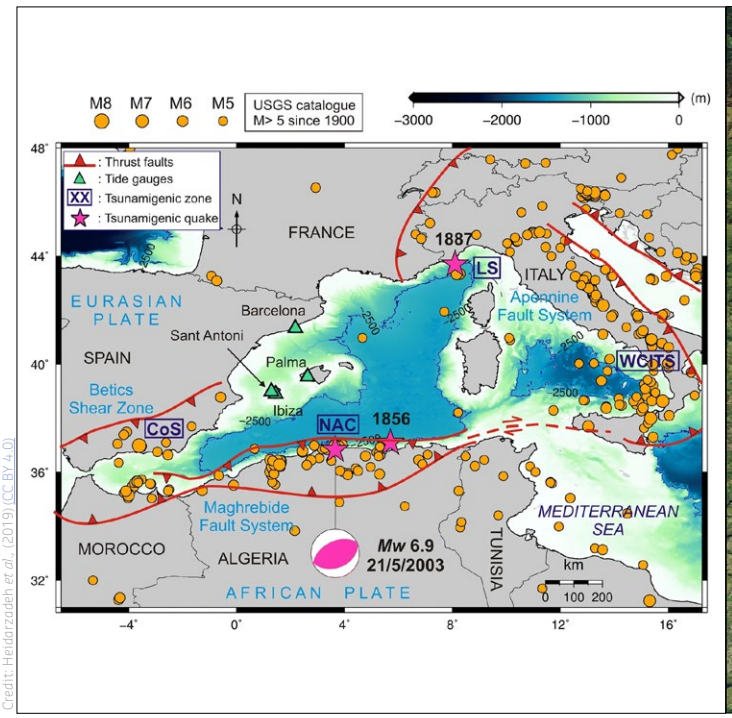

Figure 3.7. Main geological features of the Western Mediterranean Sea. The front of the main tectonic thrust belts is depicted in red, earthquake events are in orange and pink stars refer to tsunamigenic (tsunami forming) earthquakes. Tsunamigenic zones are indicated by letters (i.e. CoS, NAC, LS, and WCITS)

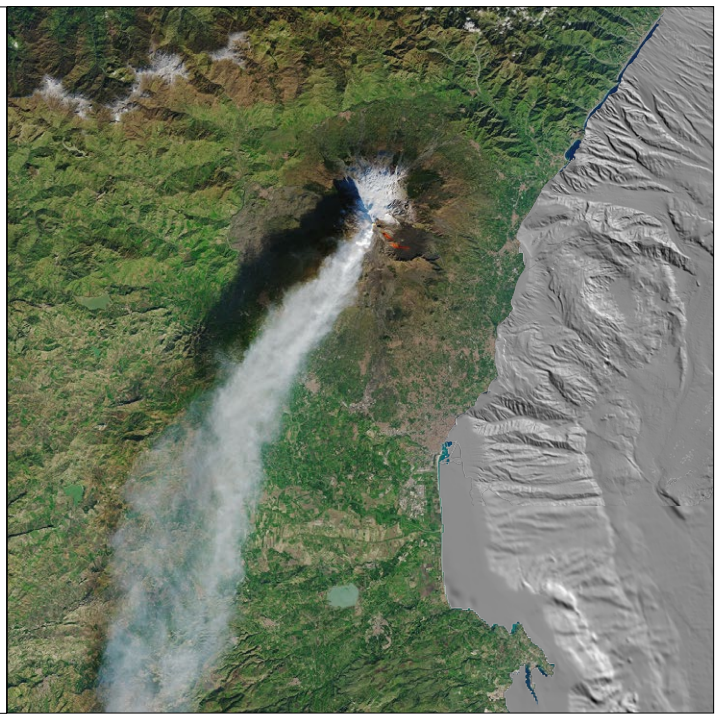

Figure 3.8. Satellite image of erupting Mount Etna and the city of Catania south of the volcano, and a multibeam bathymetry of the facing Ionian Sea based on data from EMODnet bathymetry and University of Rome 'Sapienza'. Catania was destroyed in 1663 by a volcanic eruption that reached the sea and in 1693 by a strong earthquake (M_w 7.4) and tsunami that killed 2/3 of the inhabitants of the time. Today, more than 300,000 people live in Catania. GPS data indicate that the eastern slope of the volcano is slowly sliding westwards.

Because transform faults that are unable to generate significant waves predominate in the Sea of Marmara, most tsunamis are triggered by submarine landslides from the steep slopes (up to 29 degrees) of the deep basins (Görür & Çağatay, 2010). Recent modelling results demonstrate that the generation of tsunamis is caused by waves in marine basins or bays with steep slopes, such as the Gulf of Izmit on the easternmost tip of the Sea of Marmara (Elbanna *et al.,* 2021).

The North Anatolian Fault extends from the Sea of Marmara to the northern Aegean Sea (Sakellariou & Tsampouraki-Kraounaki, 2018) and joins the rift zones in mainland Greece. The major faults in this zone can generate earthquakes up to M_w 7.5, including the 2014 (M_w 6.9) Saros Gulf earthquake and the 2001 (M_w 6.4) Skyros earthquakes (Ganas *et al.,* 2005). The North Skyros Basin had two M_w 7.2 earthquakes in 1968 and 1981 (Papazachos *et al.,* 2000). The steep margins of up to ~1600 m deep depressions in the North Aegean (i.e. Gulf of Saros, North Aegean Trough, Skyros Basin and Sporadhes Basin) are prone to submarine landslides and associated tsunamis.

The central Aegean Sea is characterized by seismogenic faults capable of generating up to M_w 7 earthquakes, such as the 1881 (M_w 6.5-7.3) Çesme-Chios earthquake and the recent 2020 (M_w 7.0) Samos-Izmir earthquake which created a 1.9 m high associated tsunami causing 117 deaths. The southern Aegean Sea straddles the Hellenic Arc and its active earthquake fault systems, and includes the volcanoes of the South Aegean Volcanic Arc (Sakellariou *et al.,* 2018). This belt of active volcanoes emits ash and gases into the atmosphere and could cause submarine caldera and flank collapses and landslides, which could in turn create associated tsunamis. In 1650, the submarine Kolumbo volcano 8 km from Santorini, erupted pyroclastic flows and volcanic gases and produced a tsunami that caused significant damage and fatalities in Santorini (Dominey-Howes *et al.,* 2000).

One of the largest volcanic eruptions recorded in Europe was the Minoan eruption of Santorini (Thera) sometime between 1627 and 1600 BCE (Friedrich *et al.,* 2006), which is claimed to have ended, or contributed to ending, the Minoan civilization in the region (Figure 3.10.). This event occurred in several phases, producing huge volumes of ash that reached Scandinavia and Gibraltar, causing the collapse of the volcano edifice and producing tsunami waves up to 40 m high (Sakellariou *et al.,* 2012). The tsunami impacted the whole Aegean Sea up to the west coast of Anatolia (Antonopoulos, 1992). Historically, only the Indonesian volcano eruptions of Tambora (1815) and Krakatoa (1883) had similar magnitudes and these each caused several tens of thousands of casualties and affected global climate (Sigurdsson *et al.,* 2006; Johnston *et al.,* 2014). Volcanic islands of the Aegean Sea are also subject to sector collapses and debris avalanches, as is seen on the seafloor off Santorini, Antiparos and Nysiros (Nomikou *et al.,* 2014).

Figure 3.9. Map of the Western Mediterranean indicating places highlighted in this document. Sources: GEBCO Compilation Group (2019) GEBCO 2019 Grid (doi:10.5285/836f016a-33be-6ddc-e053-6c86abc0788e). IHO-IOC GEBCO Gazetteer of Undersea Feature Names, www.gebco.net. DISS Working Group (2018). Database of Individual Seismogenic Sources (DISS), Version 3.2.1: A compilation of potential sources for earthquakes larger than M 5.5 in Italy and surrounding areas. http://diss.rm.ingv.it/diss/, Istituto Nazionale di Geofisica e Vulcanologia; DOI:10.6092/INGV.IT-DISS3.2.1. Mikenorton, CC BY-SA 3.0, via Wikimedia Commons

Figure 3.10. Excavation site of the Minoan settlement at Akrotiri in Santorini (Thera) Island, buried under the product of one of the two largest eruptions that have ever occurred in Europe, some 1600 BCE. The eruption is thought to have ended (or contributed to the ending of) the Minoan civilization in the Bronze Age.

3.4 The Black Sea

The Black Sea is characterized by two ~2200 m deep basins, the Eastern (EBS) and Western Black Sea (WBS) basins, separated by the Andrusov-Arkhangelsky ridge (Figure 3.11.). Prominent transform faults in the Western Black Sea appear to still be active. The area produces M_w ~7 earthquakes every 400-600 yrs, including the (M_w 7.2) Balchik earthquake in 1901. This was the most powerful earthquake in the Black Sea (Ranguelov & Gospodinov, 1994) and generated a 4–5 m high tsunami. The other historical earthquakes of M_w 6-7 in the area happened in 1738, 1802, 1838, 1940, 1977, 1986 and 1990, close to the Bulgarian and Romanian coasts (Ambraseys & Finkel, 1987). The Western Crimean Fault Zone has caused two M_w 5-7 earthquakes near the Crimean coast in the last 145 years. Multiple other faults have been mapped in the Western Black Sea region (Oaie *et al.,* 2016).

A total of 22 tsunamis were identified in the Black Sea in the last ~1500 years, triggered by earthquakes (Papadopoulos *et al.,* 2011) and submarine landslides. Two of these events, known to have caused ~7 m high surface waves, were observed in Crimea in 544 CE and north of Amasra on the Anatolian coast in 1598. The last event was most probably triggered by a submarine landslide (Altınok & Ersoy, 2000).

The Black Sea is also prone to submarine landslides (and associated tsunamis) by sediment loading, especially along its western, north-western and northern continental shelf and slopes where deltaic sediments and deep-sea sediment fans of the regions' major rivers (e.g. Danube, Dniester, Dnieper and Kuban) have accumulated. These areas are also the sites of gas seeps, gas hydrates and mud volcanoes (Oaie *et al.,* 2016), where downslope mobilization of sediments could occur by gas-escape related processes (Figure 3.11.). The Black Sea slopes are marked by submarine canyons, where turbidity currents may pose a geohazard risk to submarine engineering structures (Popescu *et al.,* 2014).

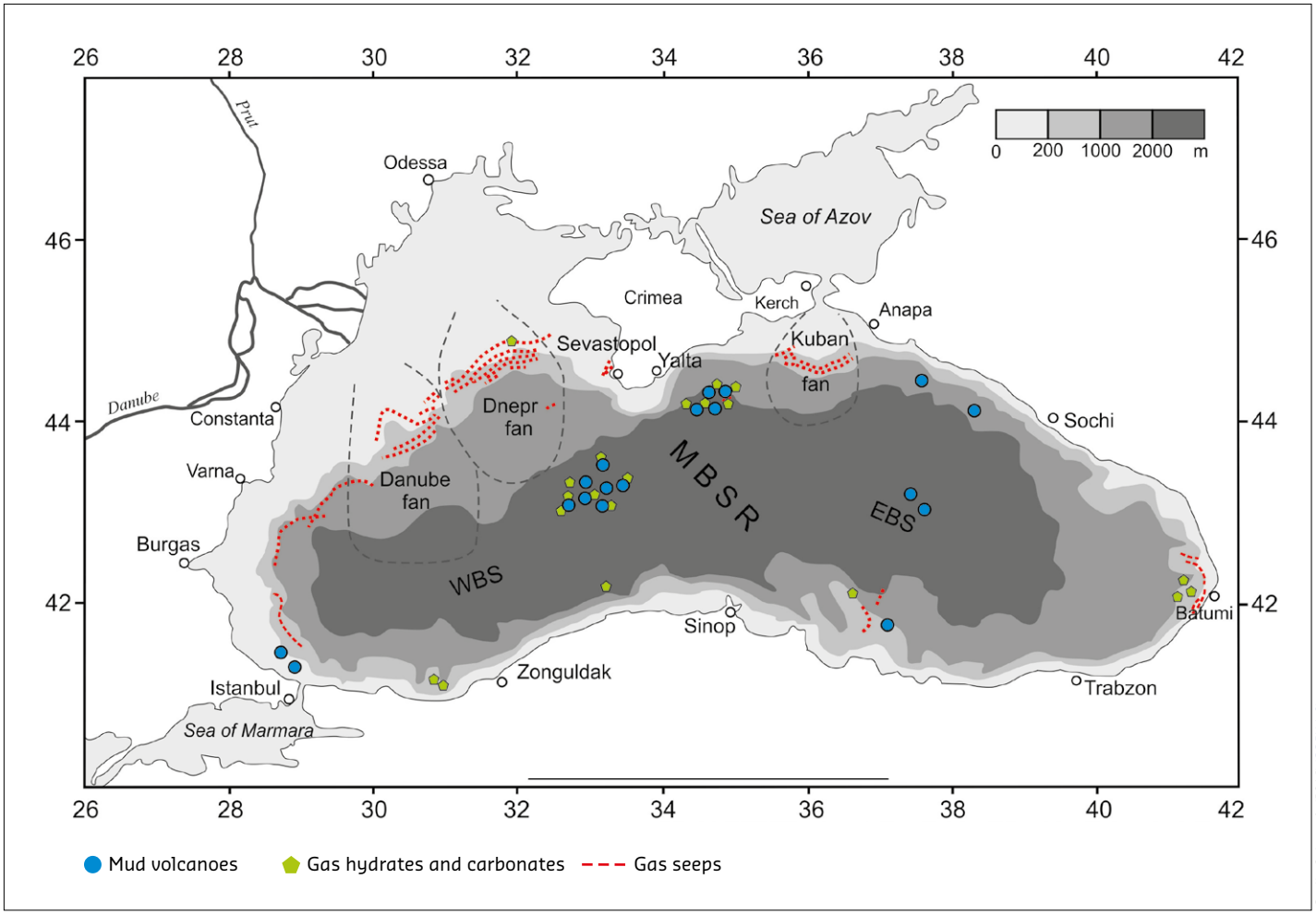

Figure 3.11. Distribution of gas seeps, mud volcanoes and gas hydrates in the Black Sea.
Abbreviations: **WBS:** West Black Sea basin, **EBS:** East Black Sea basin, **MBSR:** Mid Black Sea Ridge or Andrusov-Arkhangelsky ridge.

3.5 High-latitude and Epicontinental Seas

The North Atlantic and Arctic Ocean (Figure 3.12.) have been affected by some of the largest submarine slope failures documented anywhere on Earth. Gigantic landslides occur on steep continental slope while shallow water landslides are common in fjords. One of the most catastrophic submarine landslides, the Storegga slide, occurred off Norway's continental shelf approximately 8,200 years ago. It generated a tsunami that was recorded in the sedimentary record along the east coast of the United Kingdom and as far north as Iceland. Tsunami deposits from the Storrega slide have been found in coastal lakes up to 10-12 m above sea level in western Norway, 3-6 m in Scotland, and >20 m on the Shetland Islands (Bondevik *et al.,* 2005).

Other slides of similar size and run-up occurred off the coast of Norway and Svalbard. These slides depend on glacial processes: mainly rapid deposition of glaciogenic sediments in front of cross-shelf troughs, i.e. the valleys where the main ice streams flowed during glacial periods. While most of the slopes in front of cross-shelf troughs have already failed, some still exist in settings that may be unstable, such as the northern flank of the Storegga slide, that can fail in the future. Similar to earthquakes in the Mediterranean Sea and the Gulf of Cadiz, it is evident that these failures will occur in the future but, so far, with the available technology there is no way to predict them.

Sediment accumulation is driven by climate oscillations, the naturally reoccurring changes in climate. Glacial sediment accumulates during glacial periods of low sea level near the shelf edge and can later be mobilized or spilled over by a triggering mechanism during interglacial high sea level periods. This occurred for instance to glacial sediments making up the North Sea Fan as glaciogenic debris (Nygård *et al.,* 2007). On average, the Arctic warms much quicker than the global climate, therefore the European Arctic is a fast-evolving environment. Ice shields and glaciers retreat, and bottom water temperatures rise. This may affect submarine slope stability in two ways: 1) Warming will lead to a change of the gas hydrate stability zone and may destabilize the slopes both through the removal of cementation and through the build-up of overpressure; and 2) Ice shield retreat will accelerate surface uplift and may cause earthquakes that can trigger slope failures, a scenario that was proposed to be the cause of the Storegga slide (Berndt *et al.,* 2009).

Fjords host extensive geohazards (see Box 1) and are considered one of the major submarine landslide areas (Hampton *et al.,* 1996). Relatively small but frequent landslides occur on coasts where people and infrastructure are restricted to narrow areas close to the coastline. These events may cause significant damage and

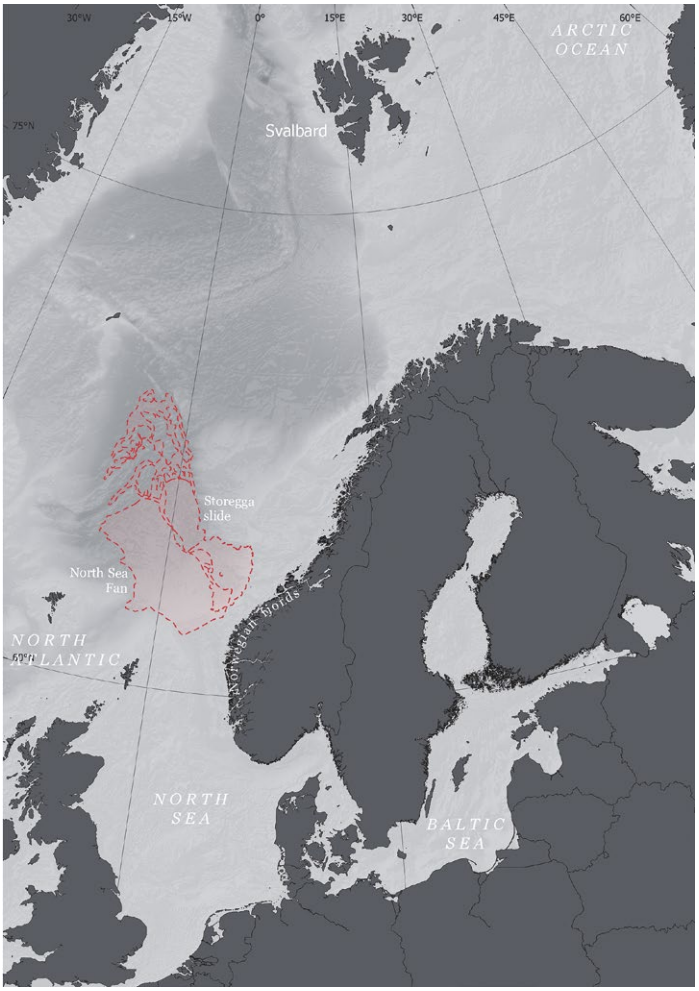

Credit: Britt Lonneville – VLIZ

Figure 3.12. Map of the European high-latitude and epicontinental seas indicating places highlighted in this document. Sources: GEBCO Compilation Group (2019) GEBCO 2019 Grid (doi:10.5285/836f016a-33be-6ddc-e053-6c86abc0788e). Contains data under Norwegian license for public data (NLOD) made available by the Geological Survey of Norway (NGU).

casualties, as happened with the Kitimat landslide (Prior *et al.,* 1982), the Balsfjord landslide (Rygg & Oset, 1996), and the Finneidfjord landslide (Figure 3.13., (Longva *et al.,* 2003)). Fjord landslides are caused by a variety of natural factors, but human activity, such as controlled use of explosives during construction works, may play an important role, accounting for or contributing to 60% of the fjord slides (L'Heureux *et al.,* 2013). Finally, rockfall on the steep fjord wall may cause tsunamis that may be funnelled and amplified by the complex fjord morphology (Blikra *et al.,* 2006).

The European epicontinental seas, the North and Baltic Seas are fairly tectonically inert, but do host some other geohazards. The North Sea in particularly poses hazards for gas and oil exploration, and increasingly, for carbon capture and storage operations and infrastructure. The primary hazard is from pockets of shallow gas or gas hydrates that can damage equipment and/or endanger oil rigs if not detected and subsequently intersected by drilling. Finally landslides have been recorded in both the Baltic and the North Sea and remain a geohazard risk.

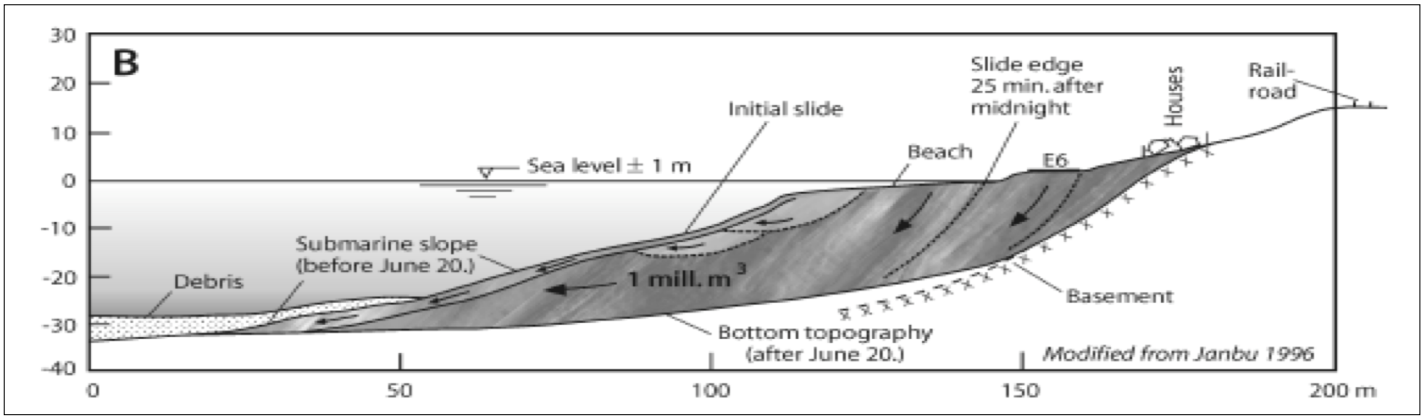

Credit: Modified from Janbu (1996)

Figure 3.13. The 1996 (1 million m³) Finneidfjord landslide dynamics are shown in the cross section. The slope failure reached the coast, destroying roads and several houses, and killing four people.

4

How do marine geohazards impact society and the Blue Economy?

Credit: Tomoki Sato via Wikimedia Commons

The European Seas have played a central role in European culture and trade since ancient times. Traditional maritime use focused on fisheries and transport, and later on tourism, hydrocarbon exploration and internet data transfer. Today the expansion of economic activities is driven by a combination of population growth, rising incomes, dwindling natural resources, responses to climate change and pioneering technologies. The 'Blue Economy' thus encompasses established Ocean-based industries as well as emerging and developing activities that are re-shaping and diversifying maritime industries (OECD, 2016). These activities include offshore renewable energy, communication, marine cruise tourism, offshore aquaculture, marine biotechnology and bioprospecting, seabed mining, aggregate extraction, Ocean monitoring, control and maritime surveillance. Further activities, for which established markets do not yet exist include carbon sequestration, coastal protection, waste disposal and conservation and restoration of biodiversity. In 2018, the EU Blue Economy directly employed close to 5 million people, and generated around €750 billion in turnover and €218 billion in gross value added (European Commission, 2020). In 2020, the COVID-19 pandemic caused a decline in Blue Economy activities, but the overall dynamic development of the sector prior to the pandemic indicates that we will see a swift recovery in the near future.

As the variety of Ocean uses is increasing and the investments in Ocean development and seafloor infrastructure are rising (Voyera & van Leeuwen, 2019; European Commission, 2020), the social and economic consequences of marine geohazards become more important (Figure 4.1.). The impacts of marine geohazards on society and the Blue Economy are as diverse as the hazards themselves. Some marine geohazards (e.g. fluid activity, migrating bedforms) will mostly affect the seafloor, while others have the potential to severely afflict coastal communities and/or generate reverberations on a transnational scale (e.g. high-magnitude earthquakes, tsunamis).

This chapter provides a perspective on societal impacts and evaluates how marine geohazards can jeopardize the different components of the Blue Economy by discussing case study examples that highlight the effects on different assets.

Credit: Sheila Heymans

Figure 4.1. Vineyards in the Azores islands are planted on rich volcanic soils and surrounded by 'currais' (corrals), geometric squares, rectangles, or semi-circles separated by walls of stacked basalt stones. This practice, protected by UNESCO World Heritage since 2004, demonstrate the cultural implications of living on a volcano.

4.1 Impact on coastal communities, livelihoods and loss of lives

The significant and increasing population along the European coast has led to increased exposure and vulnerability to marine hazards.

The most devastating hazards in terms of casualties and economic loss involve earthquakes and tsunamis. Earthquakes (or seismic shaking) severely affect building structures, local and regional infrastructure and supply chains. Earthquakes are not only a major hazard for communities situated in the vicinity or along active fault systems, but may also cause cascading effects, including landslides, tsunamis and liquefaction (a loss of shear strength of soil causing a sudden collapse of buildings).

Other than earthquakes, tsunamis have the potential to cause major damage and casualties at great distances from their origin and affect large sections of coastlines. Tsunamis are devastating for coastal communities and disrupt local or even global economies. They cause extraordinarily large numbers of casualties and distress the physical and mental health of the survivors (Dilek *et al.,* 2021; Tashiro *et al.,* 2021). Their destructive power is largely a result of inundation and the energy transported by a tsunami wave, which severely impact buildings and infrastructure that are further affected by floating debris. Additional damage occurs when the waters retreat and drain away from the coast causing erosion. Large tsunami flooding may also result in the salination of freshwater reservoirs, groundwater aquifers and lakes. Contamination of drinking water fosters the spread of infectious diseases.

As earthquakes and earthquake-generated tsunamis are the most destructive events for coastal communities and public health, we describe three past events that have particularly affected Europe.

4.1.1 The 1755 Lisbon earthquake and tsunami (Portugal, Gulf of Cadiz, Morocco)

The Lisbon earthquake occurred on the morning of Saturday 1 November 1755, at around 09:40 local time (Figure 4.2.). The earthquake caused most of the population to rush towards the docks for safety. Around 40 minutes later, the receding sea unveiled the seafloor and then a large tsunami inundated the harbour and the downtown area, moving at great speed along the Tagus river (Zitellini *et al.,* 1999; Viana-Baptista *et al.,* 2006). Intense fires in the aftermath of the tsunami lasted for five days and destroyed most of what was left of Lisbon (Baptista *et al.,* 1998). The earthquake, fires and tsunami combined almost totally destroyed Lisbon and caused enormous damage at several localities in the Gulf of Cadiz, including Cadiz, and along the Atlantic coast of Morocco, including Fez and Tanger (Figure 3.5.). Seismologists estimate that the earthquake had a magnitude of M_w 8.5–9.0, with its epicentre in the Atlantic Ocean about 200 km west-south-west of Cape St. Vincent (Figure 3.5.). It was the third known large-scale earthquake to hit the city (after 1321 and 1531). Estimates of the death toll are highly variable (because of a lack of census of the existing population) but in Lisbon alone more than 10,000 causalities have been hypothesized (Pereira, 2009). The total number of victims may have been as high as 45,000, making the 1755 Lisbon earthquake one of the deadliest earthquakes in European history. Samples of marine sediments recovered in the Horseshoe Abyssal Plain and other places around the north Atlantic coast reveal the traces of a sediment layer corresponding to the 1755 Lisbon earthquake and document the far-field effects of the disaster (Gràcia *et al.,* 2010).

Credit: "The Earthquake Engineering Online Archive" Jan Kozak Collection: KZ128 Wikimedia Commons.

Figure 4.2. Copper engraving of the 1755 Great Lisbon earthquake (and tsunami and fire), created in the same year as the event. If such an event would occur today it would have enormous consequences.

4.1.2 The 1908 Messina earthquake and tsunami (Sicily, Calabria)

The 1908 (M_w 7.1) Messina earthquake and tsunami had a much lower magnitude but were still destructive and deadly (Figure 4.3.). They caused extensive cascading effects, including coastal retreat, liquefaction, slope movement, ground settlement, and gas emission (Comerci *et al.,* 2015). Intensive ground shaking lasted for at least 30 seconds and affected a region of >4,000 km^2. Approximately ten minutes after the earthquake, tsunami waves hit the coast destroying the towns of Messina and Reggio Calabria and causing thousands of victims among the earthquake survivors (Pino *et al.,* 2009). The tsunami inundated both sides of the Messina Strait with run-up heights reaching 13 m. A comparable event today could equal or surpass the death toll of ~80,000 in 1908, especially if it occurred during the summer tourist season. The Messina event was one of the first earthquakes in Europe to occur in the instrumental period (Mercalli, 1909), and its epicentre was located in the Messina Strait between Sicily and Calabria, although its exact source remains debated (Meschis *et al.,* 2019; Barreca *et al.,* 2021). The scale of destruction from this event was tremendous. At least 91% of the buildings in the town of Messina were destroyed or heavily damaged and the town lost around half of its population. The earthquake occurred in the early morning, surprising most victims in their sleep. The town was crowded on this particular day with overnight visitors attending a performance of Guiseppe Verdi's opera Aida the previous evening (Mowbray, 1909), showing the impact of tourism even over a century ago. The shoreline experienced several centimetres of subsidence into the sea, affecting the commercial harbour. Fires and earthquake aftershocks continued to cause havoc. The historic town centre of Reggio Calabria was also almost completely levelled. Commercial, municipal, residential, military and public buildings were affected. Because civilian and military hospitals in both cities were affected, medical support for the survivors was disrupted until outside relief arrived. Communication was also interrupted due to damaged telegraph lines and railways.

Credit: Luca Comerio (1878-1940), Public domain, via Wikimedia Commons

Figure 4.3. Victims and destroyed buildings on the Messina seafront after the 1908 earthquake and tsunami.

4.1.3 The 1999 Eastern Marmara earthquake and tsunami (Turkey)

The North Anatolian Fault zone marks the transform plate boundary between the Eurasian and Anatolian-Aegean plates (Figure 4.4.). The fault experienced a remarkable series of earthquakes, with ruptures starting in 1939 on its eastern segment and progressively moving westwards towards the Sea of Marmara. The 1999 (M_w 7.6) Izmit earthquake in the eastern Sea of Marmara caused subsidence and coastal landslides along the southern coast, and a 2.5 m-high tsunami run-up along the shores (Altınok *et al.,* 2001). Earthquake shaking lasted for 37 seconds and severely damaged the town of Izmit. Ground ruptures were as wide as 5.7 m. The event resulted in more than 17,000 people dead, 24,000 injured, and more than US$10 billion of damage to the Turkish economy. The earthquake damaged 120,000 houses beyond repair and caused 20,000 buildings to collapse, making more than 250,000 people homeless after the earthquake. Damage to transportation infrastructure, including bridges and tunnels, was significant. Heavy environmental pollution occurred in the Izmit Gulf as a result of disruption to the sewerage lines, spillage from chemical and oil storage tanks and a refinery fire, which in turn led to anoxia and mass fish mortality (Balkıs, 2003; Giuliani *et al.,* 2017; Morkoc *et al.,* 2007). Attempts to extinguish the refinery fire were hampered by breakages in water pipelines, requiring the employment of aircraft to douse the flames with foam. Due to the breakdown of telephone communication and damage of roads, coupled with an initial underestimation of the earthquake's magnitude and associated destruction, rescue operations were delayed (Barka, 1999).

Today, the offshore portion of the North Anatolian Fault, which consists of several segments, is monitored by a seismological network, and by land- and submarine-based observations (Figure 4.4.). Recent observations indicate that the segment located 12 km south of Istanbul is currently not moving while the segment to the west appears to have a slow more or less continuous movement (e.g. Ergintav *et al.,* 2014; Lange *et al.,* 2019; Yamamoto *et al.,* 2019). The next earthquake is expected to occur close to Istanbul where a population of about 16 million people lives. Scenarios predict ~100,000 casualties and damage to property and industrial facilities in Istanbul as well as around the Sea of Marmara. This region accommodates ~30% of the Turkish population and ~60% of Turkish industry.

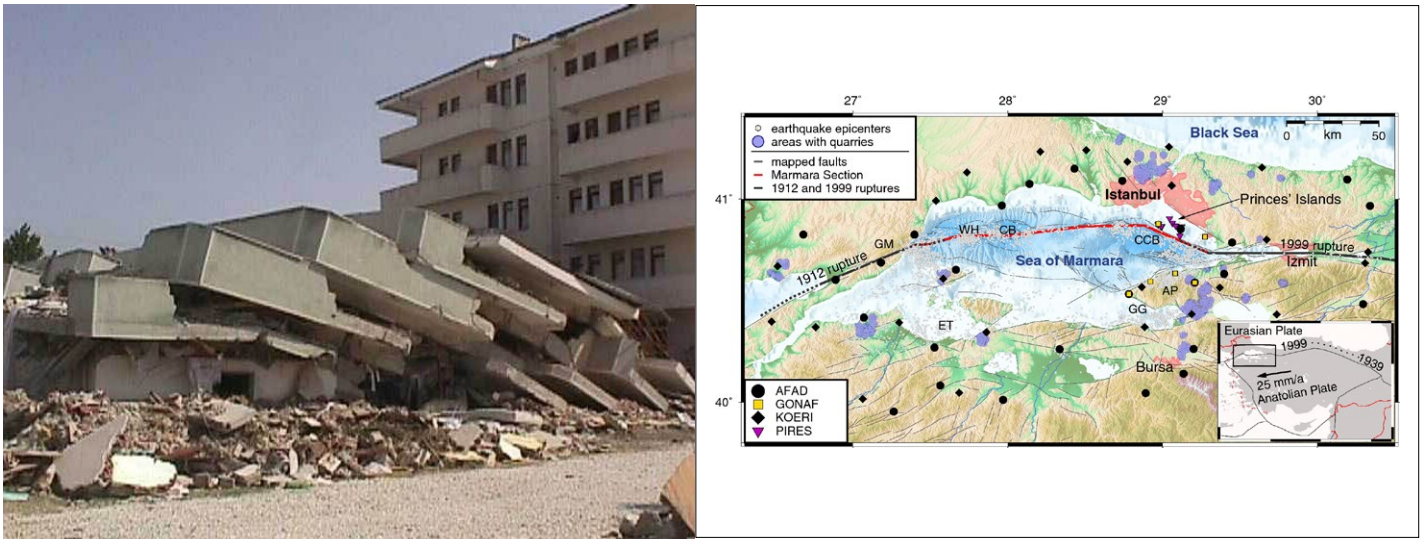

Credit: USGS Public domain, via Wikimedia Commons

Credit: Wollin *et al.* (2019) CC BY 4.0

Figure 4.4. **Left:** Collapsed buildings after the 1999 Izmit earthquake (17,000 causalities).

Right: The main faults in the Marmara Sea, part of the Northern Anatolian Fault system. The central segment, near Istanbul, is located between two segments that moved in 1912 and 1999. This seismic gap and the number of people living there implies that the seismic risk in the area is very high.

4.2 Impact on coastal infrastructure

Facilities of vital importance to socio-economic activities are often located near the shoreline and include port facilities for handling shipping, refineries, communication infrastructure, transportation facilities and power plants. Their coastal location is commonly associated with existing transportation and shipping infrastructures and, in the case of industrial plants, to their high demand for cooling water.

The orographic setting in several European regions, where steep mountain ranges arise very close to the coast, forces transportation to be confined to narrow coastal plains near or at the shoreline. Crucial infrastructure such as railways, major roads, and airports as well as industrial infrastructure are therefore often located a few hundred or even only a few tens of metres from the shore, and their failure would cause significant economic and social repercussions. This increases their vulnerability, because of the lack of a coastal buffer and because of the presence of coastal cliffs which can be subject to rockfalls. Moreover, where tectonic uplift occurs, the high sedimentation rate, the steepness of the continental slope (carved by submarine canyons whose heads often reach the coastline), and the high seismicity rate create a seafloor that is typically prone to geohazards.

Ports and harbours are intrinsically the most exposed to coastal geohazards. Earthquakes and submarine landslides have the potential to damage port structures, either directly through structural collapse, or indirectly via the tsunami that they can generate. Tsunami waves can result in strong currents in ports and harbours, that can damage and destroy structures even without

inundation (Admire *et al.,* 2014). Many harbours are located at or near canyon heads (Figure 4.5.), and thus in areas subject to landslides due to their intrinsic retrogressive (i.e. coastwards) evolution. The reason that harbours are located near canyon heads is that historically, small fishing wharves were constructed there because complex submarine canyon morphology and bathymetry dissipates storm waves because of refraction (Figure 4.5.). These small villages, as many along the coasts of the Mediterranean Sea, became towns with large harbours that now lie in a very hazardous setting.

Sometimes human activity may trigger submarine landslides in the vicinity of harbour structures. Harbour construction, maintenance or growth (e.g. widening) often require large engineering works that can overload the seafloor, causing instability. This was the cause of the Nice and Gioia Tauro events (Colantoni *et al.,* 1992; Ioualalen *et al.,* 2010) as well as for the majority of coastal landslides in Norway (L'Heureux *et al.,* 2010). One example of a region highly exposed to geohazards is the densely populated Ligurian continental margin off Nice (Western Mediterranean), where a submarine landslide in 1979 created a tsunami that caused several deaths and significant material damage. Accurate geohazard assessment of this area is particularly important because of its vicinity to Nice Airport and the connection to the steep slopes of the canyon creating a significant tsunami hazard to the area. Nice Airport is the third largest in France, and the area is one of the most significant economic centres in France, with over half a million permanent residents and millions of tourists annually. Since 2015, a subsea cabled observatory (EMSO Nice) has been collecting data through an array of *in situ* instruments to study these geohazards (Figure 4.6.).

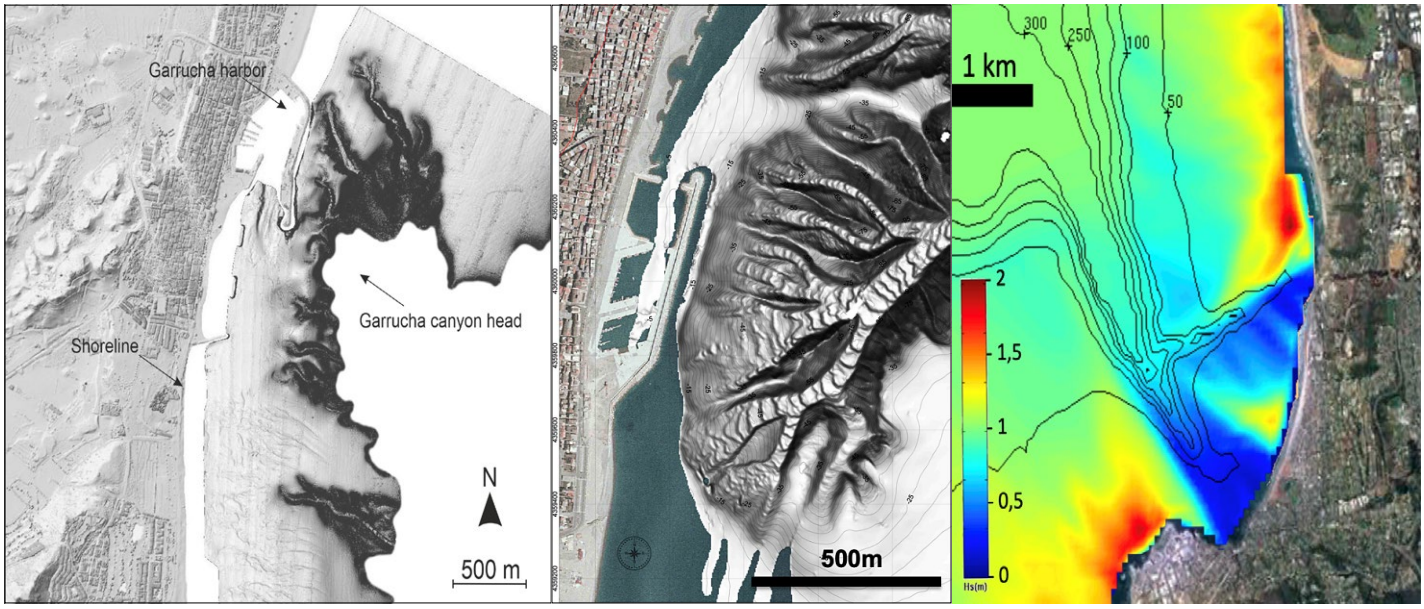

Credit Left: D. Casas ; Credit Middle: F. L. Chiocci

Credit: F. L. Chiocci, based on data from Kaihatu *et al.,* (2002). Map Data © 2011 Google

Figure 4.5. Note how the two following examples of harbours are located exactly at the canyon heads.

Left: Bathymetry map of Garrucha canyon (Almeria, Spain). **Middle:** Cirò Marina Canyon (Calabria, Italy).

Right: Modelled wave height at La Jolla canyon (California, USA). Complex bathymetry lowers the wave energy on the coast facing the canyon head. This may explain the coincidence between canyon heads and harbours and ports.

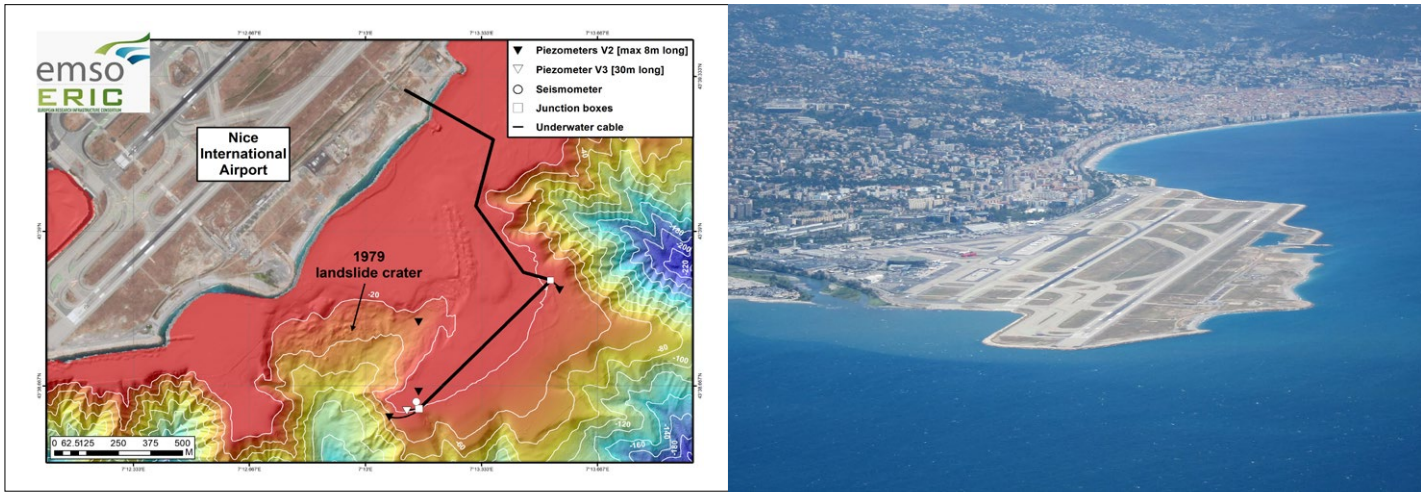

Credit: EMSO-ERIC

Credit: Olivier Cleynen, via Wikimedia Commons (CC BY 4.0)

Figure 4.6. **Left:** Bathymetric map showing the 1979 landslide scar located between Nice Airport and the head of the canyon. Symbols indicate an array of in situ instruments connected to a seafloor cable network (the EMSO-Ligure Nice observatory), as shown in preliminary graphs in Bompais *et al.,* (2019).

Right: Aerial view of Nice Airport with the urbanized coastline of the Baie des Anges in the background.

The increased use of the coast for urban and industrial settlements will occur both by expanding existing infrastructures, by establishing new infrastructures and by reclamation of marine areas. Airports, container terminals, and even amusement parks (e.g. Hong Kong Disneyland) have been built on land reclaimed from marine areas. Such coastal engineering works require deep knowledge of possible geohazards. In Greece, the new Patras harbour was built in an area affected by active fluid seepage from the seafloor, which has already been activated twice by earthquakes. (Hasiotis *et al.,* 1996; Christodoulou *et al.,* 2003; Christodoulou, 2010).

Nuclear power plants are one of the most sensitive infrastructures to tsunami hazards, as the 2011 Fukushima Daiichi incident in Japan demonstrated. On the Mediterranean coast of Spain, the Vandellòs nuclear power plant (Figure 4.7.) is located in the town of Vandellòs i Hospitalet de l'Infant (Tarragona), and is constructed on a 20 m high platform to protect against rising sea level. However, the Vandellòs nuclear power plant is situated in an area where active fault systems onshore and offshore have been identified as a possible geohazard, with the potential to trigger a tsunami that would affect the plant and the surrounding (densely populated) coast (Perea *et al.,* 2012). Similarly, Turkey is currently constructing a nuclear power plant in Akkuyu on the Mediterranean coast, which like numerous other locations around Europe may be prone to marine geohazards.

Figure 4.7. The Vandellós nuclear plant located on the shores of the Mediterranean Sea in Spain.

4.3 Impact on offshore infrastructures

Natural hazards are a major threat to all offshore industrial activities, i.e. oil and gas facilities (rigs and pipelines), communication cables, wind farms, aquaculture and the many other activities that will be developed in the future (renewable energy from waves and tides, deep sea mining, etc.).

Landslides, shallow gas and gravity flows may cause hydrocarbon infrastructures to fail and that may lead to the release of hazardous materials (DNV, 2002). Earthquakes and volcanic activity pose risks to seabed structures. Such hazards triggered five incidents at fixed seafloor structures between 1970 and 2013[7]: Three in the North Sea and two in the Caspian/Black Sea. Two of these events were related to submarine gas eruptions.

There are approximately 600 oil and gas rigs operating in the North Sea. The North Sea is not known for its earthquakes and volcanoes, but nevertheless these have accounted for some damage and accidents (Necci *et al.,* 2019). In 2016, a potentially catastrophic incident in the North Sea Troll field was reported when large quantities of fluid and gas were released from the reservoir below the Songa Endurance drill rig. Drilling personnel had to activate the blowout preventer and non-essential personnel had to be evacuated from the platform[8]. The incident could have resulted in the loss of lives and the significant release of hydrocarbons, as happened in 2010 in the Gulf of Mexico with the Deep Water Horizon incident (Bly, 2011).

The global network of submarine communication cables plays an increasingly crucial role in our modern society. More than 95% of international communication traffic is routed via submarine fibre-

[7] https://www.dnv.com/services/world-offshore-accident-database-woad-1747?&utm_campaign=plant_phast_safeti&utm_source=google&utm_medium=cpc&gclid=CjwKCAjw_o-HBhAsEiwANqYhp3umslU4QZne3uM70__U1lMt81VEzHD8Uh3bmrGlh0wZxnP2Z2Sg7xoCTdUQAvD_BwE&gclsrc=aw.ds

[8] https://www.equinor.com/en/news/well-incident-songa-endurance.html

optic cables (Carter *et al.,* 2009). Seafloor telecommunication cables are increasing in number due to the exponential need for internet data transfer (Figure 4.8.). These cables lie on the seafloor or are buried in the shallow subsurface and could be affected by earthquakes, volcanic eruptions, submarine landslides and runout sediment flows. Although less than 10% of cable faults are caused by natural hazards, this number rises to about 30% for cables in water deeper than 1,500 m and away from zones of human offshore activities (Carter *et al.,* 2009).

Soon after the first deployment of submarine cables in the second half of the 19th century, geohazards started causing cable damage. The first significant cable break was report in 1883 after the tsunami triggered by the Krakatoa volcanic eruption (Winchester, 2003). The eruptions of Mount Pelée in Martinique and La Soufrière in St Vincent, both on 7 May 1902 were accompanied by the loss of submarine cable contact (Carter *et al.,* 2009). The occurrence of the 1902 and 1907 submarine volcanic eruptions in the Azores Islands was inferred from the observation of the recovered cables showing melting of their insulation material (1902), and from cable burial due to volcanic products deposition (1907), and evidence of cable corrosion attributed to hydrothermal vents was reported as the origin of cable failures (Chaves, 1904, 1915).

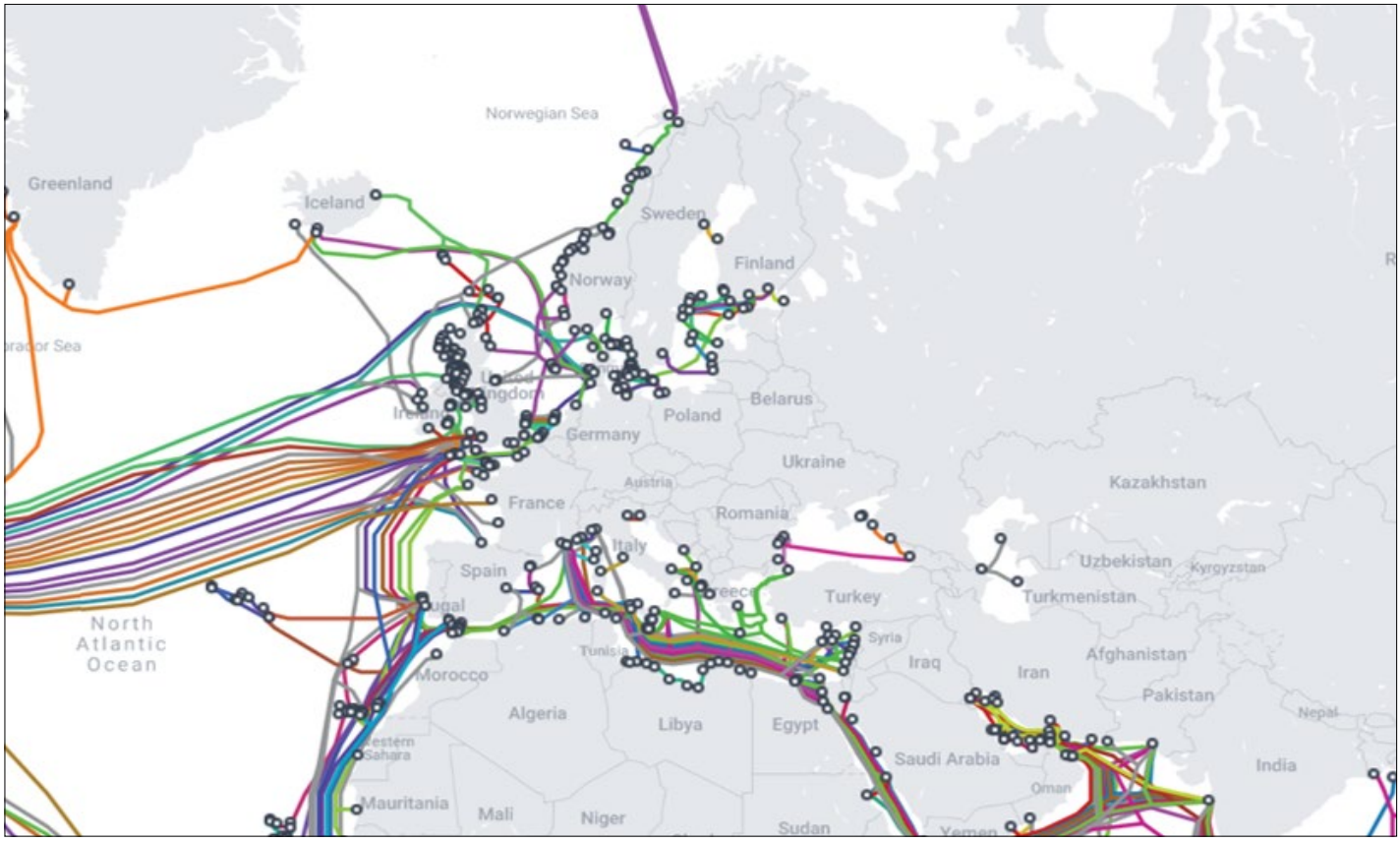

Figure 4.8. Sketch of submarine cables in European seas.

The 1929 Grand Banks (Canada) earthquake and associated landslide is the first documented evidence of turbidity currents breaking telegraph cables (Piper *et al.,* 1988; Fine *et al.,* 2005). The Mediterranean Sea has also experienced several cable breaks caused by turbidity currents since the Messina 1908 earthquake (Ryan & Heezen, 1965). Both the human-induced 1977 Gioia Tauro port and the 1979 Nice airport submarine landslides broke submarine cables crossing the canyons where the landslides occurred (Mulder *et al.,* 1997). The Boumèrdes 2003 earthquake (see figure 2.12) caused 29 submarine cable breaks at the foot of the Algerian continental slope over a distance of ~150 km (Cattaneo *et al.,* 2012). Cables breaks disrupt internet communications, electronic banking and commerce. By using a global database of subsea fibre-optic cables, Pope *et al.,* (2017) reported about 8 cases of cable breaks following earthquakes in the Mediterranean Sea. These results show the need to develop geohazard reconnaissance, prevention programs and mitigation plans to reduce the vulnerability of strategic and costly telecommunication infrastructures.

Similar to coastal infrastructure, offshore industrial activity can generate hazards such as seismicity associated with energy production, which caused the interruption of the Castor project (Section 2.7). Induced seismicity poses a hazard to the exposed population and structures (Cesca *et al.,* 2021). Induced seismicity may also be caused by injecting carbon dioxide into exhausted reservoirs, where the aim is to sequester carbon dioxide captured from fossil fuel production or other sources into the Earth's crust as a tool for climate change mitigation.

Pockmark fields and other fluid-escape geological features are an additional cause for concern for industry, as the geotechnical and topographic properties of the subsurface hinder rigs or pipeline construction, limiting the space that can be used for such constructions (Hovland *et al.,* 2002).

4.4 Impact on tourism and fisheries

The impact of marine geohazards adversely affect local economies of coastal areas, as events such as the eruption of a submarine volcano or an earthquake make those areas less attractive as they may be deemed as not safe, even if no lives are lost. Related navigation hazards, pollution or damage in ports and harbours as the consequence of marine geohazards could also affect fisheries activities and the local economy. The series of events that occurred near El Hierro in 2011 and afterwards show the impact that marine geohazards have on local communities, tourism and fisheries.

The Canary Islands are a highly appreciated tourist destination, but they are also a volcanically active archipelago located in the north-eastern Atlantic margin. El Hierro is the youngest of these islands and the latest to have recorded a volcanic eruption. On 10 October 2011, after more than 10,000 earthquakes recorded in a three-month period, a volcanic tremor marked the beginning of a submarine eruption (Santana-Casiano *et al.,* 2017). The volcano, later named Tagoro, is located 2 km south of El Hierro Island (Figure 4.9.), in the margin of the 'Mar de las Calmas' marine reserve, one of the richest biodiversity areas in the region. On this island of roughly 10,000 habitants, around 500 people had to be evacuated from their homes, and the main traffic tunnel of the island was closed as a precaution. In the end, the eruption did not cause any personal or material damage, but the impact on the economy was severe. The eruption directly affected three of the main economic activities on the island: tourism, artisanal fishing, and diving. Despite the fact that the eruption was proven not to be dangerous to the population, potential visitors still perceived it as a threat, even after 2011, severely harming the tourism sector. The population was already affected by the 2008 global financial crisis, and the economic situation on the island was extreme. The economic losses due to the 2011 volcanic crisis were estimated to be as high as €20 million, while the financial aid provided by the Spanish government was only €2–5 million.

The eruptions came to an end in March 2012 (Jurado *et al.,* 2020). The local marine biota quickly recovered, and the fully restored ecosystem is now an international attraction for diving and a constant source of fish. In addition, the volcano has evolved into a hydrothermal system that still remains active, and has become a scientific reference point for shallow volcanic and hydrothermal systems. The volcanic event was also a learning experience for the development of specific and advanced protocols for the protection of the population in case of similar events in the region. Similar events occurred in Europe in Serreta (Azores Islands) in 1999-2000 and in Pantelleria (Sicily Channel) in 1891.

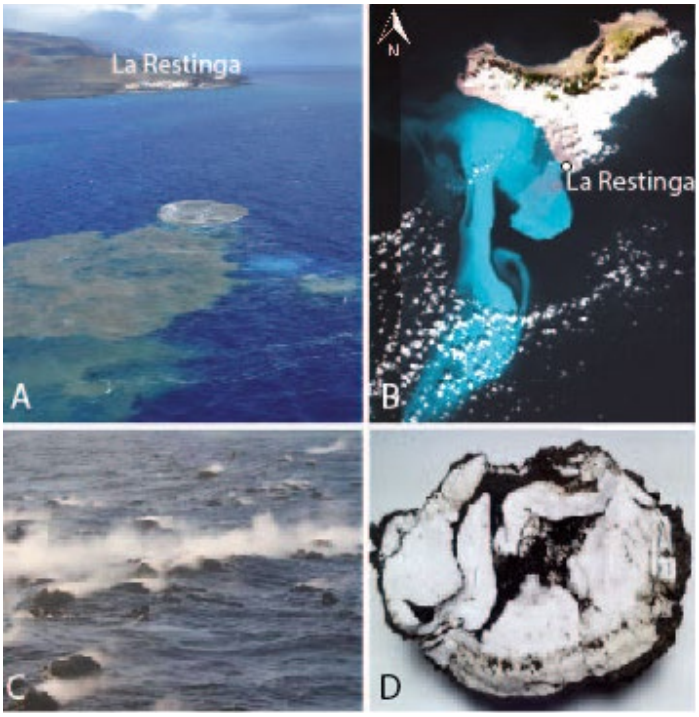

Credit: J. C. Carracedo

Figure 4.9. The eruption of El Hierro. **A.** Aerial photo of the plume of dissolved gases and suspended matter. **B.** Gas plumes on the ocean surface. **C.** Degassing and rock fragments that caused large bubbles up to 15 m high. **D.** Dissection of a rock fragment. For further information see Carracedo *et al.,* (2012).

4.5 Perception and consideration of marine geohazards by society, industry and public authorities

The sea is often considered a tranquil and contained water mass and for the general public it is difficult to perceive and evaluate marine geohazards (Cerase et al., 2019), which virtually come 'out of the blue'. This misperception can cause people to flock to the beach to observe a sea-level retreat even though this is a tell-tale sign of, for instance, a landslide-generated tsunami, or to wander curiously towards the newly emerged seafloor rather than to run for their lives away from the coast and the incoming tsunami waves (Guastello *et al.,* 2008).

In contrast, understanding of marine geohazard risks within offshore engineering is very high. In fact, industries (including those linked to rigs, wind farms, cables and pipelines) are well aware of marine geohazards and they conduct marine geological surveys that are always site-specific, i.e. performed in the vicinity of the seafloor location where the infrastructure will be placed. In comparison, public authorities responsible for the management and development of coastal communities and infrastructures are typically more aware of land-based natural hazards than of potential offshore threats, until they occur. This is because the technologies needed to highlight marine geohazard features are relatively new and there was limited use of the seafloor even until a decade ago. There is also a lack of specific legislation concerning marine geohazards (see Box 4), and marine geohazards are not considered in for instance Integrated Coastal Zone Management

or in Maritime Spatial Planning. Although Maritime Spatial Planning is conducted based on a broad range of integrated expertise, marine geohazards are often not included. The possibility of catastrophic events, including small-scale events related to extensive risk (see Box 1) such as submarine landslides or a collapse at the head of a canyon, should be included in these plans. These hazards should not only be included because of their potential to cause tsunamis but also because they should guide the placement of structures, the granting of permits, the definition of scenarios, and the setting-up of procedures to manage specific emergencies resulting from marine geohazards. At present, the Maritime Spatial Planning Directive completely lacks this aspect, and it would be beneficial to mitigate the ecological and socio-economic effects of marine geohazards in Europe more explicitly.

BOX 4: A MAGIC FAILURE, WHEN KNOWLEDGE IS NOT ENOUGH

Following the 2002 tsunami generated by a submarine landslide at Stromboli in Italy, the Civil Protection Department funded a €5.25 million project to identify and map marine geohazards. The project, named MaGIC (Marine Geohazards along the Italian Coasts), involved the whole Italian Marine Geology community including three institutes of the National Research Council (CNR), seven universities, and the Institute of Experimental Geophysics and Oceanography (OGS). The study produced a detailed, coordinated, standardized map of the geohazard features present on the Italian Continental Margin (Chiocci & Ridente, 2011). The project delivered 72 maps at 1:50,000 scale (see Figure 4.10.) and detailed publicly-available monographs[9]. The Civil Protection Department transferred this knowledge to the local authorities, however, this knowledge is likely to remain operationally unused, as there is currently no framework to transform the hazard information into mandatory legislation that imposes constraints or emergency plans.

For onshore volcanic hazards, alert levels and emergency plans exist; legislation constrains specific construction depending on local onshore seismic hazards; detailed mapping and land-use of potentially flooded river valleys is mandatory. By contrast, marine geohazards are not considered in legislation.

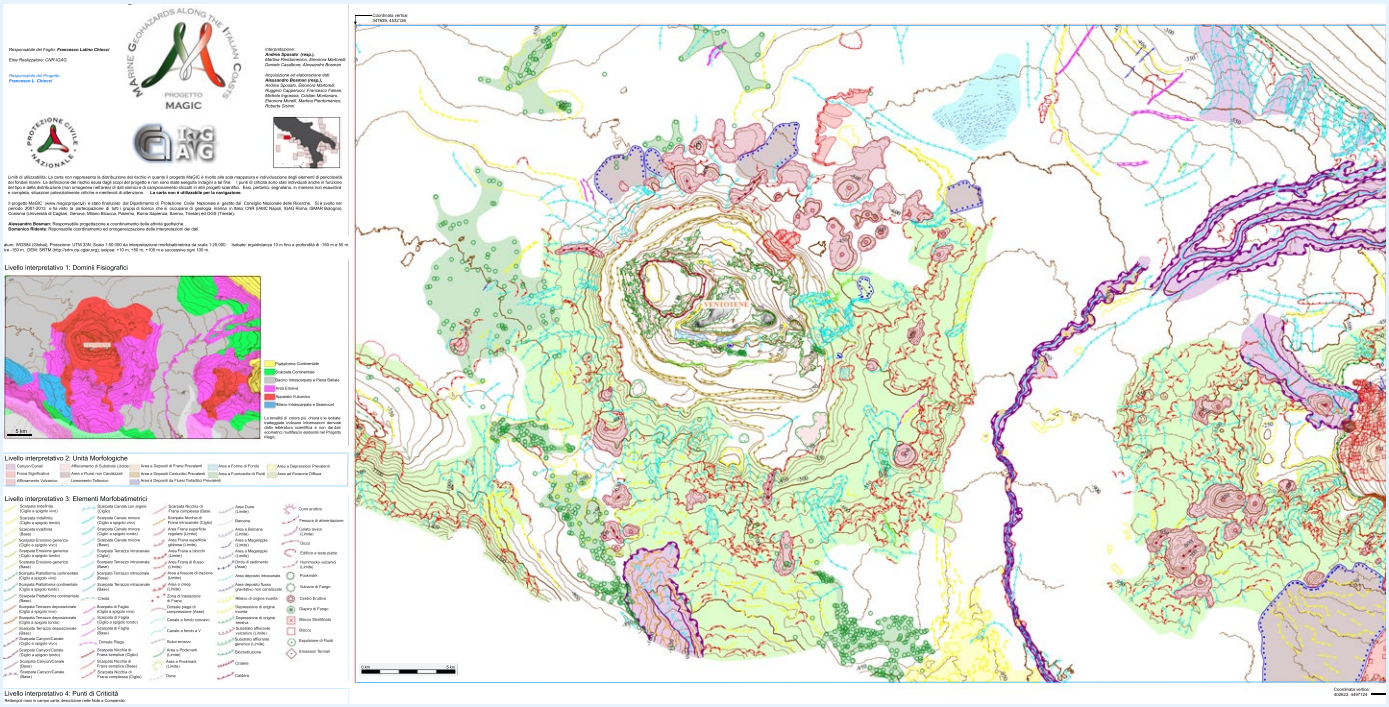

Figure 4.10. One of the 72 sheets at 1:50,000 scale produced by the MaGIC project, which mapped geohazard features in Italy: violet = canyon, green fluid = escape, red = landslide, reddish brown = volcanic vent. All sheets are available at https://github.com/pcm-dpc/Magic.

[9] https://github.com/pcm-dpc/Magic

5

How can science transform hazard assessment in Europe?

Credit: Felix Gross, GEOMAR (CC BY 4.0)

Scientific research on marine geohazards is crucial to understanding the characteristics, magnitude and recurrence intervals of events (i.e. how often do they occur at the same location). This is the basis and prerequisite for a thorough assessment of the related risks (Ercilla *et al.*, 2021). For instance, the magnitude of an earthquake that a fault may generate depends on its geometric characteristics and relationship with deep-rooted active geological structures; the tsunamigenic potential of a volcano depends on the explosivity of its eruption(s) in the past and stability of its flanks. The scale of the geohazard is very different if an area is subject to a landslide every year, once every ten years, once a century, or once a millennium. Scientific studies on marine geohazards therefore focus on: 1) identifying past geohazard events and evaluating their frequency, as well as 2) monitoring current active processes that may evolve into a marine geohazard. Both approaches are discussed in the following sections.

5.1 Characterizing past geohazard events and assessing their frequency

Forensic analysis of past events to compile catalogues of their occurrence is essential to develop and validate future scenarios (including cascading phenomena) as well as to assess their possible occurrence in a probabilistic way. Features and traces of marine geohazards on the seafloor are obviously difficult to access and therefore their detection is strongly dependent on the technological advancements that allow the imaging of the seafloor and subsurface structures. For instance, the development of multibeam systems a few decades ago (Figure 5.1.) have allowed allowed us to discover the widespread presence of geohazard features on continental margins. Similarly, in active geological areas such the Mediterranean Sea and the Gulf of Mexico, mass wasting deposits were found to cover 18% and 27% of the seafloor respectively (McAdoo *et al.*, 2000; Urgeles *et al.*, 2013). However, due to the scarcity of studies, only a tiny fraction of marine geohazard seafloor features are reported in the scientific literature. Depending on the source of data, the density of geohazard features varies widely. Casas *et al.*, (2016) defined some >400 submarine landslides in the Gioia Basin (Italy), built on full-coverage seafloor mapping, accounting for one scar per 8 km^2. In this studied area, where a census was done based on published data only, a density of one landslide scar per 4,000 km^2 for the Mediterranean Sea was estimated (i.e. 3.5 orders of magnitude lower).

The main archives of marine geohazard events are the marine sedimentary successions, and historical and archaeological reports. The locations and recurrences of earthquakes and tsunamis are compiled in various catalogues for regions such as the Mediterranean, where long historical records are available (Guidoboni *et al.*, 1994; Ambraseys, 2002; Guidoboni *et al.*, 2005; Ambraseys & Synolakis, 2010). Although such records extend back two or three millennia, they are often too short to cover several event cycles. In addition, historical records include uncertainties about the location and magnitude of the events and may be scarce for certain regions.

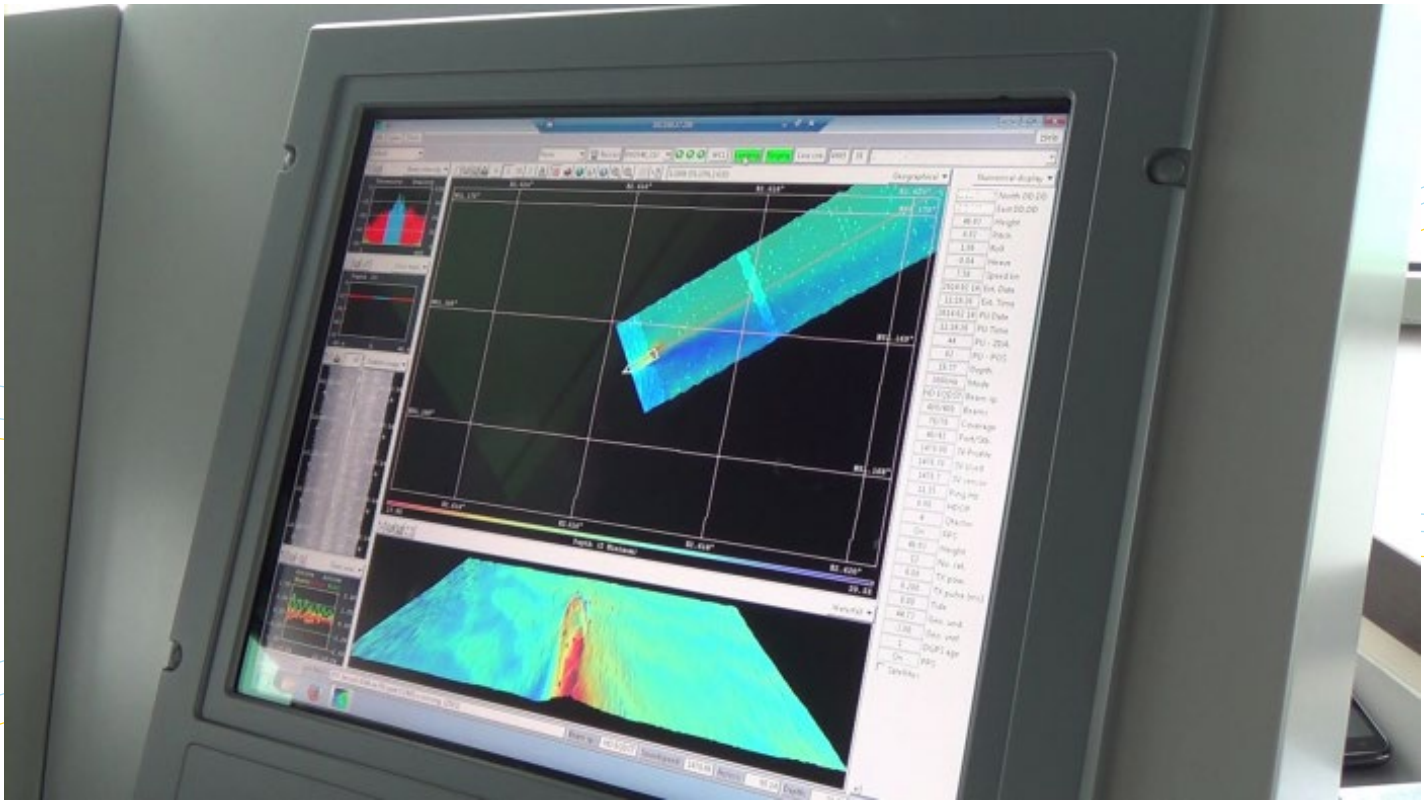

Credit: Maritieme Archeologie en Varend Erfgoed (Demerre, Ine) (CC BY-NC-SA 4.0)

Figure 5.1. A multibeam sonar display. Multibeam systems are used to map the seafloor. They are widely used to investigate geological features or locate wrecks or other objects.

In contrast, marine geological (sedimentary and morphological) records can contain information on the presence, mechanism and long-term frequency of geohazard events. However, detailed and complete maps of marine geohazards do not exist for most of the European seas. This is the reason why Figure 3.2. only shows the distribution of these hazards based on instrumental data or modelling (seismicity, earthquake-induced tsunami modelling). It was not possible to map all of the marine geohazards discussed in this document, due to the lack of complete data for all types of hazard considered in this document. Features such as active faults, landslides, fluid escape features, and even details on volcanic vents, are mainly collected only by the scientific research community, and are therefore rare, sparse and driven by scientific interest rather than by the need for a homogeneous mapping of marine geohazards in European seas (Chiocci *et al.,* 2011). However, some remarkable examples exist of censuses of geohazard features based on interpretation of full-coverage data, including the Spanish Quaternary Faults of Iberia (QAFI) for active faults[10], the Irish Infomar[11], the Norwegian Mareano[12] and the Italian MaGIC Project for marine geohazard features (Chiocci & Ridente, 2011). EMODnet[13] collects and homogenises published cartographic products for different geological features in European seas, including geohazard-bearing features. However, published data are not inherently homogeneous and often do not have full coverage, depending on the level of knowledge available in the different marine regions. Consequently, they commonly underestimate the true scale of marine geohazards in an area.

Geohazard events can be reconstructed from high-resolution seismic reflection profiling (with a resolution of few decimetres in the shallow subsurface using deep-tow instruments), high-resolution swath bathymetry (with a centimetre resolution using autonomous underwater vehicles) and by analysis of gravity/piston and drill-hole corers. The events can then be dated with high precision using radiocarbon, optically stimulated luminescence/thermoluminescence and tephrochronological techniques, and with lower precision by paleomagnetic, oxygen isotope and biostratigraphy methods.

Currently, submarine paleo-seismological investigations use high-resolution seismic data, coupled with sediment corers (Figure 5.2.) and boreholes data. The combination of this data helps to determine past fault activity and slip rates as well as long-term earthquake records in seismically active marine basins. These include convergent settings such as the Ionian Sea or plate margins around the Pacific (Pouderoux *et al.,* 2012; Polonia *et al.,* 2015; Ikehara *et al.,* 2016; Goldfinger *et al.,* 2017), as well as basins developed along transform plate boundaries such as the Sea of Marmara (Armijo *et al.,* 2005; Gasperini *et al.,* 2011; Çagatay *et al.,* 2012; Yakupoglu *et al.,* 2019). In these tectonically active basins, the long-term seismic activity has been reconstructed by analysing and dating seismically-triggered mass movement units (seismoturbidites) that show distinct sedimentary structures and textures. Past explosive volcanic activities are present as layers of volcanic ash (tephra) in marine and lake sedimentary successions. These layers range in thickness from a few mm or even dispersed volcanic glass fragments (crypto-tephra) to several metres, depending on the proximity to the volcanic centre and the wind direction at the time of the explosion. In volcanically active marine and oceanic basins, such as the Eastern Mediterranean, the tephra records are widely present in sediment corers and robust tephro-stratigraphy (tephrochronology technique) has been established (e.g. Keller *et al.,* 1978; Wulf *et al.,* 2008). In seismic sections, they are usually strongly reflective because of the marked contrast between their physical properties and the sediments that surround them. They are then matched with their volcanic source by geochemical analysis of their volcanic glass. On a larger scale, submarine volcanic vents and fissures, and their lava and volcaniclastic deposits can be mapped by high-resolution bathymetry and backscatter imagery (e.g. Nomikou *et al.,* 2013).

A specific approach is needed for submarine landslides. They are characterized by head-scars on the shelf edges and continental slopes, and their deposits are commonly termed mass transport deposits (MTD). MTDs constitute the past sedimentary record of submarine landslides, and can be imaged by seismic methods where they are characterized by transparent or chaotic inner seismic facies (Figure 5.3. and Grall *et al.,* (2014)).

[10] http://info.igme.es/qafi/
[11] https://www.infomar.ie
[12] https://www.mareano.no
[13] https://emodnet.ec.europa.eu

Credit: VLIZ (Decomble)

Figure 5.2. A sediment corer being shown at the cold storage repository at the Marine Station Ostend (MSO), managed by the Flanders Marine Institute.

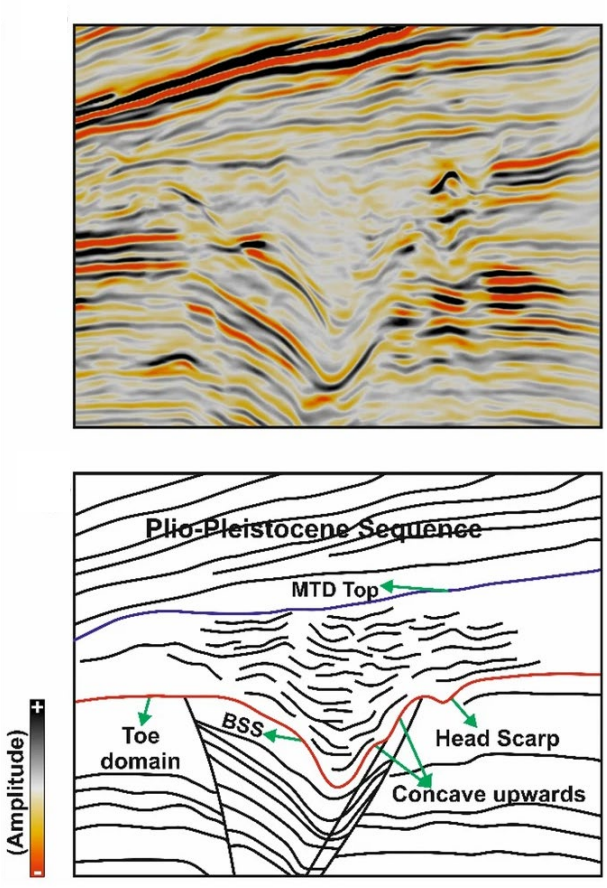

Credit: Kumar & Sain (2020) (CC BY 4.0)

Figure 5.3. A seismic section and its interpretation, showing a unit of mass-transport deposits offshore New Zealand. The mass wasting event is characterized by deformed sediment units and internally chaotic reflections, obtained by seismic reflection data.

When exposed on the seafloor, MTDs are very well imaged by high-resolution bathymetry, which can define their character and distribution in great detail. Seafloor coring/drilling (and possibly *in situ* measurements of geotechnical properties) can then be used to characterize the sediment involved and define the factors they favour (presence of weak layers, i.e. with poor geotechnical properties, gas-hydrate dissociation, pore overpressure).

Different from faults that tend to always move along the same fault plane, landslides occur in the same area but not in exactly the same location. Therefore, for the definition of recurrence times, the detailed spatial mapping of features indicating instability has to be used as a proxy to obtain the temporal frequency of these instability events that formed them. This approach is based on the assumption that sedimentation tends to smooth through time and erase features that were produced by the instability events. Exceptions may exist due to low sedimentation rate or exhumation of these features (Minisini *et al.,* 2006), but in general it is possible to assume that morphologies at the seafloor are rather recent events and therefore their number is proportional to their recurrence time in the area.

Considering the fact that landslides can also generate tsunami waves, even a small event such as a sudden failure occurring under specific conditions, e.g. in shallow water, in a densely populated areas or along coasts with dense infrastructure, may generate very high risk, as described in Box 2. Hence, there is an urgent need for new observation and monitoring techniques to identify and quantify soft sediment deformation and mass wasting (both as precursory indicators prior to the event, and as manifestations of previous events). These will be addressed in the next section.

5.2 Monitoring active processes and understanding their dynamics and mechanisms

The advance from studying and quantifying past events to monitoring active and ongoing processes transformed our understanding of geohazards. Combining the available technologies with a number of emerging strategies on how to go beyond the state-of-the-art in the near future, we summarize the main techniques, their challenges, and their potential, before trying to identify precursors to geohazards. The following sub-sections provide a summary of systems for hazard and process monitoring, and present advanced and emerging technology that will allow a multi-hazard approach for past and current events, especially when employing a combination of methods.

Marine geohazards monitoring and observation techniques require dedicated infrastructure and sensors that are able to withstand the challenging environmental conditions in the deep-sea. These include autonomous equipment, seafloor stations, networks or arrays of sensors, and sub-seafloor systems. All these sensors share the challenges of high pressure in deep water, limited energy supply and the need for precise navigation on the seafloor.

5.2.1 Repeated bathymetry surveys

Multibeam echo-sounder technology and the accuracy of positioning systems are constantly evolving and the use of autonomous and remotely operated systems for deep water investigations are growing. All these efforts allow the detection of rapid seafloor morphological changes with an unprecedented degree of resolution at any water depth. Seafloor changes are estimated by computing the difference between two co-registered digital elevation models generated from repeated multibeam echo-sounder surveys. The resulting 'difference map' quantifies the changes in elevation. The volumes associated with surface changes are obtained by integrating the difference in depth over the areas of interest. This approach has been used to detect and monitor co-seismic seafloor displacements (Fujiwara *et al.,* 2017), volcanic eruptions (Caress *et al.,* 2012; Bosman *et al.,* 2014; Ercilla *et al.,* 2021), landslides and their morphological evolution (Chiocci *et al.,* 2008; Biscara *et al.,* 2012; Casalbore *et al.,* 2012; Kelner *et al.,* 2016), submarine deltas (Hill *et al.,* 2008; Clare *et al.,* 2017), canyons (Guiastrennec-Faugas *et al.,* 2020) and channels in fjords (Conway *et al.,* 2012; Normandeau *et al.,* 2014; Gales *et al.,* 2019). These data sets include repeated surveys performed over months to decades and are used to characterize specific phenomena (Figure 5.4.). By contrast, recently the most detailed time-lapse mapping of any marine system was realized for the Squamish pro-delta in British Columbia (Stacey *et al.,* 2019). It consists of almost 100 daily bathymetric surveys performed over a period of 4 months, which detected more than 100 turbidity currents and assessed their control on the morphological evolution of the channels (Vendettuoli *et al.,* 2019 and references therein).

The integration of repeated multibeam surveys with hydroacoustic monitoring has resulted in a powerful tool for the detection of active submarine volcanoes (especially given that volcanic eruptions only occasionally reach the sea surface) and to identify submarine eruptive processes (Somoza *et al.,* 2017; Tepp *et al.,* 2019).

5.2.2 Monitoring seafloor deformation

Seafloor geodesy

The rise of satellite-based monitoring and observation techniques is arguably one of the greatest breakthroughs in geosciences since the concept of plate tectonics. Space-based methods are routinely used in onshore hazard research to monitor active movement of tectonic plates, the movement of fault zones and plate boundaries as well as volcanic and fluid activity (e.g. Owen *et al.,* 2000; Reilinger *et al.,* 2006; Tong *et al.,* 2010; Walter *et al.,* 2019). However, this is not possible offshore, as electromagnetic waves used in satellite-based approaches cannot penetrate the water column.

Seafloor geodetic techniques (without connections to satellites) detect seafloor deformation and the corresponding small changes in length and volume associated by tectonic stresses with providing relative or absolute positioning information. This information is provided at the same high-resolution level than satellite-based approached on land (Figure 5.5.). Seafloor geodesy uses acoustics

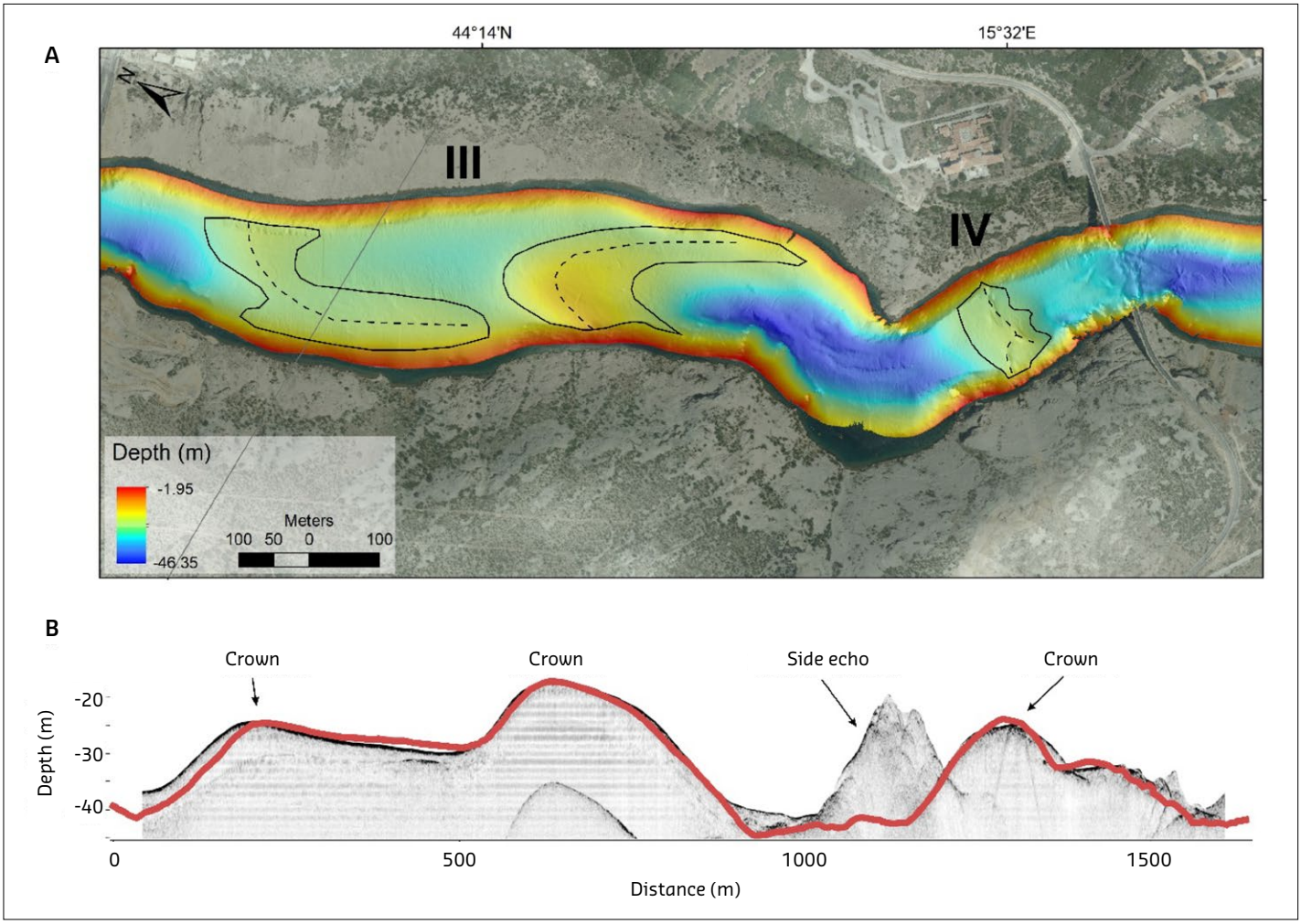

Figure 5.4. **(A)** Detailed multibeam echosounder bathymetry map of tufa barriers (III and IV) in the Zrmanja River estuary on the eastern Adriatic coast, Croatia, with the outlined barriers and their crests (dashed line).

(B) Sub-bottom profile of barriers III and IV that are overlain with the actual bathymetry profile over the central part of the canyon (red line).

to either detect relative seafloor deformation, or to transfer the seafloor position to the global reference frame (GPS-Acoustic or GPS-A) (Petersen *et al.,* 2019). This is achieved by deploying seafloor nodes which can work autonomously for up to 10 years. Measurements of millimetre-level displacement across tectonic lineaments reveal the movement of active tectonic faults. Seafloor geodesy is also used for high-precision monitoring of potentially unstable volcanic flanks or continental slopes, as depicted in Figure 5.5. There, downslope movement increased from 2 cm/yr at the shore to 4 cm/yr offshore, indicating that flank deformation is intensifying offshore. Shoreline-crossing observations will yield the full spectrum of deformation, which may differ in the offshore domain compared to measurements on land.

Seafloor geodetic studies are still in their infancy and the integration of autonomous surface vehicles such as wave gliders to enable data transmission from the seafloor to the surface and then via satellite to land is crucial. Ocean-bottom pressure sensors should be linked to all acoustic geodesy installations. Installation of seafloor nodes, which can remain on the seafloor for decades offer the opportunity to re-visit these sites multiple times. Real-time or near-real time data transfer from seafloor geodesy networks is a prerequisite for early warning schemes in cabled or autonomous systems. In addition, standardized file and data formats will enhance data and knowledge transfer in the future in order to expand seafloor geodesy missions in Europe.

Fibre-optic technology

Fibre-optic technology is mostly used by telecommunications companies to transmit telephone signals, internet communication and television signals. It is also used for light guides, imaging tools, lasers, sonar, or hydrophones for detecting seismic waves (earthquakes). Recently, scientists have used fibre-optics with sensors in boreholes to monitor temperature, strain or seismology, to provide continuous temporal and spatial observations. Fibre-optic cables record seismic signals at a much higher density, comparable to placing a broadband seismometer every few metres. A recent application in marine geophysics supported by the Monterey Accelerated Research System (USA), recorded a minor earthquake and identified multiple submarine fault zones (Lindsey *et al.,* 2019). The observations lasted just a few days, but allowed for the mapping of an unknown fault system and the detection of several dynamic processes in the water column above.

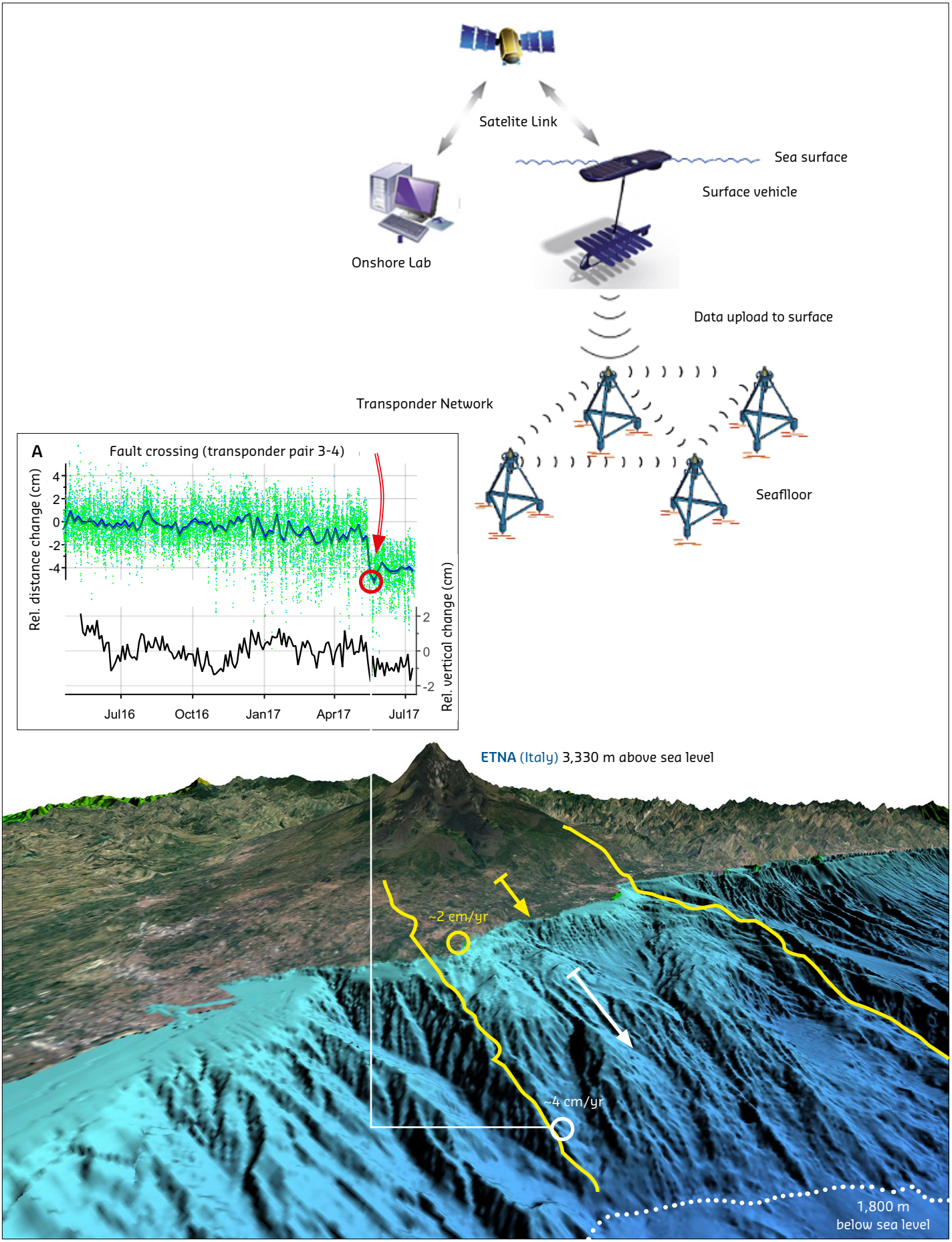

Figure 5.5. **Top:** Concept of a seafloor geodesy array with data upload via an autonomous surface vehicle (wave glider) and a satellite link.
Bottom: Detection of a 4 cm movement downslope on the flank of Mount Etna in Sicily, see red circle on the graph.

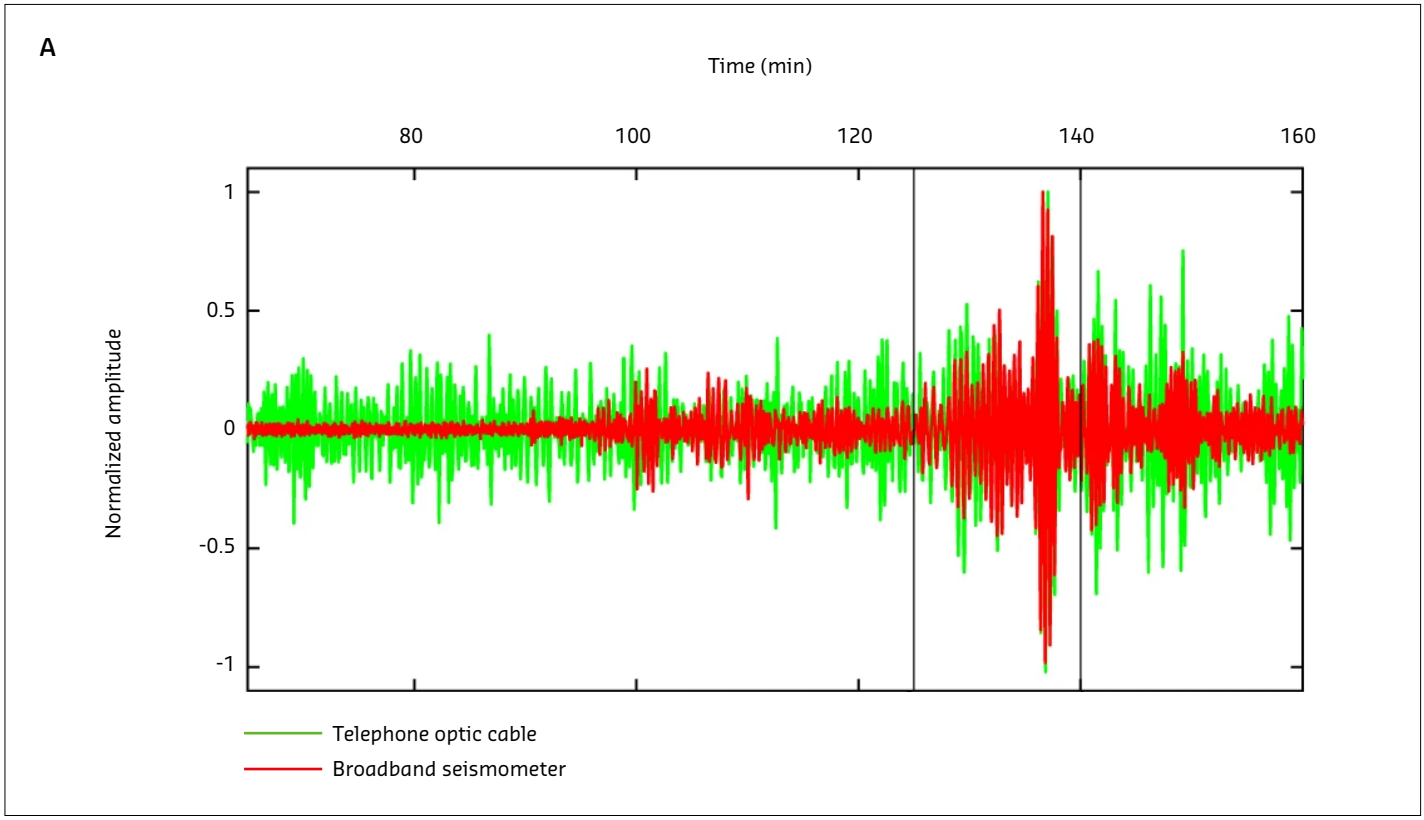

Figure 5.6. Record of an earthquake on a fibre-optic cable (green) and a broadband seismometer (red). The comparison shows the good phase correspondence between the two sensors.

Recently, optical fibres (OF) have been turned into seismo-acoustic sensors. The breakthrough came with the discovery that earthquakes can be detected by analysing the phase stability of state-of-the-art lasers across thousand-kilometre-long seafloor telecommunication cables (Marra *et al.,* 2018). However, this approach provides only one measurement that is integrated over the entire length of the cable. Thus, Distributed Acoustic Sensing techniques (DAS, Figure 5.6.) exploits the phase of light that is backscattered by the inherent irregularities of the silica fibre to provide densely spaced, high-rate measurements of strain. DAS provide high frequency (1 kHz) acoustic measurements with metric spacing, effectively turning OF cables into dense linear seismic arrays (Jousset *et al.,* 2018). This effectively means that instead of one seismometer spaced every hundreds of meters or even kilometres apart, we now have a set up that is equivalent to having a seismometer every two meters, which renders much more detailed information of the subsurface. Sladen *et al.,* (2019) demonstrated that regional seismicity (e.g. a M_w 1.9 micro-earthquake located 100 km away) can be monitored with signal characteristics comparable to those of a coastal seismic station.

Future developments call for the integration of sensors into undersea telecommunication cables. The SMART (Science Monitoring and Reliable Telecommunications) subsea cables initiative would combine these infrastructures to create a seafloor-based global ocean observing network (Howe *et al.,* 2019). Enabling telecommunication cables on the seafloor to sense their environment could potentially reduce the time to detect earthquakes that may trigger a tsunami by approximately 20% (Tilmann *et al.,* 2017).

Seismic imaging

Seismic imaging provides the most accurate information when analysing the geology below the seafloor and forms the basis of most marine geohazard studies. There is a trade-off between resolution and penetration. With seismic methods that can look 5 km below the seafloor, it is possible to resolve geological features of about 50 m, but with seismic methods that only penetrate the top 25 m, the resolution can be as high as 25 cm. Studies of slope stability typically employ seismic systems that image the top 1,000 m at 5 m resolution, while earthquake studies have to image the entire continental crust down to about 30 km. Modern systems are able to image the subsurface in three dimensions. Like in a medical CT-scan the entire subsurface is revealed and can be interrogated in all directions. This reveals the main tectonic structures, such as tectonic faults along which earthquakes occur (Figure 5.7. and Karstens & Berndt (2015)), and the deposits of past landslides, that provide information on which parts of the continental margins are unstable and how often landslides occur in a particular region.

Credit: C. Berndt

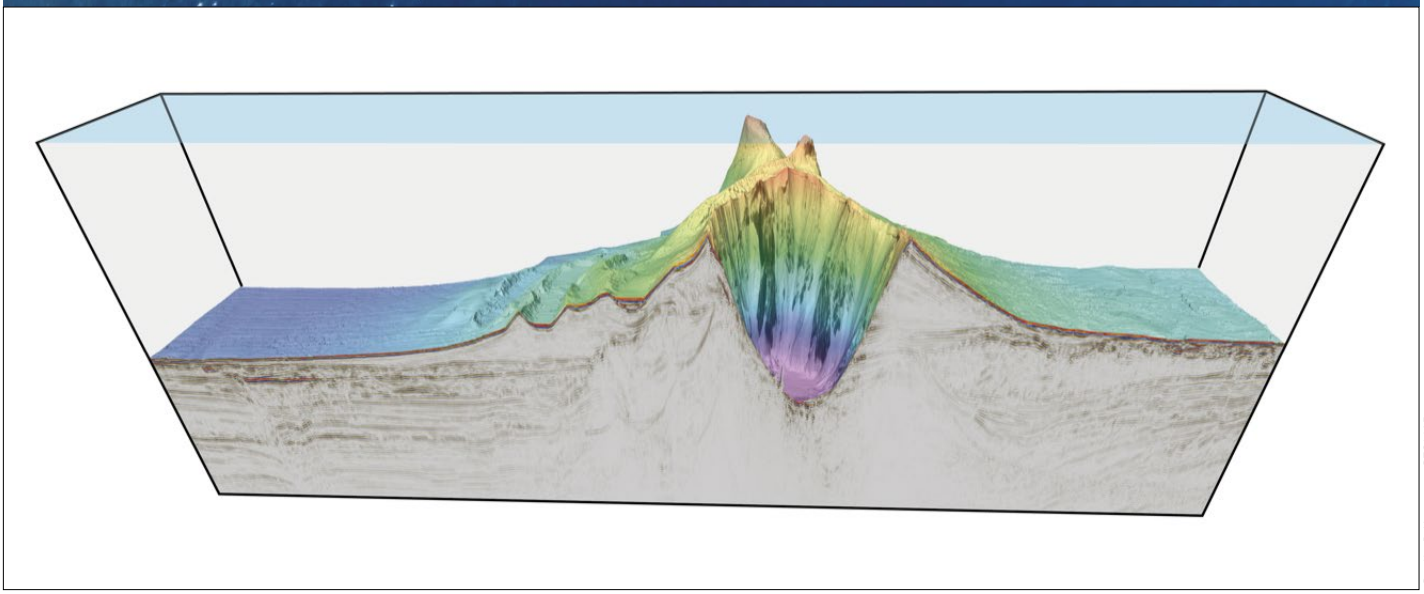

Credit: J. Karstens, GEOMAR

Figure 5.7. **Top:** Aerial photograph of a 3D-seismic experiment.
Bottom: 3D seismic data covering the submarine volcano Kolumbo in the Aegean Sea.

There are two recent developments in seismic technology that have redefined the field of marine geohazard research. The first is the development of high-resolution 3D seismic capabilities available at only three European academic institutions, i.e. IFREMER, GEOMAR, and the University of Tromsø (Planke *et al.,* 2009). If the issue of having the required equipment is solved, making this technique available to the wider community would boost European marine geohazard research (see EMB Position Paper 25 on Next Generation European Research Vessels for further information on sharing equipment and trans-national access (Nieuwejaar *et al.,* 2020)). The second advance is IFREMER's development of a deep-towed,high-resolution seismic system, which can image the top 50 m below the seafloor at 25 cm resolution even in deep ocean basins (Ker *et al.,* 2014). If these two technologies were combined into a deep-tow seismic system that could image the subsurface in three dimensions, it would lead to unprecedented insights into the geological processes that control geohazards. But developing a 3D-system to be towed at great water depth is technically challenging and would require a joint European effort.

5.2.3 Drilling the seafloor to understand geohazards at depth

Seafloor drilling devices

Robotic seafloor drills (Freudenthal & Wefer, 2013) are state-of-the-art remotely controlled devices that can drill up to 200 m into the seafloor. They can penetrate shallow fault zones, the detachment planes of submarine landslides, but also crustal rock or other strata can be penetrated by either push coring or rotary coring. A suite of logging tools exists to collect continuous records of petrophysical parameters. Samples can also be taken using an autoclave system, so gas hydrate-bearing sediment can be recovered at their *in situ* pressure and temperature. In addition, a suite of borehole observatories has been developed for the slim MeBo drillholes (Kopf *et al.,* 2015, Figure 5.8.) to seal the borehole to the Ocean above, sample fluids, and to transfer data from the seafloor to the sea surface. Electrical conductivity probes (that measure salinity), hydrophones or a slim seismometer may be mounted to the drill, and multiple holes with such systems could monitor their relative distance and would be powerful in seafloor geodesy.

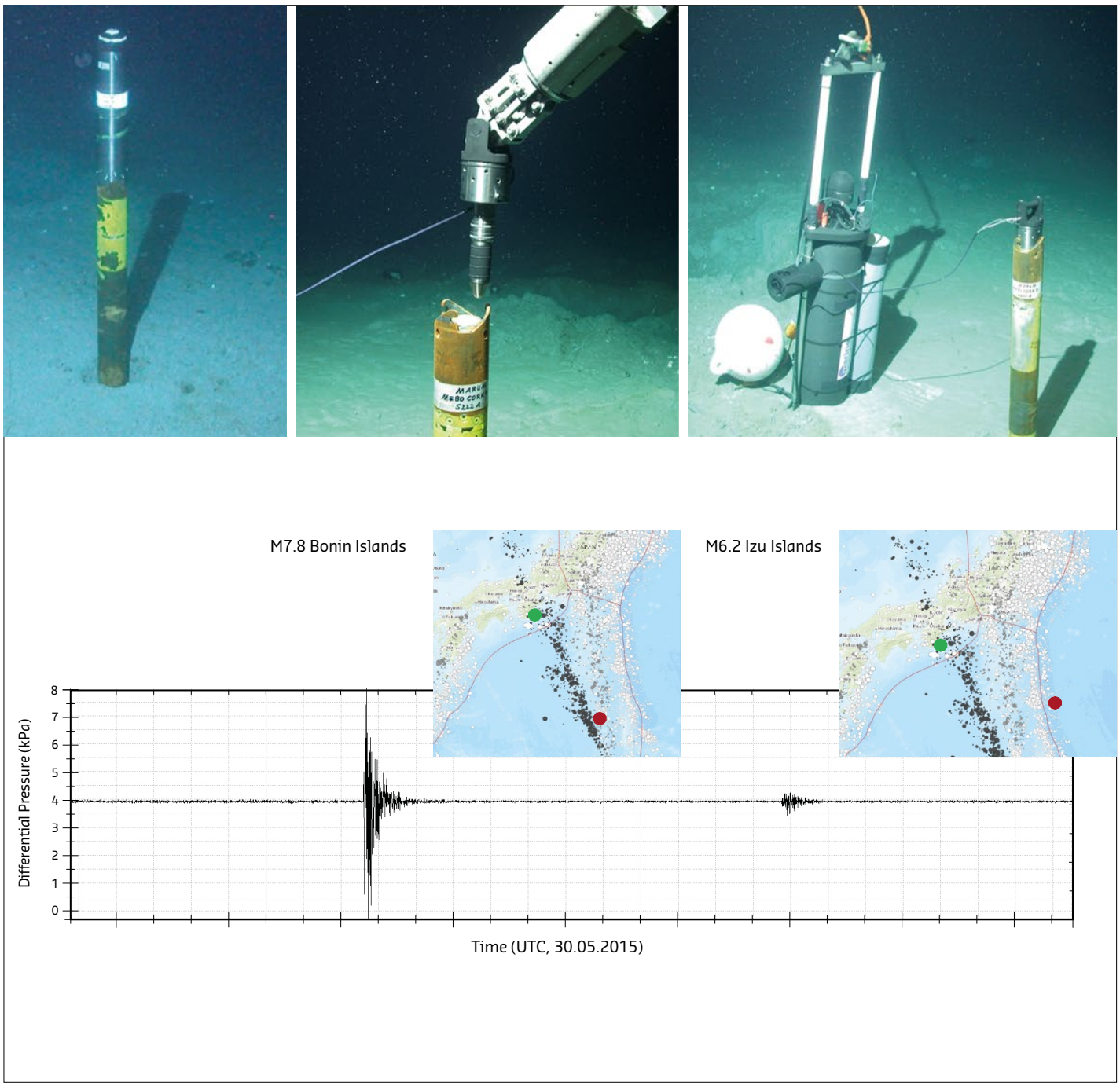

Credit: MARUM Bremen (CC BY 4.0)

Credit: Achim Kopf, MARUM, unpubl. data

Figure 5.8. **Top:** Different MeBo drill rig bore hole observatories.

Bottom: Example of the formation pressure response of a MeBo observatory in Nankai (Japan) when two earthquakes in the near-field (see inset maps, MeBo instrument = green dots, earthquakes = red dots) stroke in May 2015. The Bonin Islands event has a larger magnitude and is also situated on the same subduction system, hence causing the stronger pressure anomaly.

Long-term borehole monitoring system (LTBMS)

Long-term borehole monitoring systems (Figure 5.9.), also known as CORK (Circulation Obviation Retrofit Kit), are state-of-the-art borehole observatories that seal the subsurface borehole from the ocean water body, allowing the *in situ* monitoring of deep-seated processes in the borehole. There have been numerous CORK designs over the past decades, which are described in Solomon *et al.,* (2019) and references therein.

More recently, very complex long-term borehole monitoring systems (LTBMSs) were developed and deployed off Japan, comprising an array of sensors designed to monitor slow crustal and sediment deformation (Wallace *et al.,* 2016). Pore pressure records from these monitoring systems can detect extensional and compressional sediment deformation before an earthquake occur. The configurations of these 100 m-long observatories include: (1) pressure ports, (2) volumetric strain-meters, (3) broadband seismometers, (4) tiltmeters, (5) three-component geophones, (6) three-component accelerometers, and (7) thermometer arrays. Unlike the CORKs, the LTBMSs can operate in self-contained mode but also as part of a powered, real-time seafloor cabled network, making them suitable for geohazard mitigation and early warning. Examples of the outcome of such research activities for earthquake assessment include the very precise location of earthquakes and associated seafloor movement offshore (Wallace *et al.,* 2016), and the ultraprecise quantification of earthquake slip and tremors and how this relates to the plate kinematic stress accumulation and future risk (Araki *et al.,* 2017).

5.2.4 Observing physical parameters governing geohazards

Ocean-Bottom Seismometers (OBS)

Ocean-Bottom Seismometers (OBS) are deployed on the seafloor to record acoustic and seismic events from natural and anthropogenic sources, such as earthquakes and tremors or human-made acoustic signals (Figure 5.10. and Kopp *et al.,* (2011)). Processing and analysing the data yields information on the type and location of the acoustic or seismic source, and the physical properties and geology of the sub-seafloor sediments, Earth crust and mantle. OBS may be equipped with geophones in addition to a hydrophone and require enough capacity to record wide-angle seismic profiles (Sallarès *et al.,* 2013). OBS can operate for up to ~12 months for long-time autonomous monitoring. The instruments shown in Figure 5.10. are rated to 8 km water depth and are thus capable of being deployed in most oceanic regions.

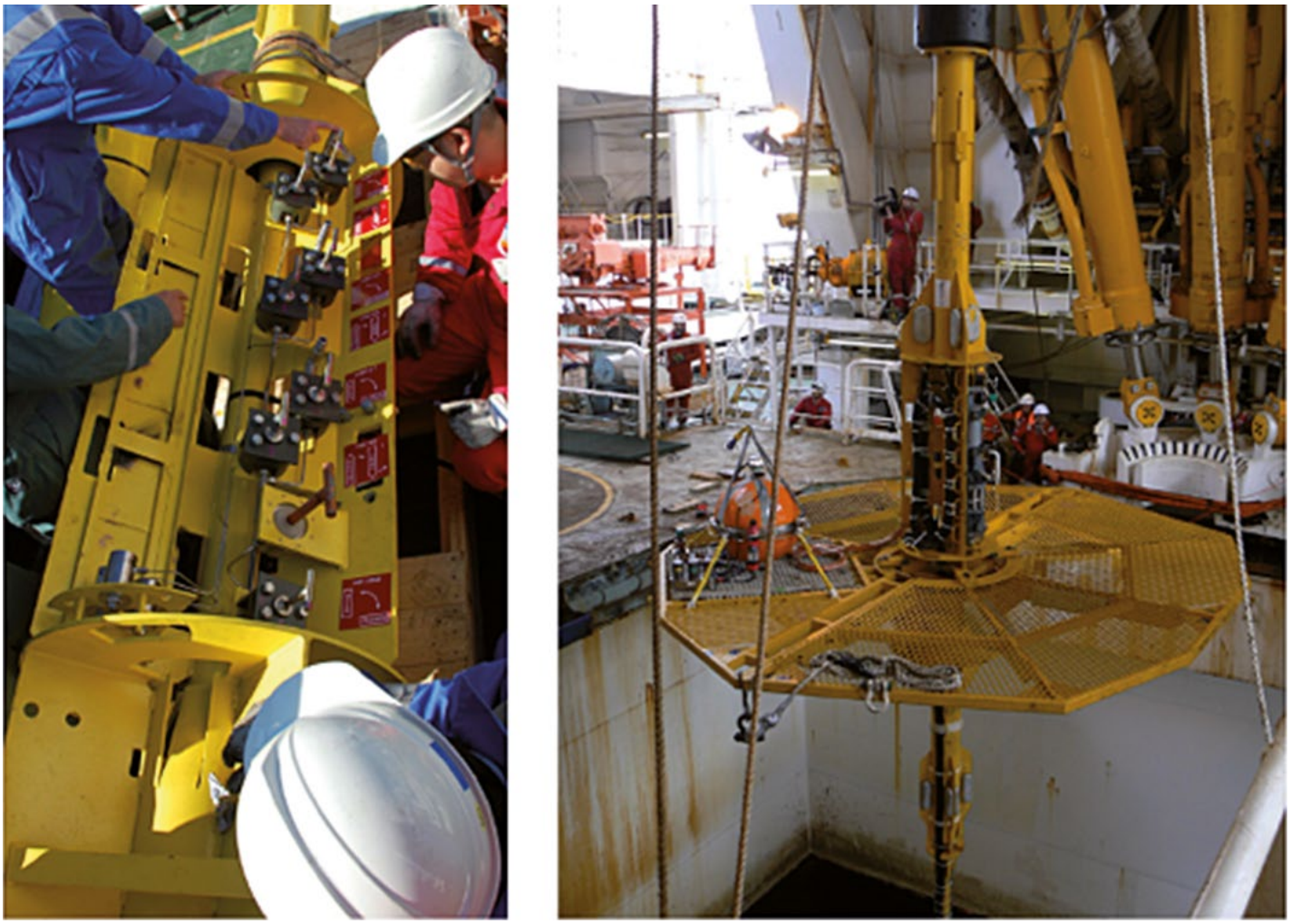

Credit: A. Kopf/MARUM (CC BY 4.0)

Figure 5.9. **Left:** One of the payload bays on the LTBMS head showing ROV-operable valves that allow fluid sampling as well as pump tests in the formation at up to several 100 meters sub-seafloor depth. **Right:** Head of an LTBMS surrounded by the ROV landing platform that also hosts a data recorder when it is lowered into the moonpool of DV Chikyu.

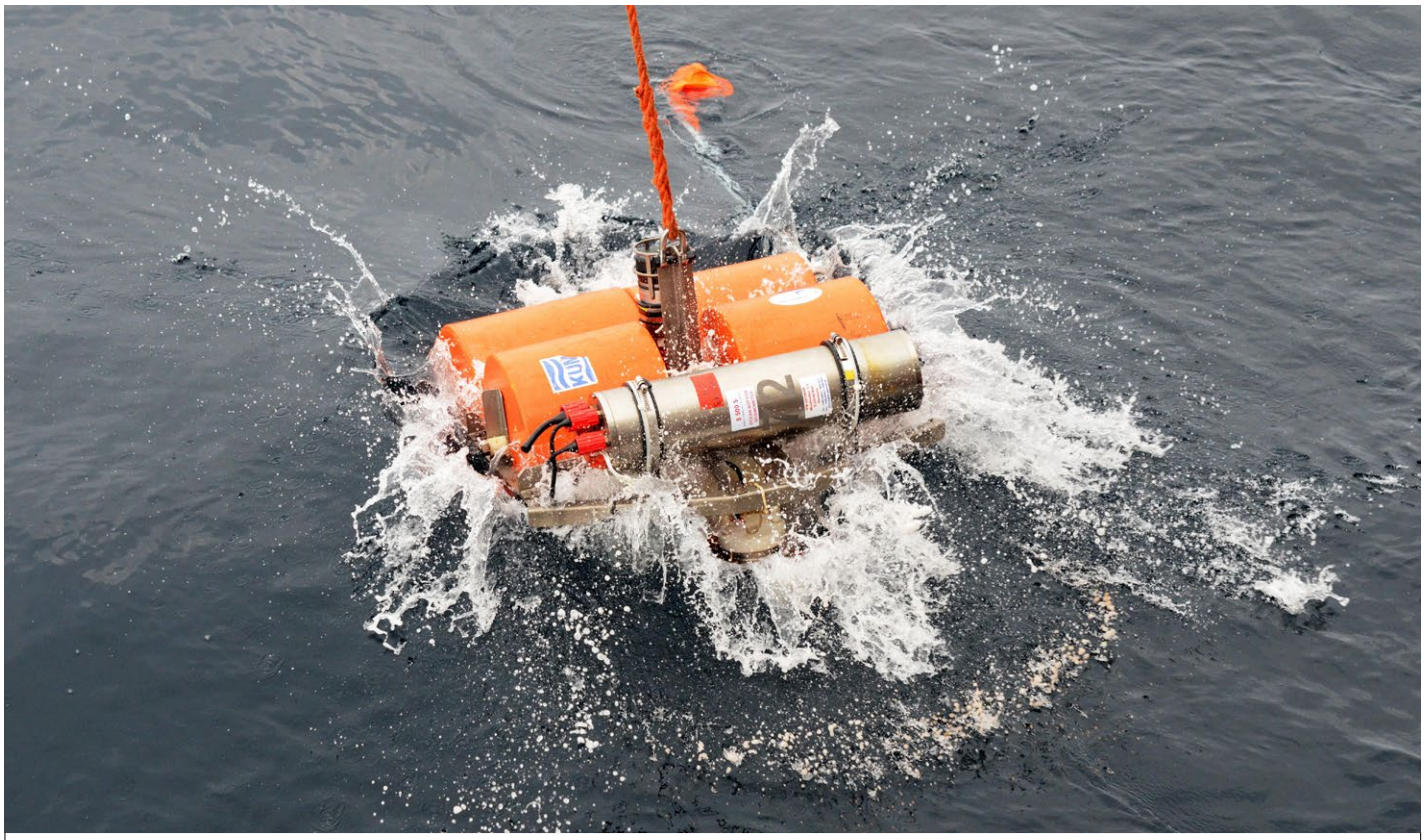

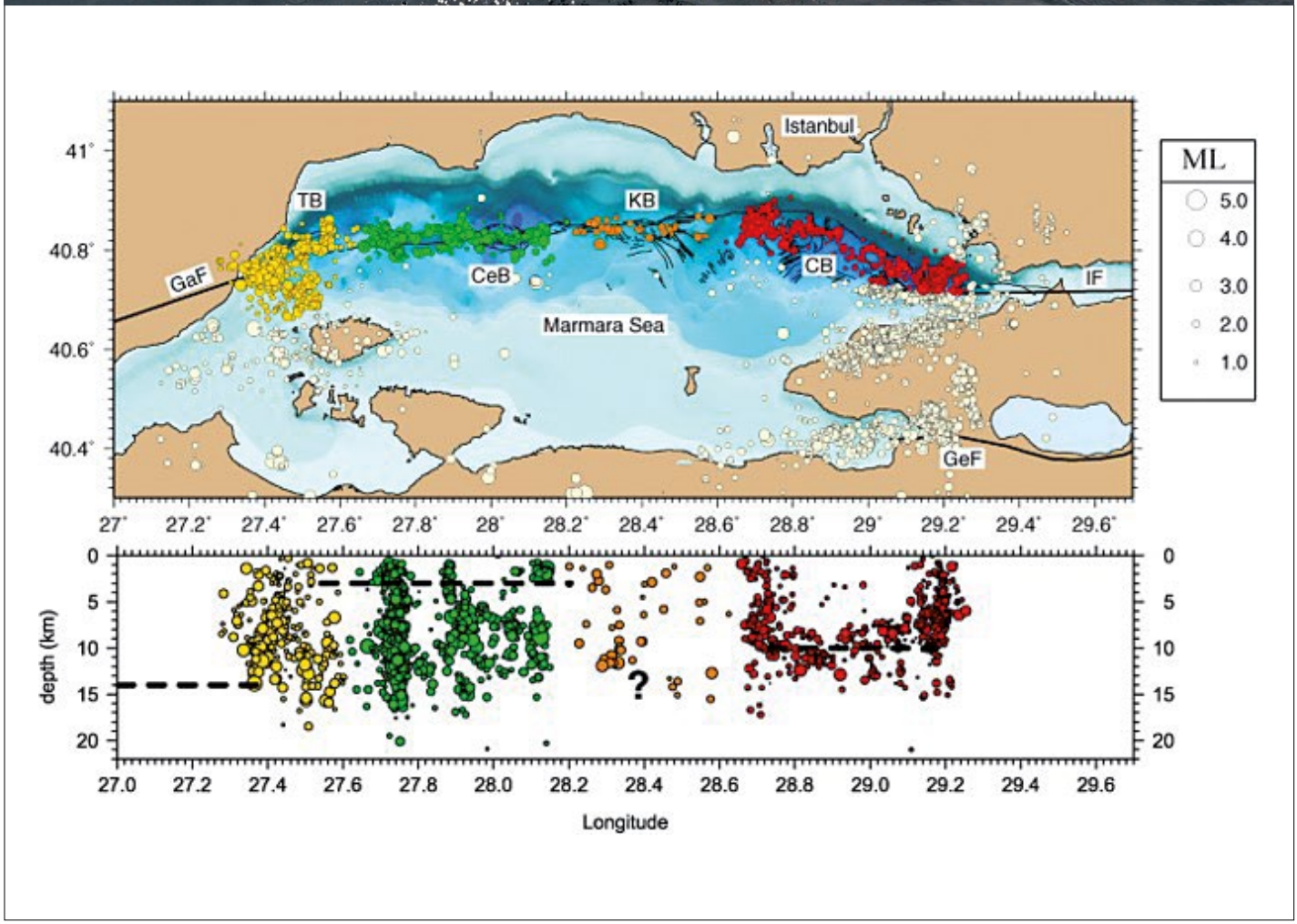

Figure 5.10. **Top:** Ocean bottom seismometer being deployed.

Bottom: Geographical distribution (top) and cross section of the seismicity (bottom) along the Main Marmara Fault during the period 2007–2012. Different domains were identified (TB, CeB, KB, CB) based on the earthquake distribution (colored dots) and the dotted lines in the depth section show the estimated fault depth of each domain.

Credit: Earl Davis

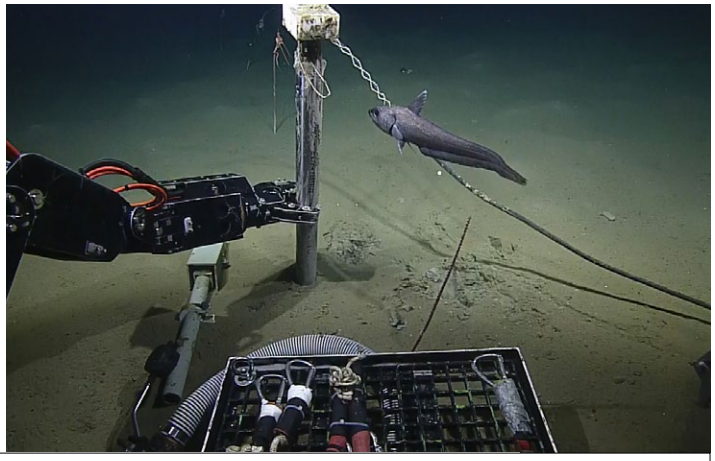

Credit: Ocean Networks Canada/OET/Nautilus Live (CC BY-NC-SA 3.0)

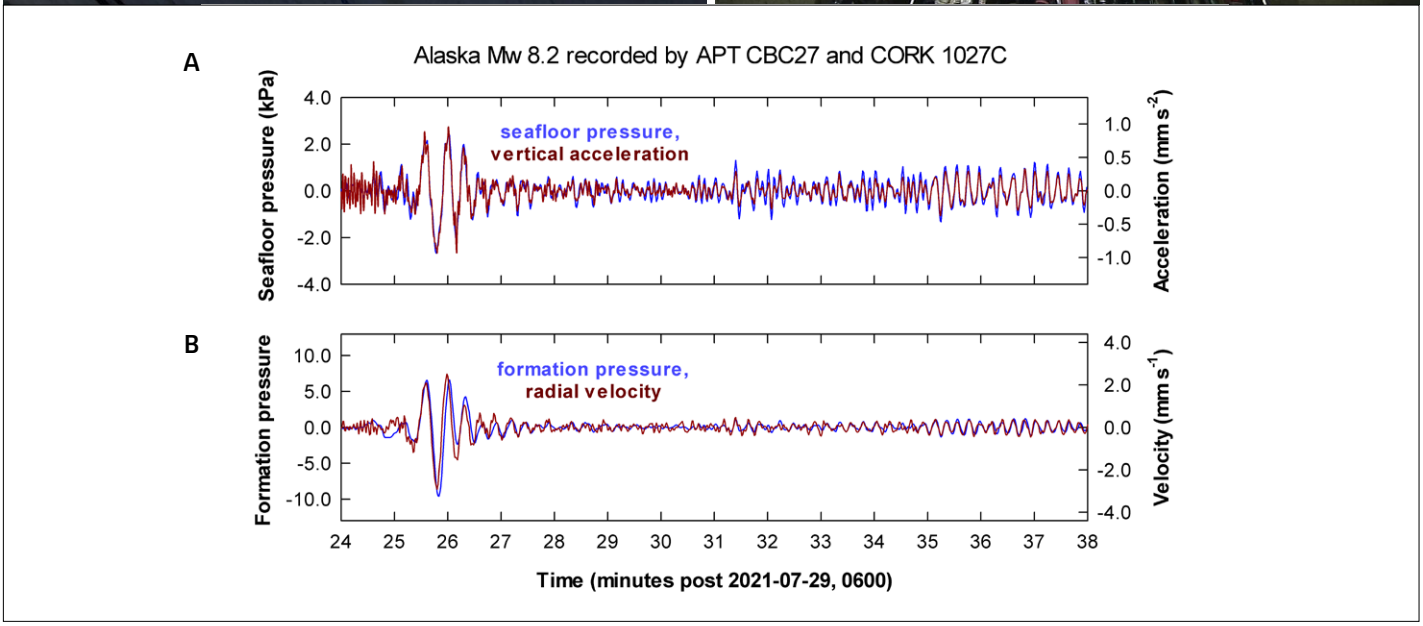

Credit: E. Davis, unpubl. data

Figure 5.11. **Top left:** Photo of an acceleration, pressure, and temperature (APT) tool being tested in a salt water tank.

Top right: An APT device being adjusted with the help of a Remotely Operated Vehicle (ROV) (see section 5.2.5).

Bottom: Example of APT data **(A)** and a CORK borehole observatory data **(B)** in detecting a Mw 8.2 earthquake in Alaska, USA. The advantage of the small size APT devices is that the ultra-precise measurements mimics much larger and more expensive technologies, such as the CORK borehole observatory. In addition, these graphs demonstrate the value of using pressure data as a proxy for earthquakes/seismic waves in cases where only pressure observations exist (matching between the measurements of the seismic surface wave vertical ground acceleration (red curve) and the seafloor pressure (blue curve)).

OBS will in future be integrated into submarine cabled real-time observation systems (Wallace *et al.,* 2016), which are developed as earthquake monitoring and tsunami early warning systems that continuously stream data to shore, such as Japan's fully operational DONET and S-net networks[14] (Mulia & Satake, 2021). In the future low-cost and lightweight OBS will allow deployment of large number of instruments (several hundred per mission) to increase our observation and monitoring capabilities. Optimized power consumption will enable long-term autonomous deployments of sensors beyond the scope of what is possible today, with data transmission solutions via modem and satellite offering non-permanent links for data transfer.

Acceleration/pressure/temperature (APT) device

The APT (Accelerator, Pressure, Temperature, see Figure 5.11.) is a new seafloor device that monitors seafloor acceleration, pressure and temperature using established transducers in a very robust device (Davis *et al.,* 2019). Similar to a CTD (conductivity [=salinity], temperature, depth [=pressure]), a set of key parameters is measured with an increased level of precision and in an affordable way. The APT is pushed into sediment or clamped into a borehole, providing extremely high resolution and accuracy due to its high-frequency period counter. Advantages include large dynamic ranges, high sensitivities and broad bandwidth. The APT monitors strong and weak seismic ground motion, tidal loading, and slow and rapid geodynamic deformation with a single tool.

Piezometer probes

Piezometer probes (Figure 5.12.) are devices designed to record formation pressure and temperature at the seafloor. Temperature variations at the seafloor are an indicator of fluid movement, and the formation pressure can be used as a proxy for strain and/or fluid flow. Piezometers and piezocone probes have been widely deployed in landslide research (Sultan *et al.,* 2010, 2020; Stegmann *et al.,* 2011). Numerous systems exist in the scientific community, with the modular devices developed by IFREMER being one of the most versatile. The sensing is done by individual modules that are connected by spacer rods, so that the depth

[14] http://www.jamstec.go.jp/donet/e/

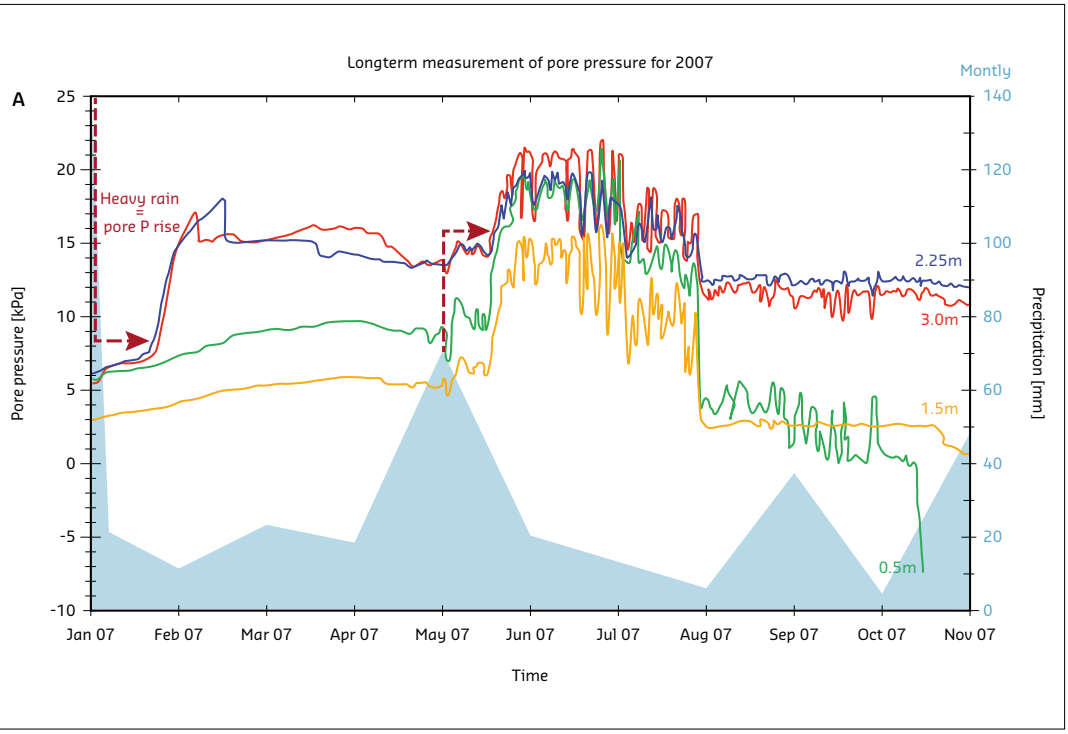

Figure 5.12. **Left:** Deployment of a piezometer probe.

Right: Long-term pore pressure monitoring (1 year, 2007) in the 1979 Nice Airport Landslide area (colored lines). Each curve represents measurements from the same piezometer probe at different depth. The monthly precipitation rate measured at Nice Airport (light blue area) is shown for comparison. Weeks after heavy precipitation, the pore pressure increases (arrows) because the aquifer is then charged with water and causes submarine groundwater seepage in the shallow slope. If pore pressure exceeds the (shear) strength of the sediment, the slope could collapse again (see calculations in Stegmann *et al.*, (2011)). Precipitation data from HYDRO database, from Le Service Central d'Hydrométéorologie et d'Appui à la Prévision des Inondations.

below seafloor in which the measurement takes place is defined prior to the deployment. The systems are self-contained with battery packs and buoyancy for recovery. Future use of cabled systems in larger seafloor networks will allow a broader spatial coverage of measurements.

Pore Pressure Sensors

The Penfeld penetrometer (Figure 5.13.) is a seagoing cone penetrometer with pore pressure sensing (CPTu). It was developed by IFREMER and has recently been upgraded to explore sub-seafloor depths down to 50 m. The self-contained system uses a regular CPTu piezocone at the tip of 50 m-long coiled tubing, which is straightened before the probe is pushed to measure pore pressure in the upper sedimentary succession. Recently, the device was modified with a decoupling mechanism, which can deploy a coiled long-term instrument of up to 50 m length. The presence of coarse sediments is shown by high values of the tip resistance. Decrease from the corrected tip resistance, indicate probably a precursor to a future shear, a zone where potential landslide can occur (see Sultan *et al.*, (2010)). Once this system is in the ground, the string is decoupled and the Penfeld is retrieved. TIPS (Temperature, Inclination and Pressure Sensors) is one example of such a custom-built pore pressure sensor developed within the ANR MODAL[15] project with the aim of identifying landslide precursors prior to failure events. TIPS is a modular *in situ* monitoring unit that measures pore pressure and temperature at different levels along a 50 m drive rod equipped with tilt sensors helping in accurately measuring tilt and inclination using accelerometers.

Figure 5.13. Launch of penetrometer Penfeld.

[15] modal-project.cnrs.fr

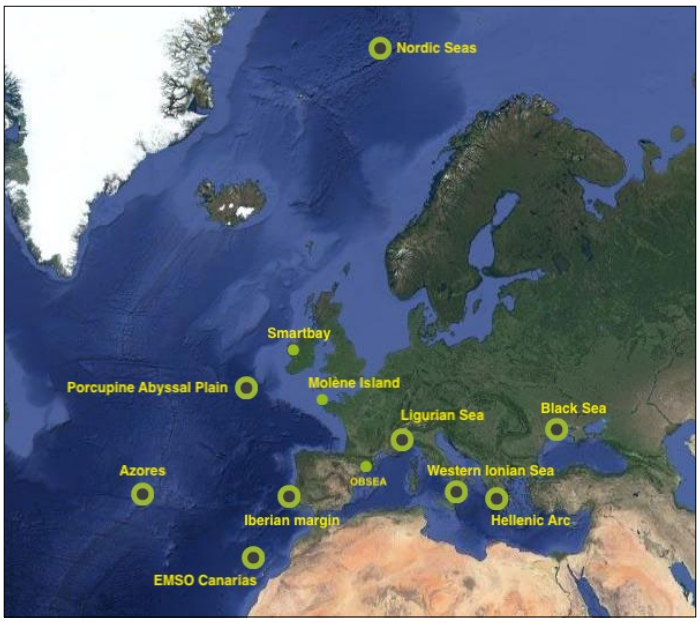

Figure 5.14. The EMSO regional facilities (black and green dots) and test facilities (green dots).

Permanent multidisciplinary seafloor observatories

Permanent seafloor observatories have been developed to complement the mobile sensors and equipment introduced above, which are commonly deployed only during research campaigns or for a limited period. Permanent observatories are platforms equipped with multiple sensors, placed along throughout the water column and on the seafloor to make recordings over a longer period of time. Depending on their target sites and attached sensors, seafloor observatories may have different configurations. They may be autonomous, acoustic or cabled.

Monitoring the seafloor using permanent observatories started in the 1990's. In 1995, the Instituto Nazionale di Geofisica e Vulcanologia (INGV, Italy) was the first institution to start monitoring submarine infrastructures, to develop new technologies for long-term underwater observation (Favali & Beranzoli, 2006). During the last two decades, many countries have started to establish multidisciplinary observatories and observatory networks. For example, in the north-east Pacific, Ocean Networks Canada (ONC) operates the cabled East Pacific Time-series Underwater Networked Experiments (NEPTUNE) to monitor seismic and volcanic activities. The Ocean Observatories Initiative (OOI) cabled array in the USA supports near-continuous geophysical monitoring of seismicity at the Cascadia margin and the Juan de Fuca and Gorda Ridges.

The European Multidisciplinary Seafloor and Water column Observatory (EMSO-ERIC) (Best *et al.*, 2016), which consist of a system of regional facilities placed at key sites in the European seas[16] (Figure 5.14.), constantly measure different biogeochemical and physical parameters relevant to marine geohazards. EMSO observatories include those installed on the Iberian Margin (Portugal/Spain); on the Porcupine Abyssal Plain in the North Atlantic, at a depth of 4840 m (operated by NOC, United Kingdom); at a depth of 3630 m off the Canary Islands (operated by PLOCAN, Spain); at a depth of 1700 m in the Hellenic Arc (operated by HCMR in Greece); and at a depth of 95 m in the Black Sea (operated by GeoEcoMar in Romania). EMSO-ERIC has also proposed the establishment of observatories in the Marmara Sea, a high-risk area with strong earthquakes, submarine landslides and tsunamis. Other observatories operate close to unstable margins, such as that off the coast of Norway, affected by numerous and recurrent submarine slides, that may damage offshore oil and gas installations, and generate tsunamis.

Globally, the United Nations Decade of Ocean Science for Sustainable Development (2021-2030) endorsed a programme called 'One Ocean Network for Deep Observation'. This programme is proposing the development of deep-sea science observatories and survey technologies at various sites of the global ocean to help protect people from natural hazards, among other objectives.

Off the Azores Islands on the Mid-Atlantic Ridge, the MoMAR observatory[17] operated by IFREMER-CNRS in France, continuously monitors volcanic, seismic and benthic faunal activity at the Lucky Strike hydrothermal field (1700 m depth), using an array of sensors and cameras. At 2100 m depth, the western Ionian Sea NEMO-SN1[18] multidisciplinary cabled observatory operated by INGV, INFN and CNR in Italy monitors offshore seismicity related to offshore faults and volcanic activity from Mount Etna (Sgroi *et al.*, 2019).

The Ligurian Sea shallow cabled observatory is an example where physical and chemical parameters in the sub-seafloor are monitored in concert to identify landslide precursors and potential triggers. These include local seismicity (see OBS above), pore pressure and tilt (see piezometer and TIPS above), and also CTD (Conductivity – Temperature – Depth), and Radon and other radionuclides. The latter two measures serve to identify changes in the pore volume of the marine sediments that may cause ground failure or successive weakening as a result of leaching in groundwater-bearing sediments. Groundwater pulses from the Maritime Alps, and in particular snow melt events in spring that enhance signals from precipitation, have been documented to cause destabilization and landslides (Dan *et al.*, 2007). As a result, recent studies use the KATERINA sensor, an autonomous *in situ* detection system for radioactivity, to measure radionuclide abundance as a proxy for groundwater seepage (Tsabaris *et al.*, 2011). See also Section 5.3. on precursors where such measurements were used at times of prominent earthquakes (e.g. Tsunogai & Wakita, 1995).

5.2.5 Underwater vehicles

Remotely Operated Vehicles (ROV)

A ROV (Figure 5.15.) is a non-autonomous remotely operated underwater vehicle, operated by a crew on board a research vessel, that is controlled and powered using a customised telemetry, optical fibres for communication, and a high voltage cable for power and hydraulics (Barreyre *et al.*, 2012). ROVs are a routine tool for monitoring and maintenance of offshore industrial infrastructure but they may also be used for scientific exploration. Most ROVs are equipped with high-definition still and video cameras and lights, and may include sonar systems (Dyment *et al.*, 2018), robotic arms (multi-function hydraulic manipulators), and sampling devices (i.e. baskets for seafloor fauna, sediment/rock, and gas/fluid samplers).

[16] http://www.emso.eu
[17] http://www.ipgp.fr/fr/momar-d-a-technological-challenge-to-monitor-the-dynamics-of-the-lucky-strike-vent-ecosystem
[18] http://www.esonet-noe.org/About-ESONET/Organization/East-Sicily

Over the past decade, ROVs have included *in situ* instruments that can measure bottom water and sub-seafloor temperature (up to >400°C at hydrothermal vents), physical or biogeochemical parameters. They can also contain *in situ* mass spectrometers used to trace the (isotope) geochemistry of deep fluids, and special devices such as the ROV-drill to extract hard rock samples to provide ground-truth information. Future demand requires novel, more dedicated sensors and smart solutions, such as advanced control of ROVs using immersive displays, and robotic tasks, live footage from the deep sea (telepresence), or manipulator motion compensation for observatory work (e.g. underwater mate-able connections, valve manipulation, data download).

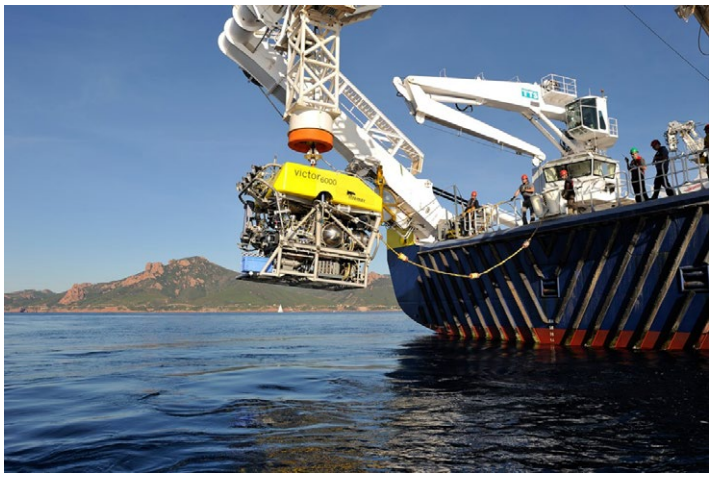

Credit: IFREMER, Michel Gouillou

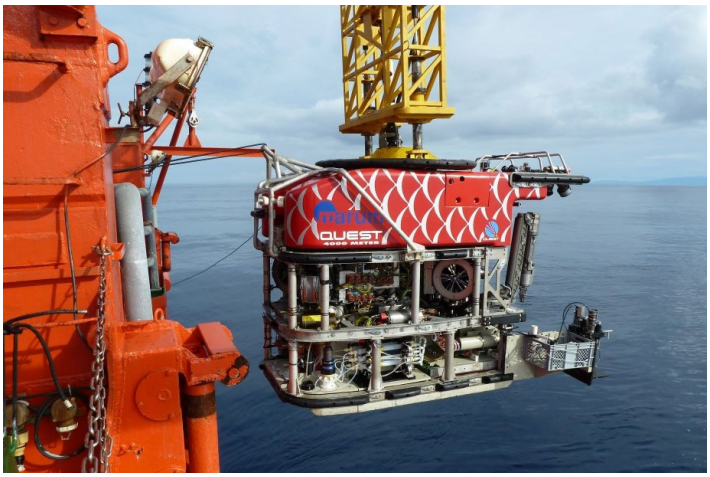

Credit: MARUM, Univ. Bremen (CC BY 4.0)

Credit: VLIZ

Figure 5.15. **Top Left:** IFREMER's Remotely Operated Vehicle (ROV) Victor 6,000 being deployed from *RV Pourquoi pas?*
Top Right: *ROV Quest* 4,000 m operated by MARUM being launched from *RV Sonne*.
Bottom: The control room of *ROV Zonnebloem* from the Flanders Marine Institute.

Autonomous Underwater Vehicles (AUV)

An AUV is a robot capable of underwater missions without requiring constant input from an operator because of its battery-powered propulsion, pre-programmed mission planning and other AI-controlled functions. Most AUVs contain sonar systems to survey bathymetry and backscatter imaging of the seafloor at high spatial resolution, given their low altitude relative to the seafloor (Kwasnitschka *et al.,* 2016). A variety of sensors can be attached to AUVs to measure the concentration of various elements, the absorption or reflection of light, and the presence of microscopic life. Examples include conductivity-temperature-depth sensors (CTDs) and pH sensors.

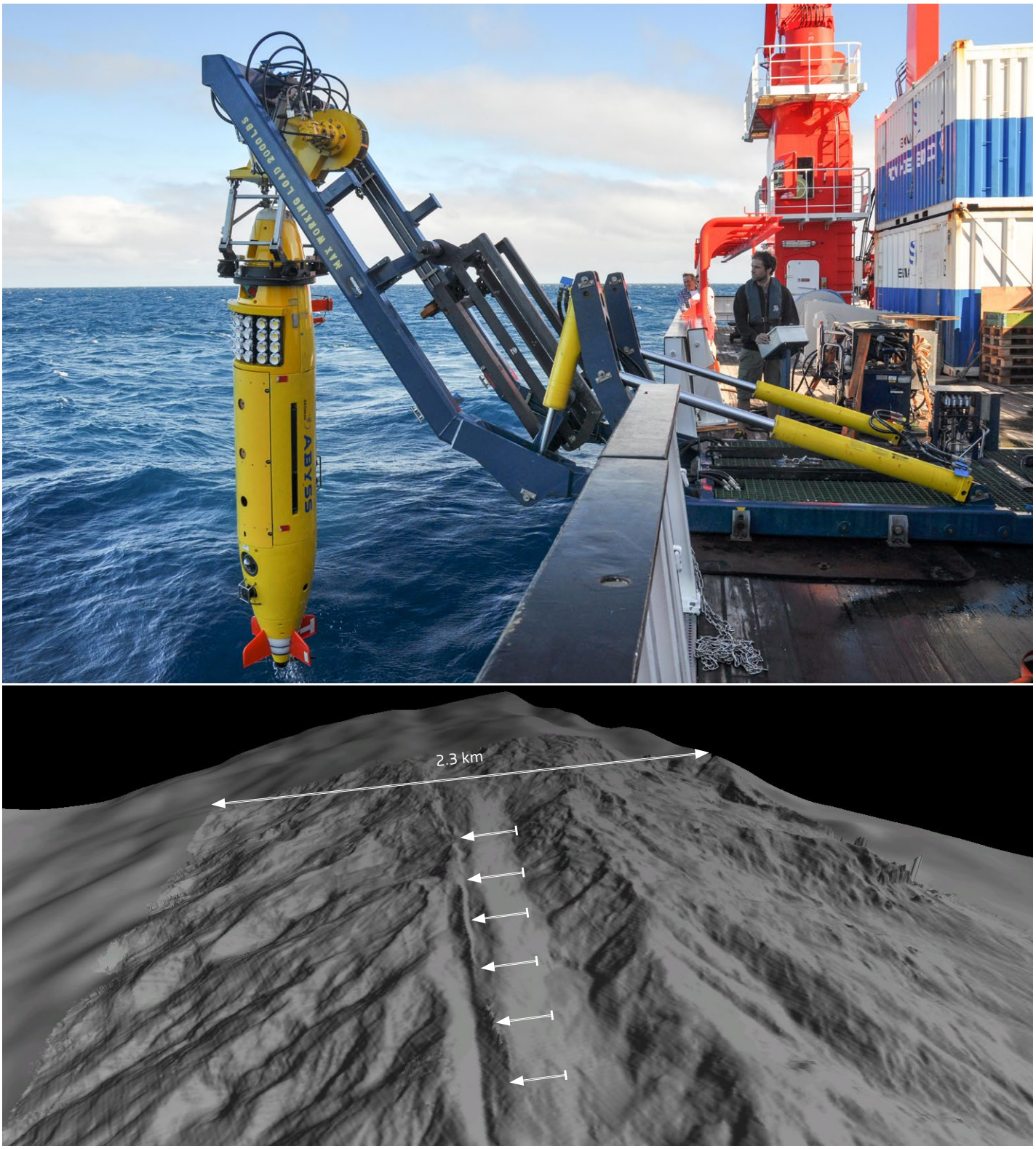

Credit: Emanuel Wenzlaff, GEOMAR (CC BY 4.0)

Credit: M. Urlaub

Figure 5.16. **Top:** The AUV ABYSS on *RV Sonne II* during the SO242/1 expedition.

Bottom: High-resolution seafloor map showing a fault zone (white arrows) on the flank of Mount Etna. Bathymetry data were acquired with an AUV at a resolution of 0.05 m.

AUVs can be used as a fleet of robots: new multi-vehicle/multi-sensor/multi-ship systems (MVSS; see Figure 5.16.) augmented with remote sensing and data assimilation technologies, as well as with cloud-based planning and control software, will enable ocean observation with unprecedented adaptive spatial and temporal resolution. MVSS are particularly suited to find, track and sample physical, chemical and biological features at the sub-mesoscales (e.g. spills of hazardous materials), combining AUVs in the water column with ships or smaller Unmanned Surface Vehicles (USVs, e.g. wave gliders) for communication towards sea level, followed by satellite links. This is because the different vehicles, equipped with a variety of sensors, operating at nominal speeds over a long time can be dynamically combined to address different observation/scientific needs such as exploration, targeted sampling of geohazard precursors with specific sensors, or continuous coverage for these spatial-temporal scales. Autonomous vehicles will benefit from innovative algorithms (underwater decision-making, energy-efficient path planning, hibernation) and upgraded sensors (all the way to floating observatory level with smart transducers).

5.3 Recording and recognizing precursors to geohazards

Robust forecasting of marine geohazards involves expanding our knowledge of the drivers of the relevant physical processes behind geohazards, with a major focus on identifying, understanding and exploiting the build-up phase of these events. The identification of temporal variations and the last stages before a hazardous event is crucial. This information, when coupled with innovative data mining strategies (see EMB Future Science Brief 6 on Big Data in Marine Science for further information (Guidi *et al.,* 2020)), will provide the potential to detect changes that deviate from the background signals (Pritchard *et al.,* 2020). These results in turn can be combined with advanced modelling schemes (discussed in Section 5.4) to evaluate if such changes might indicate a forthcoming event (so-called precursors). Variations in the fluid chemistry, and in particular devolatilization processes, are very common, but have not yet been in the focus of geohazard research. The marine environment has several advantages for identifying e.g. potential earthquake precursors: (1) It is easier to hydrologically seal shallow boreholes in a fully saturated environment, so measuring pore pressure becomes straightforward once a hole is sealed. (2) Seafloor mud volcanoes are less sensitive to atmospheric changes or local disturbances than onshore mud domes (Martinelli *et al.,* 1995). Thus, long-term seafloor monitoring may produce more stable data records and transient changes may be more significant and easier to detect. The marine environment is therefore the ideal test ground for techniques that can later be applied outside the Ocean.

Onshore, Radon (Figure 5.17.) is a powerful tracer because positive Radon anomalies are commonly (but not always) observed prior to earthquakes (Igarashi & Wakita, 1990; Martinelli *et al.,* 1995; Kuo *et al.,* 2009). Radon probes have been modified for (shallow) marine use (Tsabaris & Wakita, 2008), but studies in seismically active areas have not been performed yet. Similar to Radon, anomalies in subaqueous release of methane gas may occur pre-, co- or post-seismically through pockmarked areas on the shelf (Hasiotis *et al.,* 1996) or in mud volcanoes (Kopf *et al.,* 2010). However, data from continental slopes are rare, although ionic concentrations of some elements have been shown to vary in sub-seafloor pore waters. An example is observations from a borehole intersecting the frontal thrust in the Costa Rica subduction zone by Solomon *et al.,* (2009), whose model suggests seismic fault slip events being the cause of variations of ionic Strontium, Magnesium, Lithium or Potassium. Onshore, similar fluctuations in ionic concentration have been observed in groundwater associated with the M_w 7.2 Kobe (Japan) earthquake (e.g. Tsunogai & Wakita, 1995), and the M_w 7.3 Chi-Chi (Taiwan) earthquake (Song *et al.,* 2003).

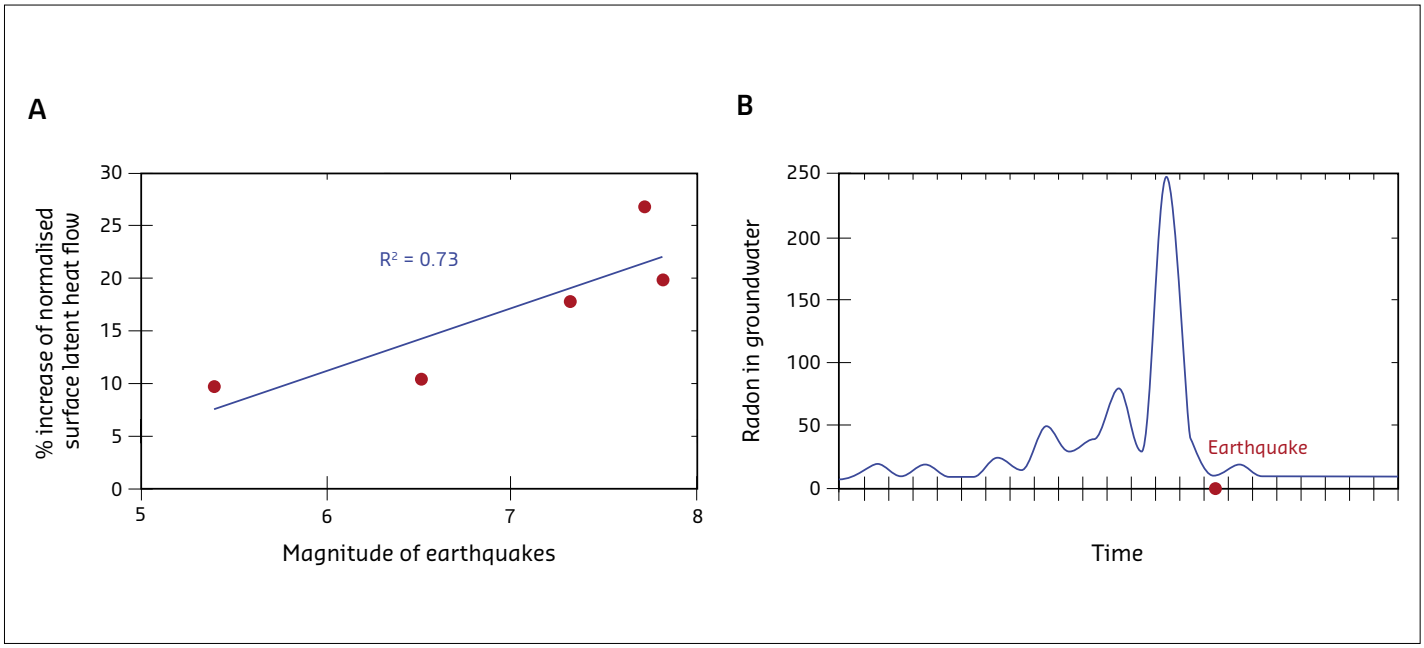

Figure 5.17. Examples of transient phenomena related to earthquakes. **Left:** Positive relationship between percentage of increasing surface latent heat flow and earthquake magnitude. **Right:** Radon has been known to increase in groundwater in the preceding months leading up to earthquakes (red dot in figure), as described by Igarashi *et al.,* (1995).

The 2011 (M_w 9.1) Tohoku earthquake is one of the best-recorded seismic events, due to the dense sensor arrays offshore and onshore in Japan. Prior to the earthquake, a number of observations pointed to the possibility of a large seismic rupture in north-eastern Japan. However, due to the lack of interdisciplinary understanding of the hazard potential, the results from individual methods did not provide a consensus assessment of the hazard (Uchida & Bürgmann, 2021). Even though temporal variations along the plate boundary and enhanced seismic activity were documented prior to the event, this did not cause an alert, so the large-magnitude (M_w >8) earthquake was not considered in the official earthquake probabilities, and the initial tsunami warning far underestimated its true size (Hoshiba & Iwakiri, 2011). Although discrepancy in the plate coupling models derived from seismic and geodetic studies was recognized prior to the Tohoku event (Kanamori *et al.,* 2007), the origin of the diverging values was not clear. At the time of the earthquake, mostly onshore measurements were used and the resolution of processes occurring far offshore was limited as the seafloor arrays were still lacking a critical number of stations. Consequently, based on the fact that M_w ~7.5 earthquakes occurred every ~30 years, the long-term forecast for the region suggested a 90% or larger probability of rupture by a moderate to large sized (M_w <8.5) earthquake.

The M_w 7.6 Izmit earthquake along the North Anatolian Fault in Turkey was preceded by a seismic signal originating from the hypocenter 44 minutes prior to the main shock (Bouchon *et al.,* 2011). The signals consisted of a succession of repetitive seismic bursts, accelerating with time, and increased low-frequency seismic noise. These signals were interpreted to be due to a phase of slow slip occurring at the base of the brittle crust, with the slip accelerating slowly initially, and then rapidly in the 2 minutes preceding the earthquake. Precursory seismic activity prior to the M_w 9.1 Tohoku Earthquake was even more marked. The increasing seismic activity prior to the Tohoku main event culminated in a M_w 7.3 foreshock two days before the main event.

Precursory anomalies were identified from the unique data set that the Tohoku event provided. Small, repeating earthquakes (M_w ~4) and transient slow slip were observed prior to the earthquake, but ceased after the event, indicating that seismicity patterns change during a seismic cycle (Uchida & Bürgmann, 2021). The Tohoku earthquake greatly improved our understanding of earthquake dynamics because of the diverse networks and arrays of sensors placed on the island of Japan and its offshore domain. It has highlighted the multidisciplinary need to better link the observations from diverse fields (seismology, geodesy, geology, geomorphology, structural tectonics, forensic seismology) and recognize their significance, at least for intermediate-term earthquake forecasts and probabilities.

For cascading or cumulative hazards, the situation is more complex and challenging. A combination of space-borne and ground-based techniques resolved the cascade of precursors leading up to the 2018 sector collapse of Anak Krakatoa (Figure 5.18.), an Ocean island volcano located between the islands of Java and Sumatra in Indonesia, which resulted in a fatal tsunami (Walter *et al.,* 2019). Flank motion and increasing volcanic activity were detected prior to a small-sized earthquake that preceded the sector collapse by about 2 minutes. The flank collapse removed a significant portion of the island and its shallow volcanic magma reservoir, causing an explosive eruption and the associated landslide triggered the tsunami.

While the flank movement, anomalous degassing, thermal anomalies, and seismic activity were observed prior to the tsunami, they were considered individually and their significance as precursors to the complex cascade of events evolving at Anak Krakatoa over a period of months was not recognized. This lack of understanding of cascading hazards prevented an accurate prediction of the event, even though a volcano-induced tsunami was anticipated for Anak Krakatoa (see Section 2.2). The failure to correctly interpret the anomalous behaviour as precursor activities leading to a geohazard emphasizes the urgency to develop multi-hazard observation

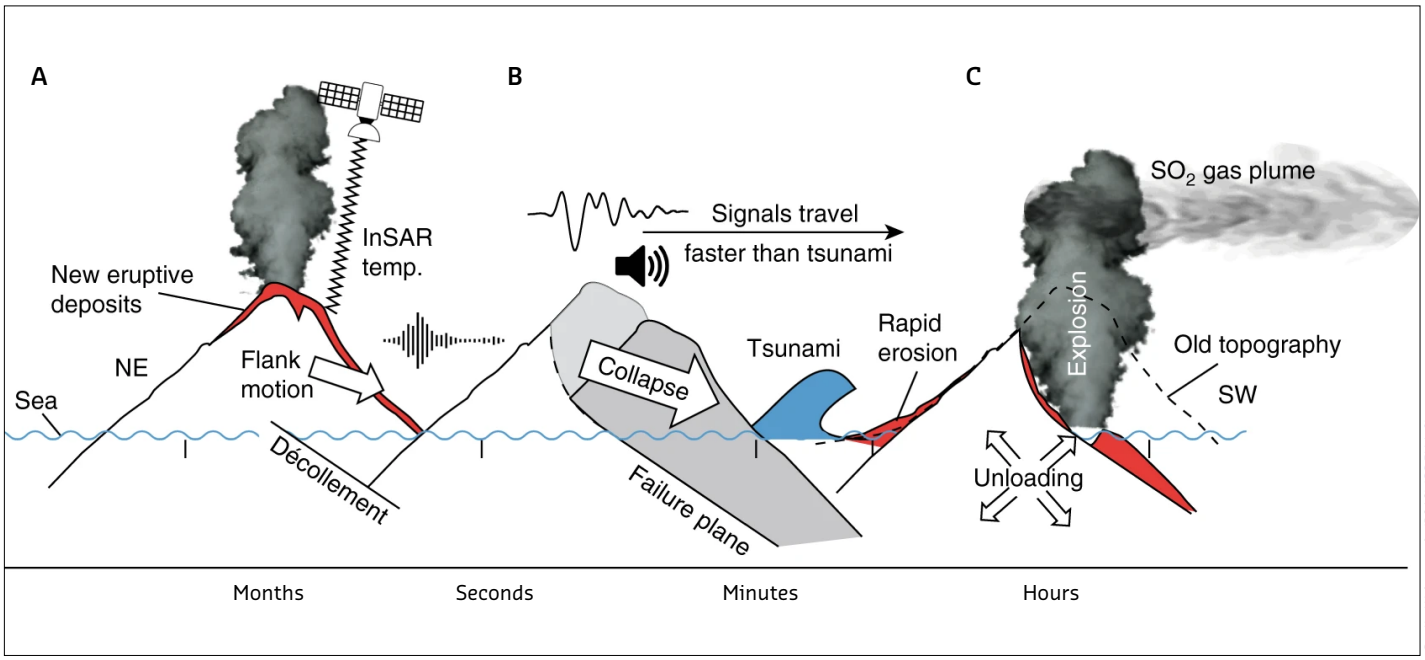

Credit: Walter *et al.*, (2019) (CC BY 4.0)

Figure 5.18. Schematic sequence of events leading to the hazard cascade during the 2018 flank collapse of Anak Krakatoa, Indonesia. Flank movement (indicated by the white arrow in the left panel) and volcanic eruptions (dark cloud in left panel) were precursors to the flank collapse, which may have been triggered by an earthquake (seismic signals). Mass movement during flank collapse generated a tsunami (central panel), which reached the adjacent shores within minutes and caused ~400 casualties. The events lead to a decapitation of the volcanic island (right panel), causing rapid erosion.

capabilities and monitoring techniques to enable a shift from a single hazard perspective to a cascading hazard perspective, and to account for the specific complexity of a region or area, as discussed in Section 2.8.

Monitoring of active processes is crucial to understand their underlying dynamics and mechanisms and to enable us to recognize the significance of precursory signals. Laboratory and field observations show that the transition from slow build-up to its release in hazardous events occurs as a brief process in which the onset of deformation is accompanied by changes in material properties. These changes may occur not only over minutes and hours as thought a decade ago, but could also occur over time scales of years. For example, changes that lasted several years were observed preceding large earthquakes such as the 2011 M_w 9.1 Tohoku earthquake in Japan (Mavrommatis *et al.,* 2014). The aim of identifying these changes is to distinguish between a geosystem in equilibrium from one approaching instability, thus triggering a hazardous event. This requires the development of the next generation of observation systems and techniques to transform our observing and monitoring capabilities and to advance our interpretation and modelling frameworks. It is necessary to quantify the thresholds and transitions towards instability and to improve our assessment of the hazard potential of threatened sites around Europe.

5.4 Defining hazard through numerical and physical modelling

Recently, the development of mathematical models for hazard definition, geotechnical measurements, data collection in the field and in laboratories, and event dating has gradually increased. These tools can be applied to understand the formation and the mechanisms of marine geohazards and their consequences, but also to develop warning systems prior to these disasters.

Tsunamis

To minimize the impact of a tsunami and to reduce the infrastructure destruction along the coast, understanding tsunami land inundation over the coastal areas is crucial. For that, numerical modelling is a powerful tool, and over the last few decades, numerical models have advanced rapidly due to improved numerical schemes and computational resources. Scenario-based modelling can provide information on potential inundation areas based on knowledge of the bathymetry and potential sources of tsunamis. Physical tsunami models are used to better understand tsunami inundation in coastal areas (Bridges *et al.,* 2011; Palermo *et al.,* 2012; Kihara *et al.,* 2015; Thomas *et al.,* 2015; Prasetyo *et al.,* 2016; Yasuda *et al.,* 2016).

When tsunamigenic sources are well constrained and detailed bathymetric and coastal topography data are available, numerical models allows for accurate estimates of offshore tsunami propagation and inundation (Prasetyo *et al.,* 2019). However, there are still limitations in data availability and the ability of current numerical schemes to reconstruct tsunami inundation and run-up associated with complex bathymetry and topography (Park *et al.,* 2013; Pringle & Yoneyama, 2013; Miyashita *et al.,* 2015; Adriano *et al.,* 2016). Validation of the numerical models is challenging due to limitations in observational data, particularly for extreme tsunami events. This makes it challenging to constrain certainty in propagation and inundation.

Interaction between laboratory and numerical modelling communities is mutually beneficial and allows for the development of an iterative process using both techniques to test numerical models against data derived from the physical models. Scaled laboratory experiments allow us to observe and understand physical processes and test basic assumptions, and the numerical simulations can be used to quantify processes that are too complex, large, or long-lasting to be reproduced in the laboratory, making the approaches highly complementary.

Probabilistic tsunami hazard assessment (PTHA) is an approach used to quantify tsunami hazard. A PTHA combines all potential tsunamigenic sources that may affect a region to provide the probabilities that various tsunami heights might be exceeded. These analyses provide information on event probabilities and can therefore feed directly into risk management plans. PTHA was inspired by probabilistic seismic hazard assessment (PSHA) for earthquakes, and is currently a topic of intense research. Behrens *et al.,* (2021) provide an elaborate overview of current state-of-the-art and research gaps in probabilistic tsunami hazard and risk assessment, summarizing the large uncertainties that arise from inadequate knowledge of the physics and geological complexity of the tsunamigenic sources, particularly those triggered by landslides and volcanoes. Furthermore, uncertainties propagate across disciplines assessing risks, where our understanding in the level of vulnerability and exposure to different hazards is still immature (Behrens *et al.,* 2021). Basili *et al.,* (2021) present a state-of-the-art PTHA for earthquake-generated tsunamis in the north-eastern Atlantic, the Mediterranean, and connected seas (NEAM), which underscores the importance of exploiting data from different scientific fields and disciplines (Figure 5.19.). Landslide-generated tsunamis will benefit from such a region-wide approach, as the source, size and possible generating mechanisms may be inferred from high-resolution bathymetry.

Tsunami early detection and warning systems (TEWS) have been operational in the Pacific since the late 1940s. These systems combine seismological monitoring with sea bottom pressure sensors (Deep-ocean Assessment and Reporting of Tsunami - DART Buoys) to detect, and later confirm, potentially tsunamigenic earthquakes in order to issue warnings to the threatened coastal areas. Following the 2004 Indian Ocean tsunami, there have been widespread efforts to develop tsunami warning and mitigation systems in several other regions, including the Indian Ocean (ICG/IOTWMS), the NEAM region (ICG/NEAMTWS) and the Caribbean. In addition to Ocean-wide systems, local warning systems are in place for tsunamis triggered by large rock avalanches. One such example is the Åkneset slope in Norway, which is threatening to fail and would thereby generate a massive tsunami that could wipe out settlements along the Storfjorden fjord system (Harbitz *et al.,* 2014). Another example is the Stromboli Sciara del Fuoco in the southern Tyrrhenian Sea that experienced a landslide-generated tsunami in 2002.

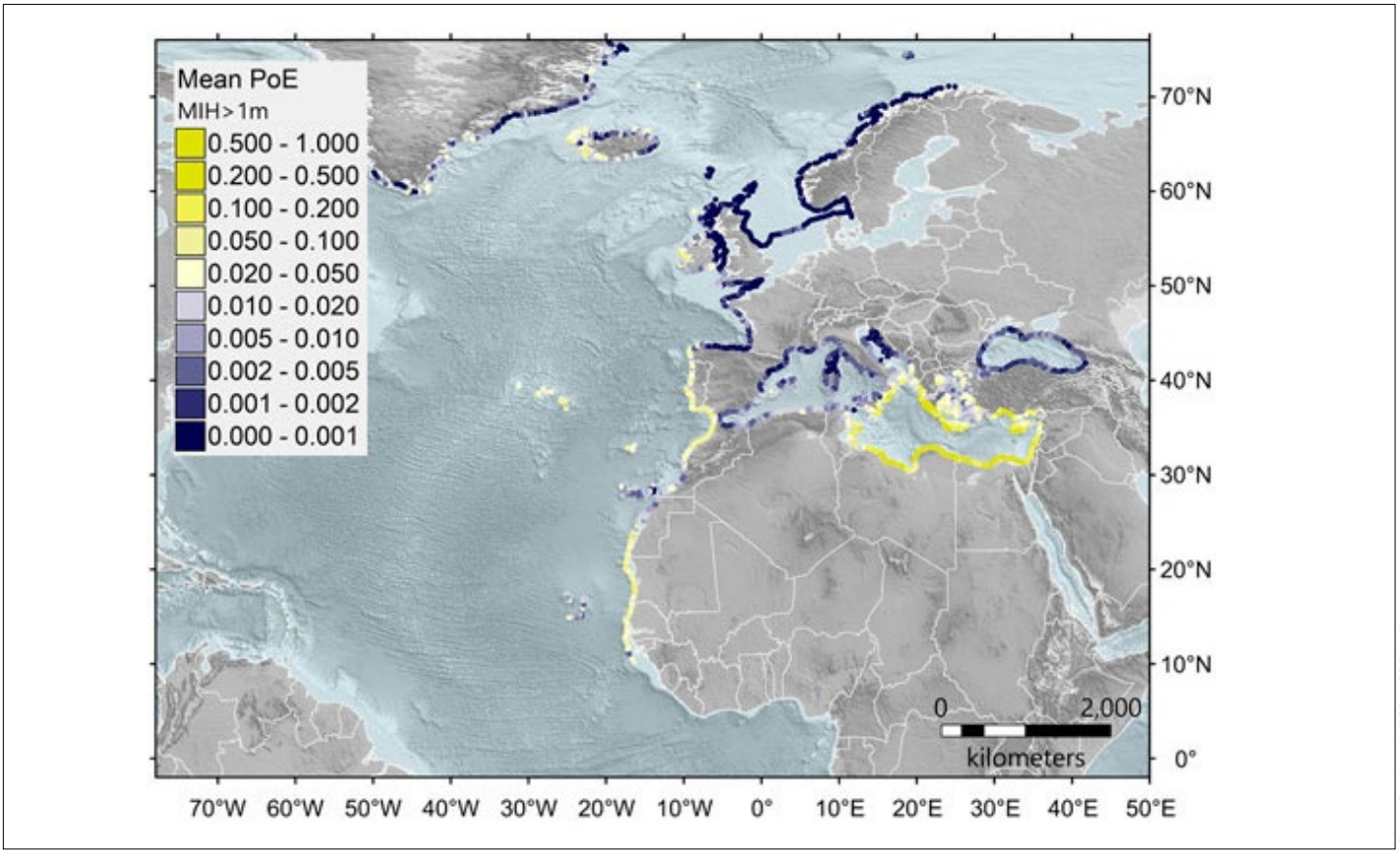

Figure 5.19. A probability map for maximum inundation height larger than 1 m modelled by the North-Eastern Atlantic, the Mediterranean, and connected seas (NEAM) Tsunami Hazard Model 2018 (NEAMTHM18). The larger the number (between 0 and 1), the higher the probability that an earthquake-generated tsunami would inundate the coast with a wave larger than 1 m high.

Earthquakes

Similar to tsunamis, scenarios can be used to assess the ground shaking hazards of earthquakes, either probabilistically or deterministically. The probabilities and estimated motion of the ground can be fed into building regulations and used for planning purposes (Figure 5.20.).

Probabilistic seismic hazard assessment (PSHA) was developed in the 1960s (e.g. Cornell, 1968), and although the tools and methods have been improved recently, the basic concepts and assumptions remain the same. In a PSHA, all potential earthquake sources that could affect a given area are considered with their individual earthquake magnitude-frequency distribution (the relationship between the magnitude and frequency of the earthquakes is inverse, i.e. low magnitude earthquakes are more frequent). Combining this information with ground motion prediction models, in which earthquake ground shaking is given as a function of distance, magnitude and potentially other source parameters, provides an estimation of the probability of various levels of ground shaking at a given location.

In a deterministic model, the source of the earthquake is assumed, e.g. a 'worst-case' or 'most likely' event, and the corresponding ground shaking is calculated. Such models have been developed for a wide range of scenarios using both fairly simple 1D stochastic models (e.g. Atkinson & Assatourians, 2015) and much more complex 3D numerical models (e.g. Chaljub *et al.,* 2010).

Submarine landslides

Predicting the generation, propagation and trigger of tsunami waves can help to reduce the losses caused by submarine landslides. This is done by providing an estimate of the threatened areas and the intensity of the hazard, allowing for the design of appropriate protective measures. Marine models are fundamental tools to assess the direct and indirect (tsunami-related) hazards to offshore and coastal human settlements and infrastructures caused by submarine- and/or coastal landslides. Modelling is fundamental in the assessment of the stability of submerged slopes, where catastrophic failure or significant deformation can damage inhabited areas or infrastructures on the slope itself, and in propagation areas (e.g. Zhu & Randolph, 2010). In the case of medium to large failures, propagation of tsunami waves generated by landslides can be simulated with numerical models to predict the distribution of wave height and run-up in the surrounding areas.

In the last two decades, models have been significantly improved by the development of large-strain stress numerical techniques for the analysis of triggering and propagation stages (large-strain finite element analyses or the material point method; Dey *et al.,* 2016; Soga *et al.,* 2016); the application of smoothed particle hydrodynamics (SPH) techniques to analyse the runout of the tsunami wave; the development of models for gas-hydrate sediments (Sultan & Garziglia, 2011); models of sediment shear band theories (e.g. Zhang *et al.,* 2020); and the assessment of the effect of seismic/cyclic loading on the slope failure in homogeneous sediments or with weak soil horizons.

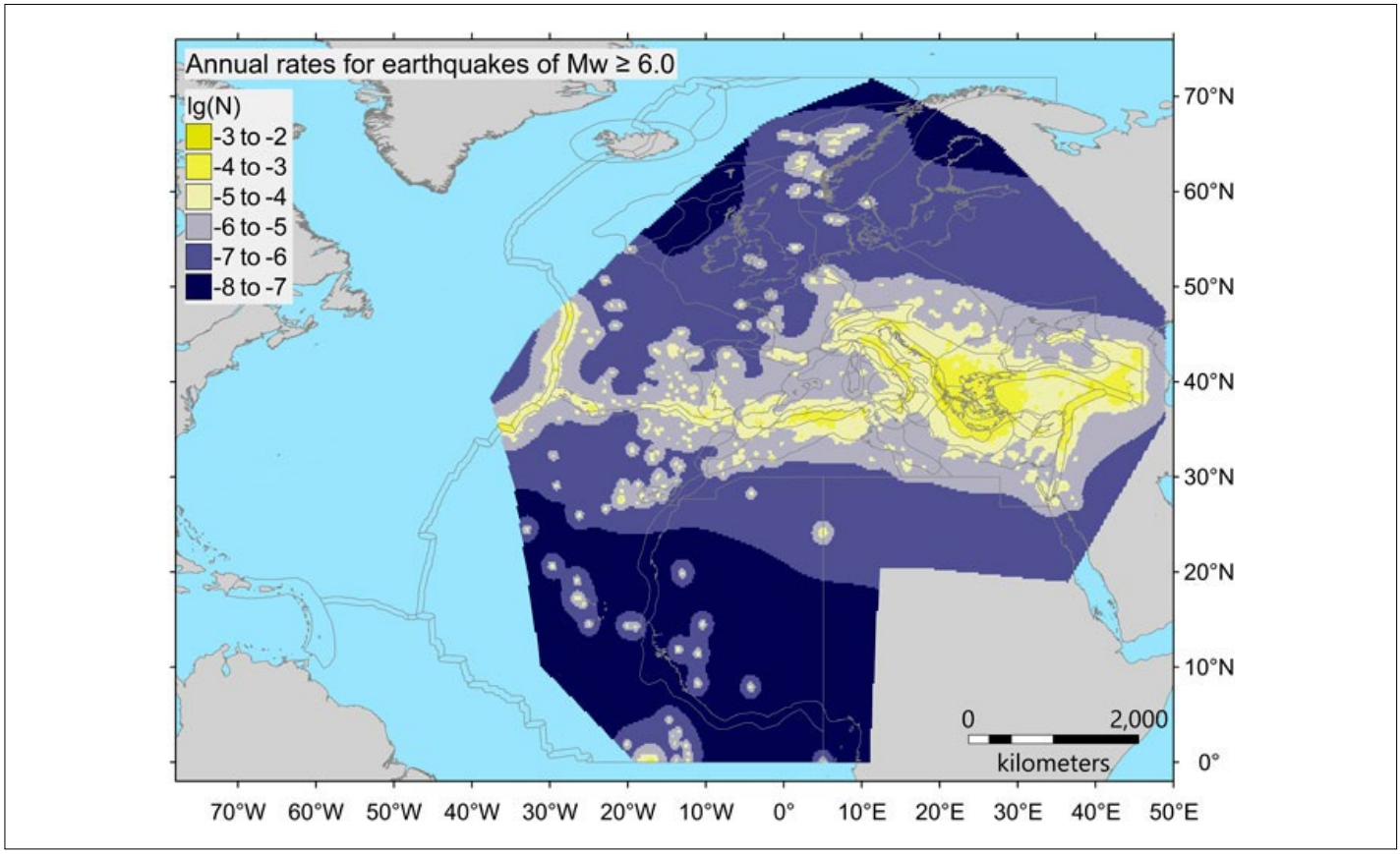

Figure 5.20. Map showing the geographic distribution of annual earthquake rates for $M_w \geq 6.0$ for two seismicity model types. Using a common logarithm scale, lower numbers (dark purple) means lower annual earthquake rates.

A lack of geotechnical data hampers the prediction power of submarine slope models. Although the reconstruction of morphological features and seismic stratigraphy through geophysical investigations is detailed and covers large areas, it does not provide all the input data needed by the models used for hazard assessments. Thus, substantial effort is needed to collect experimental data both *in situ* and in the laboratory, on the mechanical behaviour of sediments, pore pressure regime and sub-bottom structural and geological features of slopes that can control the slope behaviour under static and seismic/cyclic loading (e.g. in the presence of gas-hydrates). The collection of such data is only possible if both offshore and *in situ* facilities in near seafloor conditions are available to European research institutions.

At present, the three main methods to investigate submarine landslides and the associated landslide-generated waves are laboratory experiments, analytical solutions and numerical modelling. Ideally, these should be used in combination: analytical solutions are only appropriate for simple cases; laboratory experiments represent the most straightforward way to study the landslides and their induced waves, but provide challenges in terms of scaling of the problem; and scaled physical experiments can be both time-consuming and costly. By contrast, numerical models, if properly validated with laboratory experiments or observed data, are a more flexible and efficient tool, which can easily provide flow variables at any point in space and are therefore better for a detailed study of the underlying physical processes.

Heidarzadeh *et al.,* (2014) provided an excellent review of the state-of-the-art numerical tools used for modeling landslide-generated waves. They divided the landslide tsunami models into: (1) models treating the moving mass as a fluid (Kawamata *et al.,* 2005); (2) models estimating the initial water surface (Lynett & Liu, 2002); and (3) models fed by transient seafloor deformation (Lynett *et al.,* 2002; Satake, 2012). The selection of a particular model depends on the dimensions of the source, the available computing capacities, the availability of a fine bathymetric grid, and the purpose of the models.

Volcanoes

The hazard impacts of volcanic processes cover a diversity of phenomena, ranging from magma eruptions, to lava balloons on the sea surface, to ash dispersal in the stratosphere. Given the scope of the potential impact on society and the Blue Economy, a multidisciplinary approach is crucial for modelling volcanoes. Integrating scaled laboratory experiments (such as building of scaled models with analogue materials) with numerical simulations allows systematic evaluation of the model outcomes, which then need to be tested against observations and measurements.

As our understanding of the physical processes in volcanology is evolving, the conceptual modelling framework needs to be adapted to include new insights (Kavanagh *et al.,* 2018). Model boundary conditions are based on diverse data sources, including geophysics, geochemistry and petrology, in combination with input from fluid dynamics, engineering or material science. Advancements in technological observation capacities, such as drones or autonomous systems, coupled with increasing data resolution, especially in geochronology, are advancing the modelling abilities in volcanology and will allow the quantification of complex physical processes and their impact on hazard assessment.

BOX 5: GRAND CHALLENGES IN MARINE GEOHAZARD SCIENCE

1. A thorough characterization of past geohazard events and an assessment of their frequency has to feed into a census of geohazard features and manifestations in European seas. This is the only feasible pathway **to provide a better database on the recurrence of certain events and to gather crucial data for probabilistic risk assessment**, e.g. for reinsurance companies and other stakeholders, which in turn will be of broad societal benefit, in particular in settlements close to the coast.
2. Monitoring of active geodynamic processes and the understanding of the underlying mechanisms is expensive. It requires both designated natural marine geohazard laboratories, and national and overarching **integrated European efforts such as European deep-sea monitoring infrastructures.** These efforts will enable permanent geophysical monitoring of the seafloor to expand submarine observatory arrays to multi-scale, multi-method surveillance. **A transformative multi-hazard assessment will provide better management of present-day risks** such as slope movements, sub-seafloor fluid flow, and other destabilizing factors with tsunami potential, and is important for protecting coastal communities and their infrastructures and hence, the EU Blue Economy.
3. One key aspect in geohazard research is time, i.e. at what stage can a certain event or risk unambiguously be identified. Consequently, innovative technologies (including artificial intelligence, smart sensors, etc.) are required to record and recognize precursors to significant geohazard events. The reliability, integrity and coverage of early warning networks based on seismological, geotechnical and other emerging methods is key. This will result in increasing warning times and improved forecast quality, specifically focused on tsunamis. We have **to deliver the capability to effectively warn coastal societies and protect these communities, their infrastructure (ports, harbours, buildings, energy and aquaculture platforms, etc.), as well as the ecosystems and their services.**
4. Apart from the (mostly) geophysical approaches in geohazard monitoring, one key aspect in a changing climate is the potential link to how climate change may enhance geohazards, e.g. by changing ocean temperature and currents, causing more abundant storm events (and associated run-off, sediment remobilization, etc.), groundwater charging, etc. Questions remain regarding whether we can **identify (and quantify) a climate-induced increase in natural hazards** and potentially geohazards, and whether the probability of their occurrence could be modelled. Specifically, to model geological processes, larger time-scales are needed for both hindcast and predictive models. Modelling past tsunami wave propagation, wave height and inundation, and landslide reconstruction have been successful. In the future, **machine learning approaches** using (big) data from these past events and present-day processes will be able to provide knowledge on geohazards, future mitigation measures and resilience. The momentum gained from **digitization** due to the COVID-19 pandemic and other recent advances should be used to this end.

Credit: Sheila Heymans

6 Recommendations

Credit: Dzintra Grinbergs

Marine geohazards are a serious threat to European communities and infrastructure both on the coast and offshore. Such events can have far-reaching effects on the Blue Economy and on our closely interwoven societies in Europe. Europe's increasing reliance on high-technology industry, including the exponential increase in offshore infrastructure for renewable energy, communication and resource extraction raises our vulnerability to marine geohazards.

In view of future destructive events due to marine geohazards, we need to enhance our understanding of the processes that trigger marine geohazards, advance our ability to assess and forecast these hazards, and transfer this scientific knowledge to practical mitigation actions, in order to augment society's resilience.

It is therefore essential to prepare public authorities that manage coastal and marine areas, and the communities that live there (Section 6.1). This requires improved understanding of where and why marine geohazards occur, in order to provide the basic knowledge needed to forecast and assess hazards and provide it to civil protection in a timely manner (Section 6.2).

6.1 Advancing hazard mitigation for policy making and the Blue Economy

1. **Increase awareness of marine geohazards among public authorities and communities.** For safe and sustainable use of the seafloor, public authorities and policymakers responsible for coastal and maritime management and planning need to be aware of the significance of marine geohazards. National and local public bodies responsible for coastal communities and infrastructures are well aware of land-based natural hazards, but the potential of offshore threats remain mostly unknown. The reasons for this lack of attention are: 1) technologies to highlight the marine geohazard features are relatively new; and 2) up to a decade ago, the use of the seafloor was limited and there was little need to manage submerged territories. Similarly, public awareness of natural marine hazards is often low, even though the two very large tsunamis that hit Asia in 2004 (Indonesia) and 2011 (Japan), demonstrated how real marine geohazards can be and that they are not 'a thing from the past'.

   We recommend that marine geohazards are included as natural hazards in all policies relating to risk mitigation and land management, at European, regional, national and local levels.

2. **Address marine geohazards in administrative management rules.** A specific obstacle in managing marine geohazards is the lack of an appropriate policy framework in which to frame them. Because of the novelty of the tools to detect and quantify marine geohazards, national- and EU-level legislation is often poorly defined. Local agencies in charge of land management should be required to transform scientific knowledge acquired on marine geohazards into regulatory guidelines or restrictions to be applied, and co-develop with Civil Protection Agencies (or other similar) actions to be taken in case of emergency (see Box 4).

   We recommend that marine geohazards are considered in local, national and EU legislation such as the EU Maritime Spatial Planning Directive, legislation pertaining to Integrated Coastal Zone Management, and that pertaining to the safe development of the Sustainable Blue Economy.

3. **Require industrial technology to be available for marine geohazard research.** The technological advancement in offshore energy production and data transfer will allow more infrastructure to be placed on the seafloor. If these infrastructures were equipped with sensors they would offer a unique opportunity to have real-time *in situ* measurements. The SMART cables initiative described in Chapter 5 is a good start but any powered industrial offshore installation that can transmit data could be used as a monitoring tool if required to do so by legislation.

   We recommend that public authorities require all seafloor infrastructure installations to also be used for environmental and geohazards monitoring.

4. **Model the potential impact of marine geohazards** that could be quantified using hazard maps or risk models to set up early warning and rapid response systems. Marine geohazards are usually treated as individual hazards, monitored separately, and assessment without considering other phenomena that can trigger, or be triggered by, marine geohazards. It is therefore crucial to consider the cascading effect of marine geohazards (Chapter 2) that may significantly amplify the risk. For instance, seismic hazard assessment should include the possibility of tsunamis generated by submarine landslides triggered by ground shaking, as such effects may be comparable or even higher than the earthquake itself (Chapter 3).

   We recommend that all mayor coastal settlements and industrial infrastructures develop probabilistic scenarios of marine geohazard risks.

5. **Enhance scientific research on marine geohazards at all levels** (infrastructure development, technological advancement, knowledge transfer) and stimulate education and public outreach on the understanding of the processes, impacts and consequences of marine geohazards. A stakeholder forum is needed to enable a sustained dialogue between the research community and stakeholders. This is necessary to inform all stakeholders about the breadth of marine hazards that have to be taken into account and communicate new research results. It would also allow stakeholders to communicate their knowledge needs and experience to the scientific community to generate the crucial research that is required for policy development.

   We recommend that a stakeholder forum be established to identify knowledge gaps and technological needs. This could be achieved through the development of specific EU research programs on marine geohazards.

6.2 Science needed to understand processes, triggers and precursors

1. **Designate natural laboratories for marine geohazards**, i.e. areas with a seismogenic fault, a flank of an active volcano, or a submarine slope prone to failure (Chapter 3), either for individual hazards or in a multi-hazard strategy. Funding opportunities need to be set up to focus the activities of EU researchers in these natural laboratories by using different approaches, technologies, methods and data. The aim is to equip natural laboratories with (submarine) observatory networks similar to that achieved on land (geodesy, seismology, geochemistry, etc.). High-density geodetic measurements acquired onshore were instrumental in understanding fault dynamics, seismic hazards and the dynamics of landslides, and will be equally transformative at sea to identify chemical, physical, or morphological precursors of geohazard events (Chapter 5). Data produced by observatories and by research groups focusing on these natural laboratories should be fully compliant with open data policy to provide comprehensive data sets available to the scientific community and stakeholders.

   We recommend that a field laboratory for marine geohazards should be set up at a focus site in Europe to concentrate research, facilities and in situ modelling.

2. **Promote a census of geohazard features in European seas,** using homogeneous data acquisition and interpretation standards. The volume of morpho-bathymetric data already available is very large and will increase exponentially in the near future (e.g. Seabed 2030[19]). Implementing homogeneous standards for geohazard feature identification, interpretation and cartographic representation will ensure a pan-European approach for the investigation. It will also ensure the safe use of the seafloor and promote economic activities that will use this database for desktop studies. Full coverage maps of marine geohazards in Europe exist only for earthquakes and tsunamis (Chapter 3) as they are derived from land-based instrumental networks or models. No homogeneous and full-coverage maps of landslides, seismogenetic faults, fluid escapes or active volcanic features exist for European seas. On land, such maps are the primary tool for geohazard assessment and this needs to be expanded offshore.

   We recommend that a common standard for marine geohazard interpretation and mapping be promoted to ensure the safe development of the Blue Economy.

3. **Integrate EU marine monitoring infrastructures** such as EMSO (European Multidisciplinary Seafloor and Water-Column Observatory) and all other long-term monitoring of high-risk areas **with seafloor mapping and geohazard research**. Permanent seafloor observatories continuously collect environmental data in a fixed position, while seafloor mapping of geohazard features will provide data continuous in space but collected at one specific time (Chapter 5). As seismic, acoustic and chemical signals in the deep sea can travel for tens of kilometres, a comparison between detailed maps of geohazard features and the signals from observatories will allow us to understand the evolution of geohazard phenomena such as mass wasting, volcanic eruption, activity at faults and of gravity flows through time, and possibly define precursors.

   We recommend that long-term in situ monitoring be combined with geohazard studies in the surrounding region to identify long-range signals.

4. **Promote innovative technologies to conceive and realize novel sensors and new methods** to study submarine geohazards and their precursory signals, including through collaborative research with industry. The increase in performance (e.g. reduced power consumption) or the decrease in size and cost of existing sensors should also be promoted. Develop a new generation of models to help interpret and provide robust and innovative methods for long-term hazard assessments and short-term forecasting of marine geohazards. This approach needs to cover all time scales, from seconds to hours (landslides, earthquakes, tsunamis), days to years (volcanic eruptions, migrating bedforms, fluid activities), and years to millions of years (e.g. seafloor deformation) (Chapter 1).

   We recommend that technological advancement be supported in order to improve the detection capability and availability of sensors.

5. **Data mining, virtual access and AI.** Advances in digitalization, open data and implementation of interpretative standards will allow European researchers to virtually access data, while data interoperability may facilitate the interface between data acquisition systems and databases with high-performance computing platforms dedicated to data mining and model assimilation. These activities will be underpinned by exploiting advances in artificial intelligence (AI) and big data science and are essential to fully harvest the growing volumes of marine data.

   We recommend that holistic databases of raw data and homogeneous interpretations be created and made available to the scientific community to apply advanced techniques in support of marine geohazard studies.

[19] https://seabed2030.org

References

Admire, A. R., Dengler, L. A., Crawford, G. B., Uslu, B. U., Borrero, J. C., Greer, S. D., & Wilson, R. I. (2014). Observed and Modeled Currents from the Tohoku-oki, Japan and other Recent Tsunamis in Northern California. *Pure and Applied Geophysics, 171*(12), 3385–3403. https://doi.org/10.1007/s00024-014-0797-8

Adriano, B., Hayashi, S., Gokon, H., Mas, E., & Koshimura, S. (2016). Understanding the Extreme Tsunami Inundation in Onagawa Town by the 2011 Tohoku Earthquake, Its Effects in Urban Structures and Coastal Facilities. *Coastal Engineering Journal, 58*. https://doi.org/10.1142/S0578563416400131

Altınok, Y., & Ersoy, Ş. (2000). Tsunamis Observed on and Near the Turkish Coast. *Natural Hazards, 21*, 185–205. https://doi.org/10.1023/A:1008155117243

Altınok, Y., Tinti, S., Alpar, B., Yalçıner, A. C., Ersoy, Ş., Bortolucci, E., & Armigliato, A. (2001). The Tsunami of August 17, 1999 in Izmit Bay, Turkey. *Natural Hazards, 24*, 133–146. https://doi.org/10.1023/A:1011863610289

Ambraseys, N. N. (2002). The Seismic Activity of the Marmara Sea Region over the Last 2000 Years. B*ulletin of the Seismological Society of America, 92*(1). https://doi.org/10.1785/0120000843

Ambraseys, N. N., & Finkel, C. F. (1987). Seismicity of Turkey and neighbouring regions, 1899-1915. *Annales Geophysicae. Series B. Terrestrial and Planetary Physics, 5*(6), 701–725. http://pascal-francis.inist.fr/vibad/index.php?action=getRecordDetail&idt=7462215

Ambraseys, N. N., & Synolakis, C. (2010). Tsunami Catalogs for the Eastern Mediterranean, Revisited. *Journal of Earthquake Engineering, 14*(3). https://doi.org/10.1080/13632460903277593

Antonopoulos, J. (1992). The great Minoan eruption of Thera volcano and the ensuing tsunami in the Greek Archipelago. *Natural Hazards, 5*, 153–168. https://doi.org/10.1007/BF00127003

Araki, E., Saffer, D. M., Kopf, A. J., Wallace, L. M., Kimura, T., Machida, Y., Ide, S., Davis, E. E., & IODP Expedition 365 shipboard scientists. (2017). Recurring and triggered slow-slip events near the trench at the Nankai Trough subduction megathrust. *Science, 356*(6343), 1157–1160. https://doi.org/10.1126/science.aan3120

Armijo, R., Pondard, N., Meyer, B., Uçarkus, G., Mercier de Lépinay, B., Malavieille, J., Dominguez, S., Gutscher, M.-A., Schmidt, S., Beck, C., Çağatay, M. N., Çakir, Z., Imren, C., Eri , K. K., Natalin, B., Özalaybey, S., Tolun, L., Lefèvre, I., Seeber, L., ... Sarikavak, K. (2005). Submarine fault scarps in the Sea of Marmara pull-apart (North Anatolian Fault): Implications for seismic hazard in Istanbul. *Geochemistry, Geophysics, Geosystems, 6*(6). https://doi.org/10.1029/2004GC000896

Atkinson, G. M., & Assatourians, K. (2015). Implementation and Validation of EXSIM (A Stochastic Finite Fault Ground Motion Simulation Algorithm) on the SCEC Broadband Platform. *Seismological Research Letters, 86*(1), 48–60. https://doi.org/10.1785/0220140097

Balkıs, N. (2003). The effect of Marmara (zmit) Earthquake on the chemical oceanography of İzmit Bay, Turkey. *Marine Pollution Bulletin, 46*(7), 865–878. https://doi.org/10.1016/S0025-326X(03)00063-8

Baptista, M. A., Heitor, S., Miranda, J. M., Miranda, P., & Victor, L. M. (1998). The 1755 Lisbon tsunami: Evaluation of the tsunami parameters. *Journal of Geodynamics, 25*(1–2), 143–157. https://doi.org/10.1016/S0264-3707(97)00019-7

Barka, A. (1999). The 17 August 1999 Izmit Earthquake. *Science, 285*(5435), 1858–1859. https://doi.org/10.1126/science.285.5435.1858

Barreca, G., Gross, F., Scarfì, L., Aloisi, M., Monaco, C., & Krastel, S. (2021). The Strait of Messina: Seismotectonics and the source of the 1908 earthquake. *Earth-Science Reviews, 218*. https://doi.org/10.1016/j.earscirev.2021.103685

Barreyre, T., Escartín, J., Garcia, R., Cannat, M., Mittelstaedt, E., & Prados, R. (2012). Structure, temporal evolution, and heat flux estimates from the Lucky Strike deep-sea hydrothermal field derived from seafloor image mosaics. *Geochemistry, Geophysics, Geosystems, 13*(4). https://doi.org/10.1029/2011GC003990

Barrie, J. V., Hill, P. R., Conway, K. W., Iwanowska, K., & Picard, K. (2005). Environmental Marine Geoscience 4. Georgia Basin: Seabed Features and Marine Geohazards. *Geoscience Canada, 32*(4). https://journals.lib.unb.ca/index.php/GC/article/view/2717

Basili, R., Brizuela, B., Herrero, A., Iqbal, S., Lorito, S., Maesano, F. E., Murphy, S., Perfetti, P., Romano, F., Scala, A., Selva, J., Taroni, M., Tiberti, M. M., Thio, H. K., Tonini, R., Volpe, M., Glimsdal, S., Harbitz, C. B., Løvholt, F., ... Zaytsev, A. (2021). The Making of the NEAM Tsunami Hazard Model 2018 (NEAMTHM18). *Frontiers in Earth Science*. https://doi.org/10.3389/feart.2020.616594

Behrens, J., Løvholt, F., Jalayer, F., Lorito, S., Salgado-Gálvez, M. A., Sørensen, M., Abadie, S., Aguirre-Ayerbe, I., Aniel-Quiroga, I., Babeyko, A., Baiguera, M., Basili, R., Belliazzi, S., Grezio, A., Johnson, K., Murphy, S., Paris, R., Rafliana, I., De Risi, R., ... Vyhmeister, E. (2021). Probabilistic Tsunami Hazard and Risk Analysis: A Review of Research Gaps. *Frontiers in Earth Science*. https://doi.org/10.3389/feart.2021.628772

Berndt, C., Brune, S., Nisbet, E., Zschau, J., & Sobolev, S. V. (2009). Tsunami modeling of a submarine landslide in the Fram Strait. *Geochemistry, Geophysics, Geosystems, 10*(4). https://doi.org/10.1029/2008GC002292

Best, M. M. R., Favali, P., Beranzoli, L., Blandin, J., Çağatay, M. N., Cannat, M., Dañobeitia, J. J., Delory, E., de Miranda, J. M. A., Del Rio Fernandez, J., de Stigter, H., Gillooly, M., Grant, F., Hall, P. O. J., Hartman, S., Hernandez-Brito, J., Lanteri, N., Mienert, J., Oaie, G., ... Waldmann, C. (2016). The EMSO-ERIC Pan-European Consortium: Data Benefits and Lessons Learned as the Legal Entity Forms. *Marine Technnology Society Journal, 50*(3), 8-15(8). https://doi.org/10.4031/MTSJ.50.3.13

Bird, P. (2003). An updated digital model of plate boundaries. *Geochemistry, Geophysics, Geosystems, 4*(3). https://doi.org/10.1029/2001GC000252

Biscara, L., Hanquiez, V., Leynaud, D., Marieu, V., Mulder, T., Gallissaires, J.-M., Crespin, J.-P., Braccini, E., & Garlan, T. (2012). Submarine slide initiation and evolution offshore Pointe Odden, Gabon — Analysis from annual bathymetric data (2004–2009). *Marine Geology, 299–302*, 43–50. https://doi.org/10.1016/j.margeo.2011.11.008

Blikra, L. H., Longva, O., Braathen, A., Anda, E., Dehls, J. F., & Stalsberg, K. (2006). ROCK SLOPE FAILURES IN NORWEGIAN FJORD AREAS: EXAMPLES, SPATIAL DISTRIBUTION AND TEMPORAL PATTERN. In *Landslides from Massive Rock Slope Failure* (pp. 475–496). Springer. https://doi.org/10.1007/978-1-4020-4037-5_26

Bly, M. (Ed.). (2011). *Deepwater Horizon accident investigation report*. Diane Publishing. https://www.sec.gov/Archives/edgar/data/313807/000119312510216268/dex993.htm

Bompais, X., Garziglia, S., Blandin, J., & Hello, Y. (2019). EMSO-Ligure Nice, a Coastal Cabled Observatory Dedicated to the Study of Slope Stability. *OCEANS 2019 - Marseille,* 1–8. https://doi.org/10.1109/OCEANSE.2019.8867040

Bondevik, S., Løvholt, F., Harbitz, C. B., Mangerud, J., Dawson, A. G., & Svendsen, J. I. (2005). The Storegga Slide tsunami—comparing field observations with numerical simulations. In A. Solheim, P. Bryn, K. Berg, H. P. Sejrup, & J. Mienert (Eds.), *Ormen Lange–an Integrated Study for Safe Field Development in the Storegga Submarine Area* (pp. 195–208). Elsevier. https://doi.org/10.1016/B978-0-08-044694-3.50021-4

Bondevik, Stein, Mangerud, J., Dawson, S., Dawson, A. G., & Lohne, Ø. (2005). Evidence for three North Sea tsunamis at the Shetland Islands between 8000 and 1500 years ago. *Quaternary Science Reviews, 24*(14–15), 1757–1775. https://doi.org/10.1016/j.quascirev.2004.10.018

Bosman, A., Casalbore, D., Romagnoli, C., & Chiocci, F. L. (2014). Formation of an 'a' lava delta: insights from time-lapse multibeam bathymetry and direct observations during the Stromboli 2007 eruption. *Bulletin of Volcanology, 76*(838). https://doi.org/10.1007/s00445-014-0838-2

Bouchon, M., Karabulut, H., Aktar, M., Özalaybey, S., Schmittbuhl, J., & Bouin, M.-P. (2011). Extended Nucleation of the 1999 M_w 7.6 Izmit Earthquake. *Science, 331*(6019), 877–880. https://doi.org/10.1126/science.1197341

Bridges, K., Cox, D., Thomas, S., Shin, S., & Rueben, M. (2011). Large-Scale Wave Basin Experiments on the Influence of Large Obstacles on Tsunami Inundation Forces. *Coastal Structures*, 1237–1248. https://doi.org/10.1142/9789814412216_0107

Brown, K. M. (1990). The nature and hydrogeologic significance of mud diapirs and diatremes for accretionary systems. *JGR Solid Earth, 95*(B6), 8969–8982. https://doi.org/10.1029/JB095iB06p08969

Çağatay, M. N., Erel, L., Bellucci, L. G., Polonia, A., Gasperini, L., Eri , K. K., Sancar, Ü., Biltekin, D., Uçarku , G., Ülgen, U. B., & Damcı, E. (2012). Sedimentary earthquake records in the zmit Gulf, Sea of Marmara, Turkey. *Sedimentary Geology, 282,* 347–359. https://doi.org/10.1016/j.sedgeo.2012.10.001

Caress, D. W., Clague, D. A., Paduan, J. B., Martin, J. F., Dreyer, B. M., Chadwick Jr, W. W., Denny, A., & Kelley, D. S. (2012). Repeat bathymetric surveys at 1-metre resolution of lava flows erupted at Axial Seamount in April 2011. *Nature Geoscience, 5,* 483–488. https://doi.org/10.1038/ngeo1496

Carracedo, J. C., Torrado, F. P., González, A. R., Soler, V., Turiel, J. L. F., Troll, V. R., & Wiesmaier, S. (2012). The 2011 submarine volcanic eruption in El Hierro (Canary Islands). *Geology Today, 28*(2), 53–58. https://doi.org/10.1111/j.1365-2451.2012.00827.x

Carter, L., Burnett, D., Drew, S., Marle, G., Hagadorn, L., Bartlett-McNeil, D., & Irvine, N. (2009). Submarine cables and the oceans: connecting the world. In *UNEP-WCMC Biodiversity Series N°. 31*. ICPC/UNEP/UNEP-WCMC. http://www.unep-wcmc.org/resources/publications/%0AUNEP_WCMC_bio_series/31.aspx%0Ahttp://www.iscpc.org/publications/icpc-unep_report.pdf

Casalbore, D., Bosman, A., & Chiocci, F. L. (2012). Study of Recent Small-Scale Landslides in Geologically Active Marine Areas Through Repeated Multibeam Surveys: Examples from the Southern Italy. In *Submarine Mass Movements and Their Consequences: 5th International Symposium* (pp. 573–582). Springer.

Casalbore, D., Ingrassia, M., Pierdomenico, M., Beaubien, S. E., Martorelli, E., Bigi, S., Ivaldi, R., DeMarte, M., & Chiocci, F. L. (2020). Morpho-acoustic characterization of a shallow-water mud volcano offshore Scoglio d'Affrica (Northern Tyrrhenian Sea) responsible for a violent gas outburst in 2017. *Marine Geology, 428*. https://doi.org/10.1016/j.margeo.2020.106277

Casalbore, D., Romagnoli, C., Bosman, A., & Chiocci, F. L. (2011). Potential tsunamigenic landslides at Stromboli Volcano (Italy): Insight from marine DEM analysis. *Geomorphology, 126*(1–2), 42–50. https://doi.org/10.1016/j.geomorph.2010.10.026

Casas, D., Chiocci, F. L., Casalbore, D., Ercilla, G., & de Urbina, J. O. (2016). Magnitude-frequency distribution of submarine landslides in the Gioia Basin (southern Tyrrhenian Sea). *Geo-Marine Letters, 36*, 405–414. https://doi.org/10.1007%2Fs00367-016-0458-2

Cattaneo, A., Babonneau, N., Ratzov, G., Dan-Unterseh, G., Yelles, K., Bracène, R., Mercier de Lépinay, B., & Déverchère, J. (2012). Searching for the seafloor signature of the 21 May 2003 Boumerdès earthquake offshore central Algeria. *Natural Hazards and Earth System Sciences, 12*(7), 2159–2172. https://doi.org/10.5194/nhess-12-2159-2012

Cecchini, S., Taliana, D., Giacomini, L., Herisson, C., & Bonnemaire, B. (2011). Submarine geo-hazards on the eastern Sardinia-Corsica continental margin based on preliminary pipeline route investigation. *Marine Geophysical Research, 32*, 71–81. https://doi.org/10.1007/s11001-011-9126-0

Cerase, A., Longa, M., La Crescimbene, F., & Amato, A. (2019). Tsunami risk perception in southern Italy: first evidence from a sample survey. *Natural Hazards and Earth System Sciences, 19*, 2887–2904. https://doi.org/10.5194/nhess-19-2887-2019

Cesca, S., Grigoli, F., Heimann, S., González, Á., Buforn, E., Maghsoudi, S., Blanch, E., & Dahm, T. (2014). The 2013 September–October seismic sequence offshore Spain: a case of seismicity triggered by gas injection? *Geophysical Journal International, 198*(2), 941–953. https://doi.org/10.1093/gji/ggu172

Cesca, S., Stich, D., Grigoli, F., Vuan, A., López-Comino, J. Á., Niemz, P., Blanch, E., Dahm, T., & Ellsworth, W. L. (2021). Seismicity at the Castor gas reservoir driven by pore pressure diffusion and asperities loading. N*ature Communicationsomm, 12*. https://doi.org/10.1038/s41467-021-24949-1

Chaljub, E., Moczo, P., Tsuno, S., Bard, P.-Y., Kristek, J., Käser, M., Stupazzini, M., & Kristekova, M. (2010). Quantitative Comparison of Four Numerical Predictions of 3D Ground Motion in the Grenoble Valley, France. *Bulletin of the Seismological Society of America, 100*(4), 1427–1455. https://doi.org/10.1785/0120090052

Chaves, A. (1904). *Erupções submarinas nos Açores e a quebra de alguns dos cabos telegráficos lançados nos mares do mesmo arquipélago Archivo dos Açores, XIII: 53-60*.

Chaves, A. (1915). *Erupções submarinas nos Açores: Informações que os navegantes podem prestar sobre tal assunto, Lisboa : Tip. d'A Modesta.*

Chiocci, F. L., Cattaneo, A., & Urgeles, R. (2011). Seafloor mapping for geohazard assessment: state of the art. *Marine Geophysical Research, 32*(1–2), 1–11. https://doi.org/10.1007/s11001-011-9139-8

Chiocci, F. L., & De Alteriis, G. (2006). The Ischia debris avalanche: first clear submarine evidence in the Mediterranean of a volcanic island prehistorical collapse. *Terra Nova, 18*(3), 202–209. https://doi.org/10.1111/j.1365-3121.2006.00680.x

Chiocci, F. L., & Ridente, D. (2011). Regional-scale seafloor mapping and geohazard assessment. The experience from the Italian project MaGIC (Marine Geohazards along the Italian Coasts). *Marine Geophysical Research, 32*, 13–23. https://doi.org/10.1007/s11001-011-9120-6

Chiocci, F. L., Romagnoli, C., & Bosman, A. (2008). Morphologic resilience and depositional processes due to the rapid evolution of the submerged Sciara del Fuoco (Stromboli Island) after the December 2002 submarine slide and tsunami. *Geomorphology, 100*(3–4), 356=365. https://doi.org/10.1016/j.geomorph.2008.01.008

Chiocci, F. L., Romagnoli, C., Tommasi, P., & Bosman, A. (2008). The Stromboli 2002 tsunamigenic submarine slide: Characteristics and possible failure mechanisms. *JGR Solid Earth, 113*(B10). https://doi.org/10.1029/2007JB005172

Christodoulou, D. (2010). *Geophysical, geotechnical, sedimentological and remote sensing monitoring of active pockmarks field in high seismicity regions, Western Greece*. University of Patras.

Christodoulou, D., Papatheodorou, G., Ferentinos, G., & Masson, M. (2003). Active seepage in two contrasting pockmark fields in the Patras and Corinth gulfs, Greece. *Geo-Marine Letters, 23*, 194–199. https://doi.org/10.1007/s00367-003-0151-0

Clare, M. A., Vardy, M. E., Cartigny, M. J. B., Talling, P. J., Himsworth, M. D., Dix, J. K., Harris, J. M., Whitehouse, R. J. S., & Belal, M. (2017). Direct monitoring of active geohazards: emerging geophysical tools for deep-water assessments. *Near Surface Geophysics, 15*(4), 427–444. https://doi.org/10.3997/1873-0604.2017033

Colantoni, P. (1997). Coastal defence by breakwaters and sea-level rise: the case of the Italian Northern Adriatic Sea. In *Bulletin-Institut CIESM Science series 3, Evol. of Mediterranean*. https://ciesm.org/catalog/index.php?article=6003

Colantoni, P., Gennesseaux, M., Vanney, J. R., Ulzega, A., Melegari, G., & Trombetta, A. (1992). Dynamic processes of a submarine canyon of Gioia Tauro, Tyrrhenian Sea. *Gionale Di Geologia, 3*(54/2), 199–213.

Comerci, V., Vittori, E., Blumetti, A. M., Brustia, E., Di Manna, P., Guerrieri, L., Lucarini, M., & Serva, L. (2015). Environmental effects of the December 28, 1908, Southern Calabria–Messina (Southern Italy) earthquake. *Natural Hazards, 76*, 1849–1891. https://doi.org/10.1007%2Fs11069-014-1573-x

Conway, K. W., Barrie, J. V., Picard, K., & Bornhold, B. D. (2012). Submarine channel evolution: active channels in fjords, British Columbia, Canada. *Geo-Marine Letters, 32*, 301–312. https://doi.org/10.1007/s00367-012-0280-4

Cornell, C. A. (1968). Engineering seismic risk analysis. *Bulletin of the Seismological Society of America, 58*(5), 1583–1606. https://doi.org/10.1785/BSSA0580051583

CRED, & UNISDR. (2018). *Economic Losses, Poverty & Disasters: 1998-2017*. http://www.unisdr.org/files/61119_credeconomiclosses.pdf

Cutter, S. L. (2018). Compound, Cascading, or Complex Disasters: What's in a Name? *Environment: Science and Policy for Sustainable Development, 60*(6). https://doi.org/10.1080/00139157.2018.1517518

Dan, G., Sultan, N., & Savoye, B. (2007). The 1979 Nice harbour catastrophe revisited: Trigger mechanism inferred from geotechnical measurements and numerical modelling. *Marine Geology, 245*(1–4), 40–64. https://doi.org/10.1016/j.margeo.2007.06.011

Dan, G., Sultan, N., & Sayove, B. (2007). The 1979 Nice harbour catastrophe revisited: Trigger mechanism inferred from geotechnical measurements and numerical modelling. *Marine Geology, 245*(1–4), 40–64. https://doi.org/10.1016/j.margeo.2007.06.011

Daniell, J. E., Schaefer, A. M., & Wenzel, F. (2017). Losses Associated with Secondary Effects in Earthquakes. *Frontiers in Built Environment*. https://doi.org/10.3389/fbuil.2017.00030

Davis, E. E., Heesemann, M., Farrugia, J. J., Johnson, G. C., & Paros, J. (2019). APT: An Instrument for Monitoring Seafloor Acceleration, Pressure, and Temperature with Large Dynamic Range and Bandwidth. *Bulletin of the Seismological Society of America, 109*(1), 448–462. https://doi.org/10.1785/0120180132

de Lange, G. J., Mascle, J., Sakellariou, D., Salamon, A., Rosen, D., Panyides, I., Ceramicola, S., Migeon, S., Sultan, N., & De Martini, P. M. (2011). Marine geo-hazards in the Mediterranean: Executive Summary. In F. Briand (Ed.), *CIESM Workshop Monographs, n° 42: Marine geo-hazards in the Mediterranean* (p. 7). CIESM Publisher. http://www.ciesm.org/online/monographs/index.htm

Dey, R., Hawlader, B. C., Phillips, R., & Soga, K. (2016). Numerical modelling of submarine landslides with sensitive clay layers. *Géotechnique, 66*(5), 454–468. https://doi.org/10.1680/jgeot.15.P.111

Dey, S., & Singh, R. P. (2003). Surface latent heat flux as an earthquake precursor. *Natural Hazards and Earth System Sciences, 3*, 749–755. https://doi.org/10.5194/nhess-3-749-2003

Dilek, Y., Ogawa, Y., & Okubo, Y. (2021). Characterization of modern and historical seismic–tsunamic events and their global–societal impacts. *Geological Society, London, Special Publications, 501,* 1–22. https://doi.org/10.1144/SP501-2021-17

DNV. (2002). Marine risk assessment: Prepared by Det Norske Veritas for the Health and Safety Executive. In *OFFSHORE TECHNOLOGY REPORT 2001/063*. https://www.hse.gov.uk/researcH/otopdf/2001/oto01063.pdf

Dominey-Howes, D. T. M., Papadopoulos, G. A., & Dawson, A. G. (2000). Geological and Historical Investigation of the 1650 Mt. Columbo (Thera Island) Eruption and Tsunami, Aegean Sea, Greece. *Natural Hazards, 21,* 83–96. https://doi.org/10.1023/A:1008178100633

Dyment, J., Szitkar, F., & Levaillant, D. (2018). Ridge propagation, oceanic core complexes, and ultramafic-hosted hydrothermalism at Rainbow (MAR 36°N): Insights from a multi-scale magnetic exploration. *Earth and Planetary Science Letters, 502,* 23–31. https://doi.org/10.1016/j.epsl.2018.08.054

Elbanna, A., Abdelmeguid, M., Ma, X., Amlani, F., Bhat, H. S., Synolakis, C., & Rosakis, A. J. (2021). Anatomy of strike-slip fault tsunami genesis. *PNAS, 118*. https://doi.org/10.1073/pnas.2025632118

Ercilla, G., Casas, D., Alonso, B., Casalbore, D., García-Gil, J., Galindo-Zaldívar, S., Martorelli, E., Vázquez, J.-T., Azpiroz-Zabala, M., DoCouto, D., Estrada, F., Fernández-Puga, M. C., González-Castillo, L., González-Vida, J. M., Idárraga-García, J., Juan, C., Macías, J., Madarieta-Txurruka, A., Nespereira, J., ... Yenes, M. (2021). Offshore Geological Hazards: Charting the Course of Progress and Future Directions. *Oceans, 2*(2), 393–428. https://doi.org/10.3390/oceans2020023

Ergintav, S., Reilinger, R. E., Çakmak, R., Floyd, M., Cakir, Z., Do an, U., King, R. W., McClusky, S., & Özener, H. (2014). Istanbul's earthquake hot spots: Geodetic constraints on strain accumulation along faults in the Marmara seismic gap. *Geophysical Research Letters, 41*(16), 5783–5788. https://doi.org/10.1002/2014GL060985

European Commission. (2020). *The EU Blue Economy Report 2020.* Publications Office of the European Union. https://ec.europa.eu/maritimeaffairs/sites/maritimeaffairs/files/2020_06_blueeconomy-2020-ld_final.pdf

Favali, P., & Beranzoli, L. (2006). Seafloor Observatory Science: A Review. *Annals of Geophysics, 49*(2–3). https://doi.org/10.4401/ag-3125

Favali, P., De Santis, A., Anna, G. D., Di Sabatino, B., Sedita, M., & Rubino, E. (2006). A New Active Volcano in the Tyrrhenian Sea? *Annals of Geophysics, 49*(2–3). https://doi.org/10.4401/ag-3127

Fine, I. V., Rabinovich, A. B., Bornhold, B. D., Thomson, R. E., & Kulikov, E. A. (2005). The Grand Banks landslide-generated tsunami of November 18, 1929: preliminary analysis and numerical modeling. *Marine Geology, 215*(1–2), 45–57. https://doi.org/10.1016/j.margeo.2004.11.007

Freudenthal, T., & Wefer, G. (2013). Drilling cores on the sea floor with the remote-controlled sea floor drilling rig MeBo. Geoscientific Instrumentation, *Methods and Data Systems, 2*(2), 329–337. https://doi.org/10.5194/gi-2-329-2013

Friedrich, W. L., Kromer, B., Friedrich, M., Heinemeier, J., Pfeiffer, T., & Talamo, S. (2006). Santorini eruption radiocarbon dated to 1627-1600 B.C. *Science, 312*. https://doi.org/10.1126/science.1125087.

Fujiwara, T., dos Santos Ferreira, C., Bachmann, A. K., Strasser, M., Wefer, G., Sun, T., Kanamatsu, T., & Kodaira, S. (2017). Seafloor Displacement After the 2011 Tohoku-oki Earthquake in the Northern Japan Trench Examined by Repeated Bathymetric Surveys. *Geophysical Research Letters, 44,* 11,833–11,839. https://doi.org/10.1002/2017GL075839

Fukao, Y. (1973). Thrust faulting at a lithospheric plate boundary: The Portugal earthquake of 1969. *Earth and Planetary Science Letters, 18,* 205–216.

Gales, J. A., Talling, P. J., Cartigny, M. J. B., Clarke, J. E. H., Lintern, G., Stacey, C. D., & Clare, M. A. (2019). What controls submarine channel development and the morphology of deltas entering deep-water fjords? *Earth Surface Processes and Landforms, 44*(2), 535–551. https://doi.org/10.1002/esp.4515

Galindo-Zaldivar, J., Ercilla, G., Estrada, F., Catalán, M., D'Acremont, E., Azzouz, O., Casas, D., Chourak, M., Vazquez, J. T., Chalouan, A., Sanz de Galdeano, C., Benmakhlouf, M., Gorini, C., Alonso, B., Palomino, D., Rengel, J. A., & Gil, A. J. (2018). Imaging the Growth of Recent Faults: The Case of 2016–2017 Seismic Sequence Sea Bottom Deformation in the Alboran Sea (Western Mediterranean). *Tectonics, 37*(8), 2513–2530. https://doi.org/10.1029/2017TC004941

Ganas, A., Drakatos, G., Pavlides, S. B., Stavrakakis, G. N., Ziazia, M., Sokos, E., & Karastathis, V. K. (2005). The 2001 M_w = 6.4 Skyros earthquake, conjugate strike-slip faulting and spatial variation in stress within the central Aegean Sea. *Journal of Geodynamics, 39,* 61–77. https://doi.org/10.1016/j.jog.2004.09.001

Gasparini, P., & Garcia-Aristizabal, A. (2014). Seismic Risk Assessment, Cascading Effects. In M. Beer, I. Kougioumtzoglou, E. Patelli, & I. K. Au (Eds.), *Encyclopedia of Earthquake Engineering*. Springer. https://doi.org/10.1007/978-3-642-36197-5_260-1

Gasperini, L., Polonia, A., Ça atay, M. N., Bortoluzzi, G., & Ferrante, V. (2011). Geological slip rates along the North Anatolian Fault in the Marmara region. *Tectonics, 30*(6). https://doi.org/10.1029/2011TC002906

Giuliani, S., Bellucci, L. G., Ça atay, M. N., Polonia, A., Piazza, R., Vecchiato, M., Pizzini, S., & Gasperini, L. (2017). The impact of the 1999 M_w 7.4 event in the İzmit Bay (Turkey) on anthropogenic contaminant (PCBs, PAHs and PBDEs) concentrations recorded in a deep sediment core. *Science of the Total Environment, 590–591*, 799–808. https://doi.org/10.1016/j.scitotenv.2017.03.051

Goldfinger, C., Galer, S., Beeson, J., Hamilton, T., Black, B., Romsos, C., Patton, J., Nelson, C. H., Hausmann, R., & Morey, A. (2017). The importance of site selection, sediment supply, and hydrodynamics: A case study of submarine paleoseismology on the northern Cascadia margin, Washington USA. *Marine Geology, 384,* 4–16, 17, 25–46. https://doi.org/10.1016/j.margeo.2016.06.008

Gómez-Letona, M., Arístegui, J., Ramos, A. G., Montero, M. F., & Coca, J. (2018). Lack of impact of the El Hierro (Canary Islands) submarine volcanic eruption on the local phytoplankton community. *Scientific Reports, 8*. https://doi.org/10.1038/s41598-018-22967-6

Gómez de la Peña, L., Ranero, C. R., & Gràcia, E. (2018). The Crustal Domains of the Alboran Basin (Western Mediterranean). *Tectonics, 37*(10), 3352–3377. https://doi.org/10.1029/2017TC004946

González, A. (2014). Proyecto Castor. Relación de la secuencia sísmica con la inyección de gas. *Enseñanza de Las Ciencias de La Tierr, 22*(3), 298–302.

Görür, N., & Ça atay, M. N. (2010). Geohazards rooted from the northern margin of the Sea of Marmara since the late Pleistocene: a review of recent results. *Natural Hazards, 54,* 583–603. https://doi.org/10.1007/s11069-009-9469-x

Goto, A., Bromet, E. J., & Fujimori, K. (2015). Immediate effects of the Fukushima nuclear power plant disaster on depressive symptoms among mothers with infants: a prefectural-wide cross-sectional study from the Fukushima Health Management Survey. *BMC Psychiatry, 15*. https://doi.org/10.1186/s12888-015-0443-8

Gràcia, E., Dañobeitia, J., Vergés, J., & PARSIFAL Team. (2003). Mapping active faults offshore Portugal (36°N–38°N): Implications for seismic hazard assessment along the southwest Iberian margin. *Geology, 31*(1), 83–86. https://doi.org/10.1130/0091-7613(2003)031<0083:MAFOPN>2.0.CO;2

Gràcia, E., Grevemeyer, I., Bartolomé, R., Perea, H., Martínez-Loriente, S., Gómez de la Peña, L., Villaseñor, A., Klinger, Y., Lo Iacono, C., Diez, S., Calahorrano, A., Camafort, M., Costa, S., D'Acremont, E., Rabaute, A., & Ranero, C. R. (2019). Earthquake crisis unveils the growth of an incipient continental fault system. *Nature Communications, 10.* https://doi.org/10.1038/s41467-019-11064-5

Gràcia, E., Vizcaino, A., Escutia, C., Asioli, A., Rodés, Á., Pallàs, R., Garcia-Orellana, J., Lebreiro, S., & Goldfinger, C. (2010). Holocene earthquake record offshore Portugal (SW Iberia): testing turbidite paleoseismology in a slow-convergence margin. *Quaternary Science Reviews, 29*(9–10), 1156–1172. https://doi.org/10.1016/j.quascirev.2010.01.010

Grall, C., Henry, P., Westbrook, G. K., Ça atay, M. N., Thomas, Y., Marsset, B., Borschneck, D., Saritas, H., Cifçi, G., & Géli, L. (2014). Mass Transport Deposits Periodicity Related to Glacial Cycles and Marine-Lacustrine Transitions on a Ponded Basin of the Sea of Marmara (Turkey) Over the Last 500 ka. In S. Krastel, J.-H. Behrmann, D. Völker, M. Stipp, C. Berndt, R. Urgeles, J. Chaytor, K. Huhn, M. Strasser, & C. B. Harbitz (Eds.), *Submarine Mass Movements and Their Consequences: 6th International Symposium* (pp. 595–603). Springer. https://doi.org/10.1007/978-3-319-00972-8_53

Guastello, S. J., Koehler, G., Koch, B., Koyen, J., Lilly, A., Stake, C., & Wozniczka, J. (2008). Risk perception when the tsunami arrived. *Theoretical Issues in Ergonomics Science, 9*(2), 115–123. https://doi.org/10.1080/14639220601013919

Gudmundsson, M. T., Pedersen, R., Vogfjörd, K., Thorbjarnardóttir, B., Jakobsdóttir, S., & Roberts, M. J. (2010). Eruptions of Eyjafjallajökull Volcano, Iceland. *EOS, 91*(21), 190–191. https://doi.org/10.1029/2010EO210002

Guiastrennec-Faugas, L., Gillet, H., Jacinto, R. S., Dennielou, B., Hanquiez, V., Schmidt, S., Simplet, L., & Rousset, A. (2020). Upstream migrating knickpoints and related sedimentary processes in a submarine canyon from a rare 20-year morphobathymetric time-lapse (Capbreton submarine canyon, Bay of Biscay, France). *Marine Geology, 423.* https://doi.org/10.1016/j.margeo.2020.106143

Guidi, L., Guerra, A. F., Bakker, D. C. E., Canchaya, C., Curry, E., Foglini, F., Irisson, J.-O., Malde, K., Marshall, C. T., Obst, M., Ribeiro, R. P., & Tjiputra, J. (2020). Big Data in Marine Science. In S. J. J. Heymans, B. Alexander, Á. Muñiz Piniella, P. Kellett, & J. Coopman (Eds.), *EMB Future Science Brief 6* (Issue April). https://doi.org/10.5281/zenodo.3755793

Guidoboni, E., & Comastri, A. (2005). *Catalogue of earthquakes and tsunamis in the Mediterranean area from the 11th to the 15th century.* Istituto nazionale di geofisica e vulcanologia. https://www.nlb.gov.sg/biblio/13052528

Guidoboni, E., Comastri, A., & Traina, G. (1994). *Catalogue of ancient earthquakes in the Mediterranean area up to the 10th century* (stituto Nazionale di Geofisica (Ed.)). https://www.semanticscholar.org/paper/Catalogue-of-ancient-earthquakes-in-the-area-up-to-Guidoboni-Comastri/fc791423b7fa68ed53d37fc553310374bab45a62

Gutscher, M.-A., Baptista, M. A., & Miranda, J. M. (2006). The Gibraltar Arc seismogenic zone (part 2): Constraints on a shallow east dipping fault plane source for the 1755 Lisbon earthquake provided by tsunami modeling and seismic intensity. *Tectonophysics, 426*(1–2). https://doi.org/10.1016/j.tecto.2006.02.025

Hampton, M. A., Lee, H. J., & Locat, J. (1996). Submarine landslides. *Reviews of Geophysics, 34*(1), 33–59. https://pubs.er.usgs.gov/publication/70019390

Harbitz, C. B., Glimsdal, S., Løvholt, F., Kveldsvik, V., K.Pedersen, G., & Jensen, A. (2014). Rockslide tsunamis in complex fjords: From an unstable rock slope at Åkerneset to tsunami risk in western Norway. *Coastal Engineering, 88,* 101–122. https://doi.org/10.1016/j.coastaleng.2014.02.003

Hasan, O., Miko, S., Brunovi , D., Papatheodorou, G., Christodolou, D., Ilijani , N., & Geraga, M. (2020). Geomorphology of Canyon Outlets in Zrmanja River Estuary and Its Effect on the Holocene Flooding of Semi-enclosed Basins (the Novigrad and Karin Seas, Eastern Adriatic). *Water, 12*(10), 2807. https://doi.org/10.3390/w12102807

Hasegawa, A., Ohira, T., Maeda, M., Yasumura, S., & Tanigawa, K. (2016). Emergency Responses and Health Consequences after the Fukushima Accident; Evacuation and Relocation. *Clinical Oncology, 28*(4), 237–244. https://doi.org/10.1016/j.clon.2016.01.002

Hasiotis, T., Papatheodorou, G., Kastanos, N., & Ferentinos, G. (1996). A pockmark field in the Patras Gulf (Greece) and its activation during the 14/7/93 seismic event. *Marine Geology, 130*(3–4), 333–344. https://doi.org/10.1016/0025-3227(95)00131-X

Heezen, B. C., & Ewing, M. (1952). Turbidity Currents and Submarine Slumps, and the 1929 Grand Banks Earthquake. *American Journal of Science, 250,* 849–873. https://www.ajsonline.org/content/250/12/849

Heidarzadeh, M., Krastel, S., & Yalçıner, A. C. (2014). The State-of-the-Art Numerical Tools for Modeling Landslide Tsunamis: A Short Review. In *Submarine Mass Movements and Their Consequences: 6th International Symposium.* Springer International Publishing. https://doi.org/10.1007/978-3-319-00972-843

Heidarzadeh, Mohammad, Ishibe, T., Sandanbata, O., Muhari, A., & Wijanarto, A. B. (2020). Numerical modeling of the subaerial landslide source of the 22 December 2018 Anak Krakatoa volcanic tsunami, Indonesia. *Ocean Engineering, 195,* 106733. https://doi.org/10.1016/j.oceaneng.2019.106733

Heidarzadeh, Mohammad, Wang, Y., Satake, K., & Mulia, I. E. (2019). Potential deployment of offshore bottom pressure gauges and adoption of data assimilation for tsunami warning system in the western Mediterranean Sea. *Geoscience Letters, 6*(1), 19. https://doi.org/10.1186/s40562-019-0149-8

Hill, P. R., Conway, K., Lintern, D. G., Meulé, S., Picard, K., & Barrie, J. V. (2008). Sedimentary processes and sediment dispersal in the southern Strait of Georgia, BC, Canada. *Marine Environmental Research, 66 Supplem*, S39–S48. https://doi.org/10.1016/j.marenvres.2008.09.003

Hornbach, M. J., Braudy, N., Briggs, R. W., Cormier, M.-H., Davis, M. B., Diebold, J. B., Dieudonne, N., Douilly, R., Frohlich, C., Gulick, S. P. S., Johnson III, H. E., Mann, P., McHugh, C., Ryan-Mishkin, K., Prentice, C. S., Seeber, L., Sorlien, C. C., Steckler, M. S., Symithe, S. J., ... Templeton, J. (2010). High tsunami frequency as a result of combined strike-slip faulting and coastal landslides. *Nature Geoscience, 3,* 783–788. https://www.nature.com/articles/ngeo975

Hoshiba, M., & Iwakiri, K. (2011). Initial 30 seconds of the 2011 off the Pacific coast of Tohoku Earthquake (M_w 9.0)—amplitude and τ c for magnitude estimation for Earthquake Early Warnin. *Earth, Planets and Space, 63.* https://doi.org/10.5047/eps.2011.06.015

Hovland, M., Gardner, J. V., & Judd, A. G. (2002). The significance of pockmarks to understanding fluid flowprocesses and geohazards. *Geofluids, 2,* 127–136. https://doi.org/10.1046/j.1468-8123.2002.00028.x

Howe, B. M., Arbic, B. K., Aucan, J., Barnes, C. R., Bayliff, N., Becker, N., Butler, R., Doyle, L., Elipot, S., Johnson, G. C., Landerer, F., Lentz, S., Luther, D. S., Müller, M., Mariano, J., Panayotou, K., Rowe, C., Ota, H., Song, Y. T., ... Stuart Weinstein on behalf of the Joint Task Force for SMART Cables. (2019). SMART Cables for Observing the Global Ocean: Science and Implementation. *Frontiers in Marine Science*. https://doi.org/10.3389/fmars.2019.00424

Hugo, G. (2011). Future demographic change and its interactions with migration and climate change. *Global Environmental Change, 21,* S21–S33. https://doi.org/10.1016/j.gloenvcha.2011.09.008

Iezzia, G., Caso, C., Ventura, G., Vallefuoco, M., Cavallo, A., Behrens, H., Mollo, S., Paltrinieri, D., Signanini, P., & Vetere, F. (2014). First documented deep submarine explosive eruptions at the Marsili Seamount (Tyrrhenian Sea, Italy): A case of historical volcanism in the Mediterranean Sea. *Gondwana Research, 25*(2), 764–774. https://doi.org/10.1016/j.gr.2013.11.001

Igarashi, G., Saeki, S., Takahata, N., Sumikawa, K., Tasaka, S., Sasaki, Y., Takahashi, M., & Sano, Y. (1995). Ground-Water Radon Anomaly Before the Kobe Earthquake in Japan. *Science, 269*(5220), 60–61. https://doi.org/10.1126/science.269.5220.60

Igarashi, G., & Wakita, H. (1990). Groundwater radon anomalies associated with earthquakes. *Tectonophysics, 180*(2–4), 237–254. https://doi.org/10.1016/0040-1951(90)90311-U

Ikehara, K., Kanamatsu, T., Nagahashi, Y., Strasser, M., Fink, H., Usami, K., Irino, T., & Wefer, G. (2016). Documenting large earthquakes similar to the 2011 Tohoku-oki earthquake from sediments deposited in the Japan Trench over the past 1500 years. *Earth and Planetary Science Letters, 445*, 48–56. https://doi.org/10.1016/j.epsl.2016.04.009

Ioualalen, M., Migeon, S., & Sardoux, O. (2010). Landslide tsunami vulnerability in the Ligurian Sea: case study of the 1979 October 16 Nice international airport submarine landslide and of identified geological mass failures. *Geophysical Journal International, 181*(2), 724–740. https://doi.org/10.1111/j.1365-246X.2010.04572.x

Janbu, N. (1996). Raset I Finneidfjord — 20.juni 1996. Unpublished expert's report prepared for the County Sheriff of Nordland. In *Report Number 1, Revision 1*.

Johnston, E. N., Sparks, R. S. J., Phillips, J. C., & Carey, S. (2014). Revised estimates for the volume of the late bronze age minoan eruption, santorini, Greece. *Journal of the Geological Society, 171*(4). https://doi.org/10.1144/jgs2013-113

Jousset, P., Reinsch, T., Ryberg, T., Blanck, H., Clarke, A., Aghayev, R., Hersir, G. P., Henninges, J., Weber, M., & Krawczyk, C. M. (2018). Dynamic strain determination using fibre-optic cables allows imaging of seismological and structural features. *Nature Communications, 9*. https://doi.org/10.1038/s41467-018-04860-y

Jurado, M. J., Ripepe, M., Lopez, C., Ricciardi, A., Blanco, M. J., & Lacanna, G. (2020). Underwater records of submarine volcanic activity: El Hierro (Canary Islands 2011–2012) eruption. *Journal of Volcanology and Geothermal Research, 408*. https://doi.org/10.1016/j.jvolgeores.2020.107097

Kaihatu, J. M., Edwards, K. L., & O'Reilly, W. C. (2002). Model predictions of nearshore processes near complex bathymetry. *OCEANS '02 MTS/IEEE, 2,* 685–691. https://doi.org/10.1109/OCEANS.2002.1192052.

Kanamori, H., Miyazawa, M., & Mori, J. (2007). Investigation of the earthquake sequence off Miyagi prefecture with historical seismograms. *Earth, Planets and Space, 58,* 1533–1541. https://doi.org/10.1186/BF03352657

Karstens, J., & Berndt, C. (2015). Seismic chimneys in the Southern Viking Graben – Implications for palaeo fluid migration and overpressure evolution. *Earth and Planetary Science Letters, 412,* 88–100. https://doi.org/10.1016/j.epsl.2014.12.017

Kavanagh, J. L., Engwell, S. L., & Martin, S. A. (2018). A review of laboratory and numerical modelling in volcanology. *Solid Earth, 9,* 531–571. https://doi.org/10.5194/se-9-531-2018

Kawamata, K., Takaoka, K., Ban, K., Imamura, F., Yamaki, S., & Kobayashi, E. (2005). Model of tsunami generation by collapse of volcanic eruption: the 1741 Oshima-Oshima tsunami. In Kenji Satake (Ed.), *Tsunamis: Case Studies and Recent Developments.* Springer. https://link.springer.com/content/pdf/10.1007%2F1-4020-3331-1.pdf

Keller, J., Ryan, W. B. F., Ninkovich, D., & Altherr, R. (1978). Explosive volcanic activity in the Mediterranean over the past 200,000 yr as recorded in deep-sea sediments. *GSA Bulletin, 89*(4), 591–604. https://doi.org/10.1130/0016-7606(1978)89<591:EVAITM>2.0.CO;2

Kelner, M., Migeon, S., Tric, E., Couboulex, F., Dano, A., Lebourg, T., & Taboada, A. (2016). Frequency and triggering of small-scale submarine landslides on decadal timescales: Analysis of 4D bathymetric data from the continental slope offshore Nice (France). *Marine Geology, 379,* 281–297. https://doi.org/10.1016/j.margeo.2016.06.009

Ker, S., Le Gonidec, Y., Marsset, B., Westbrook, G. K., Gibert, D., & Minshull, T. A. (2014). Fine-scale gas distribution in marine sediments assessed from deep-towed seismic data. *Geophysical Journal International, 196*(3), 1466–1470. https://doi.org/10.1093/gji/ggt497

Kihara, N., Niida, Y., Takabatake, D., Kaida, H., Ishibayama, A., & Miyagawa, Y. (2015). Large-scale experiments on tsunami-induced pressure on a vertical tide wall. *Coastal Engineering, 99,* 46–63. https://doi.org/10.1016/j.coastaleng.2015.02.009

Kopf, A. J. (2002). SIGNIFICANCE OF MUD VOLCANISM. *Reviews of Geophysics, 40*(2). https://doi.org/10.1029/2000RG000093

Kopf, A. J., Delisle, G., Faber, E., Panahi, B., Aliyev, C. S., & Guliyev, I. (2010). Long-term *in situ* monitoring at Dashgil mud volcano, Azerbaijan: a link between seismicity, pore-pressure transients and methane emission. *International Journal of Earth Sciences, 99,* 227–240. https://doi.org/10.1007/s00531-009-0487-4

Kopf, A. J., Freudenthal, T., Ratmeyer, V., Bergenthal, M., Lange, M., Fleischmann, T., Hammerschmidt, S., Seiter, C., & Wefer, G. (2015). Simple, affordable, and sustainable borehole observatories for complex monitoring objectives. *Geoscientific Instrumentation, Methods and Data Systems, 4*(1), 99–109. https://doi.org/10.5194/gi-4-99-2015

Kopp, H., Weinzierl, W., Becel, A., Charvis, P., Evain, M., Flueh, E. R., Gailler, A., Galve, A., Hirn, A., Kandilarov, A., Klaeschen, D., Laigle, M., Papenberg, C., Planert, L., Roux, E., & Trail and Thales teams. (2011). Deep structure of the central Lesser Antilles Island Arc: Relevance for the formation of continental crust. *Earth and Planetary Science Letters, 304*(1–2), 121–134. https://doi.org/10.1016/j.epsl.2011.01.024

Korup, O. (2012). Earth's portfolio of extreme sediment transport events. *Earth-Science Reviews, 112*(3–4), 115–125. https://doi.org/10.1016/j.earscirev.2012.02.006

Kretschmer, K., Biastoch, A., Rüpke, L., & Burwicz, E. (2015). Modeling the fate of methane hydrates under global warming. *Global Biogeochemical Cycles, 29(*5), 610–625. https://doi.org/10.1002/2014GB005011

Kumar, P.C., Sain, K. A machine learning tool for interpretation of Mass Transport Deposits from seismic data. Sci Rep 10, 14134 (2020). https://doi.org/10.1038/s41598-020-71088-6

Kuo, T., Lin, C., Fan, K., Chang, G., Lewis, C., Han, Y., Wu, Y., Chen, W., & Tsai, C. (2009). Radon anomalies precursory to the 2003 M_w = 6.8 Chengkung and 2006 M_w = 6.1 Taitung earthquakes in Taiwan. *Radiation Measurements, 44*(3), 295–299. https://doi.org/10.1016/j.radmeas.2009.03.020

Kvalstad, T. J., Andresen, L., Forsberg, C. F., Berg, K., Bryn, P., & Wangen, M. (2005). The Storegga slide: evaluation of triggering sources and slide mechanics. *Marine and Petroleum Geology, 22,* 245–256. https://doi.org/10.1016/j.marpetgeo.2004.10.019

Kvenvolden, K. A. (1988). Methane hydrates and global climate. *Global Biogeochemical Cycles, 2*(3), 221–229. https://doi.org/10.1029/GB002i003p00221

Kwasnitschka, T., Köser, K., Sticklus, J., Rothenbeck, M., Weiß, T., Wenzlaff, E., Schoening, T., Triebe, L., Steinführer, A., Devey, C., & Greinert, J. (2016). DeepSurveyCam--A Deep Ocean Optical Mapping System. *Sensors, 16*(2). https://doi.org/10.3390/s16020164

L'Heureux, J.-S., Hansen, L., Longva, O., & Eilertsen, R. S. (2013). Landslides Along Norwegian Fjords: Causes and Hazard Assessment. In C. Margottini, P. Canuti, & K. Sassa (Eds.), *Landslide Science and Practice* (pp. 81–87). Springer. https://doi.org/10.1007/978-3-642-31427-8_10

L'Heureux, J.-S., Hansen, L., Longva, O., Emdal, A., & Grande, L. O. (2010). A multidisciplinary study of submarine landslides at the Nidelva fjord delta, Central Norway - Implications for geohazard assessment. *Norwegian Journal of Geology, 90* (1–2), 1–20. https://njg.geologi.no/images/NJG_articles/NJG_1_2010_LHeureux_pr1.pdf

Lange, D., Kopp, H., Royer, J.-Y., Henry, P., Çakir, Z., Petersen, F., Sakic, P., Ballu, V., Bialas, J., Özeren, M. S., Ergintav, S., & Géli, L. (2019). Interseismic strain build-up on the submarine North Anatolian Fault offshore Istanbul. *Nature Communications, 10*(1). https://doi.org/10.1038/s41467-019-11016-z.

Lay, T., Kanamori, H., Ammon, C. J., Nettles, M., Ward, S. N., Aster, R. C., Beck, S. L., Bilek, S. L., Brudzinski, M. R., Butler, R., DeShon, H. R., Ekström, G., Satake, K., & Sipkin, S. (2005). The great Sumatra-Andaman earthquake of 26 December 2004. *Science, 308*(5725), 1127–1133. https://doi.org/10.1126/science.1112250

Lindsey, N. J., Dawe, T. C., & Ajo-Franklin, J. B. (2019). Illuminating seafloor faults and ocean dynamics with dark fiber distributed acoustic sensing. *Science, 366*(6469), 1103–1107. https://doi.org/10.1126/science.aay5881

Lipscy, P. Y., Kushida, K. E., & Incerti, T. (2013). The Fukushima Disaster and Japan's Nuclear Plant Vulnerability in Comparative Perspective. *Environmental Science & Technology, 47*(12), 6082–6088. https://doi.org/10.1021/es4004813

Longva, O., Janbu, N., Blikra, L. H., & Bøe, R. (2003). The 1996 Finneidfjord Slide; Seafloor Failure and Slide Dynamics. In J. Locat, J. Mienert, & L. Boisvert (Eds.), *Submarine Mass Movements and Their Consequences: 1st International Symposium* (pp. 531–538). Springer. https://doi.org/10.1007/978-94-010-0093-2_58

Lynett, P. J., & Liu, P. L.-F. (2002). A numerical study of submarine–landslide–generated waves and run–up. *Proceedings of the Royal Society A: Mathematical, Physical and Engineering Sciences, 458*(2028). https://doi.org/10.1098/rspa.2002.0973

Ma, G., Zhan, L., Lu, H., & Hou, G. (2021). Structures in Shallow Marine Sediments Associated with Gas and Fluid Migration. *Journal of Marine Science and Engineering, 9*(4), 396. https://doi.org/10.3390/jmse9040396

Margaras, V. (2019). Demographic trends in EU regions. In *European Parliament Briefing. European Parliamentary Research Service.* https://ec.europa.eu/futurium/en/system/files/ged/eprs-briefing-633160-demographic-trends-eu-regions-final.pdf

Marra, G., Clivati, C., Luckett, R., Tampellini, A., Kronjäger, J., Wright, L., Mura, A., Levi, F., Robinson, S., Xuere, A., Baptie, B., & Calonico, D. (2018). Ultrastable laser interferometry for earthquake detection with terrestrial and submarine cables. *Science, 361*(6401), 486–490. https://doi.org/10.1126/science.aat4458

Martinelli, G., Albarello, D., & Mucciarelli, M. (1995). Radon emissions from mud volcanoes in northern Italy: Possible connection with local seismicity. *Geophysical Research Letters, 22*(15), 1989–1992. https://doi.org/10.1029/95GL01785

Mavrommatis, A. P., Segall, P., & Johnson, K. M. (2014). A decadal-scale deformation transient prior to the 2011 M_w 9.0 Tohoku-oki earthquake. *Geophysical Research Letters, 41*(13), 4486–4494. https://doi.org/10.1002/2014GL060139

McAdoo, B. G., Pratson, L. F., & Orange, D. L. (2000). Submarine landslide geomorphology, US continental slope. *Marine Geology, 169*(1–2), 103–136. https://doi.org/10.1016/S0025-3227(00)00050-5

McClusky, S., Reilinger, R., Mahmoud, S., Sari, D. Ben, & Tealeb, A. (2003). GPS constraints on Africa (Nubia) and Arabia plate motions. *Geophysical Journal International, 155*(1), 126–138. https://doi.org/10.1046/j.1365-246X.2003.02023.x

Meghraoui, M., Maouche, S., Chemaa, B., Cakir, Z., Aoudia, A., Harbi, A., Alasset, P.-J., Ayadi, A., Bouhadad, Y., & Benhamouda, F. (2004). Coastal uplift and thrust faulting associated with the M_w = 6.8 Zemmouri (Algeria) earthquake of 21 May, 2003. *Geophysical Research Letters, 31*. https://doi.org/10.1029/2004GL020466

Menapace, W., Völker, D., Sahling, H., Zoellner, C., dos Santos Ferreira, C., Bohrmann, G., & Kopf, A. (2017). Long-term *in situ* observations at the Athina mud volcano, Eastern Mediterranean: Taking the pulse of mud volcanism. *Tectonophysics, 721,* 12–27. https://doi.org/10.1016/j.tecto.2017.09.010

Mercalli, G. (1909). *Contributo allo studio del terremoto Calabro-Messinese del 28 Dicembre 1908*. https://www.worldcat.org/title/contributo-allo-studio-del-terremoto-calabro-messinese-del-28-dicembre-1908/oclc/703936236

Meschis, M., Roberts, G. P., Mildon, Z. K., Robertson, J., Michetti, A. M., & Walker, J. P. F. (2019). Slip on a mapped normal fault for the 28th December 1908 Messina earthquake (M_w 7.1) in Italy. *Scientific Reports, 9*. https://doi.org/10.1038/s41598-019-42915-2

Minisini, D., Trincardi, F., & Asioli, A. (2006). Evidence of slope instability in the Southwestern Adriatic Margin. *Natural Hazards and Earth System Sciences, 6*(1), 1–20. https://doi.org/10.5194/nhess-6-1-2006

Miyashita, T., Mori, N., Cox, D. T., Yasuda, T., & Mase, H. (2015). Quasi-3D Simulation of Tsunami Inundation in City Scale Model. *Journal of Japan Society of Civil Engineers, Ser. B2 (Coastal Engineering), 71*(2), 169–174. https://doi.org/10.2208/kaigan.71.I_169

Mizutori, M., & Guha-Sapi, D. (2020). Human Cost of Disasters: An overview of the last 20 years 2000-2019. In *Human Cost of Disasters*. https://doi.org/10.18356/79b92774-en

Mori, N., Takahashi, T., Yasuda, T., & Yanagisawa, H. (2011). Survey of 2011 Tohoku earthquake tsunami inundation and run-up. *Geophysical Research Letters, 38*(7). https://doi.org/10.1029/2011GL049210

Morkoc, E., Tarzan, L., Okay, O., Tufekci, H., Tufekci, V., Tolun, L., & Karakoc, F. (2007). Changes of oceanographic characteristics and the state of pollution in the Izmit bay following the earthquake of 1999. *Environmental Geology, 53,* 103–112. https://doi.org/10.1007/s00254-006-0622-5

Mowbray, J. H. (1909). *Italy's Great Horror or Earthquake and Tidal Wave*. (G. W. Bertron (Ed.)). Office of the Librarian of Congress.

Mulder, T., Savoye, B., & Syvitski, J. P. M. (1997). Numerical modelling of a mid-sized gravity flow: the 1979 Nice turbidity current (dynamics, processes, sediment budget and seafloor impact). *Sedimentology, 44*(2), 305–326. https://doi.org/10.1111/j.1365-3091.1997.tb01526.x

Mulia, I. E., & Satake, K. (2021). Synthetic analysis of the efficacy of the S-net system in tsunami forecasting. *Earth, Planets and Space, 73*. https://doi.org/10.1186/s40623-021-01368-6

Nakano, M., Unoki, S., Hanzawa, M., Marumo, R., & Fukuoka, J. (1954). Oceanographic features of a submarine eruption that destroyed the Kaiyo-Maru N°. 5. *Journal of Marine Research, 13,* 48–66. https://images.peabody.yale.edu/publications/jmr/jmr13-01-04.pdf

Necci, A., Tarantola, S., Vamanu, B., Krausmann, E., & Ponte, L. (2019). Lessons learned from offshore oil and gas incidents in the Arctic and other ice-prone seas. *Ocean Engineering, 185*(1), 12–26. https://doi.org/10.1016/j.oceaneng.2019.05.021

Nieuwejaar, P., Mazauric, V., Betzler, C., Carapuço, M., Cattrijsse, A., Coren, F., Danobeitia, J., Day, C., Fitzgerald, A., Florescu, S., Diaz, J. I., Klages, M., Koning, E., Lefort, O., Magnifico, G., Mikelborg, Ø., & Naudts, L. (2020). Next Generation European Research Vessels: Current status and foreseeable evolution. In P. Kellett, C. Viegas, B. Alexander, J. Coopman, Á. Muñiz Piniella, & S. J. J. Heymans (Eds.), *EMB Position Paper 25*. https://doi.org/10.5281/zenodo.3477893

Nisbet, E. G. (1992). Sources of atmospheric CH4 in early postglacial time. *JGR Atmospheres, 97*(D12), 12859–12867. https://doi.org/10.1029/92JD00743

Nomikou, P., Papanikolaou, D., Alexandri, M., Sakellariou, D., & Rousakis, G. (2013). Submarine volcanoes along the Aegean volcanic arc. *Tectonophysics, 597–598,* 123–146. https://doi.org/10.1016/j.tecto.2012.10.001

Nomikou, P., Papanikolaou, D., Tibaldi, A., Carey, S., Livanos, I., Bell, K. L. C., Pasquare, F. A., & Rousakis, G. (2014). The detection of volcanic debris avalanches (VDAs) along the Hellenic Volcanic Arc, through marine geophysical techniques. In *Submarine Mass Movements and Their Consequences* (pp. 339–349). Springer.

Normandeau, A., Lajeunesse, P., St-Onge, G., Bourgault, D., St-Onge Drouin, S., Senneville, S., & Bélanger, S. (2014). Morphodynamics in sediment-starved inner-shelf submarine canyons (Lower St. Lawrence Estuary, Eastern Canada). *Marine Geology, 357,* 243–255. https://doi.org/10.1016/j.margeo.2014.08.012

Nygård, A., Sejrup, H. P., Haflidason, H., Lekens, W. A. H., Clark, C. D., & Bigg, G. R. (2007). Extreme sediment and ice discharge from marine-based ice streams: New evidence from the North Sea. *Geology, 35*(5), 395–398. https://doi.org/10.1130/G23364A.1

Oaie, G., Seghedi, A., & R dulescu, V. (2016). Natural marine hazards in the Black Sea and the system of their monitoring and real-time warning. *Geo-Eco-Marina, 22,* 5–28. https://doi.org/110.5281/zenodo.889593

OECD. (2016). *The Ocean Economy in 2030.* OECD Publishing. https://doi.org/10.1787/9789264251724-en

Okal, E. A., Synolakis, C. E., Uslu, B., Kalligeris, N., & Voukouvalas, E. (2009). The 1956 earthquake and tsunami in Amorgos, Greece. *Geophysical Journal International, 178*(3), 1533–1554. https://doi.org/10.1111/j.1365-246X.2009.04237.x

Omira, R., Baptista, M. A., Mellas, S., Leone, F., Meschinet de Richemond, N., Zourarah, B., & Cherel, J.-P. (2012). The November, 1st, 1755 Tsunami in Morocco: Can Numerical Modeling Clarify the Uncertainties of Historical Reports? In G. López (Ed.), *Tsunami - Analysis of a Hazard - From Physical Interpretation to Human Impact*. https://doi.org/10.5772/51864

Owen, S., Segall, P., Lisowski, M., Miklius, A., Denlinger, R., & Sako, M. (2000). Rapid deformation of Kilauea Volcano: Global Positioning System measurements between 1990 and 1996. *JGR Solid Earth, 105*(B8), 18983–18998. https://doi.org/10.1029/2000JB900109

Palermo, D., Nistor, I., Al-Faesly, T., & Cornett, A. (2012). Impact of Tsunami Forces on Structures: The University of Ottawa Experience. *Fifth International Tsunami Symposium.* https://www.academia.edu/23378956/Impact_of_Tsunami_Forces_on_Structures_The_University_of_Ottawa_Experience

Papadopoulos, G. A., Diakogianni, G., Fokaefs, A., & Ranguelov, B. (2011). Tsunami hazard in the Black Sea and the Azov Sea: a new tsunami catalogue. *Natural Hazards and Earth System Sciences, 11*(3), 945–963. https://doi.org/10.5194/nhess-11-945-2011

Papatheodorou, G., Hasiotis, T., & Ferentinos, G. (1993). Gas-charged sediments in the Aegean and Ionian Seas, Greece. *Marine Geology, 112*(1–4), 171–184. https://doi.org/10.1016/0025-3227(93)90167-T

Papazachos, B. C., Komninakis, P. E., Karakaisis, G. F., Karakostas, B. G., Papaioannou, C. A., Papazachos, C. B., & Scordilis, E. M. (2000). *A Catalogue of Earthquakes in Greece and Surrounding Area for the Period 550 B.C.-1999.* Publication of Geophysical Laboratory, University of Thessaloniki. http://geophysics.geo.auth.gr/ss/catalogs_en.html

Papazachos, B. C., & Papaioannou, C. A. (1999). Lithospheric boundaries and plate motions in the Cyprus area. *Tectonophysics, 308*(1–2), 193–204. https://doi.org/10.1016/S0040-1951(99)00075-X

Park, H., Cox, D. T., Lynett, P. J., Wiebe, D. M., & Shin, S. (2013). Tsunami inundation modeling in constructed environments: A physical and numerical comparison of free-surface elevation, velocity, and momentum flux. *Coastal Engineering, 79,* 9–21. https://doi.org/10.1016/j.coastaleng.2013.04.002

Paulatto, M., Pinat, T., & Romanelli, F. (2007). Tsunami hazard scenarios in the Adriatic Sea domain. *Natural Hazards and Earth System Sciences, 7*(2), 309–325. https://doi.org/10.5194/nhess-7-309-2007

Perea, H., Masana, E., & Santanach, P. (2012). An active zone characterized by slow normal faults, the northwestern margin of the València trough (NE Iberia): a review. *Journal of Iberian Geology, 38*(1), 31–52. https://doi.org/10.5209/REV_JIGE.2012.V38.N1.39204

Pereira, A. S. (2009). The Opportunity of a Disaster: The Economic Impact of the 1755 Lisbon Earthquake. *The Journal of Economic History, 69*(2), 466–499. https://doi.org/10.1017/S0022050709000850

Petersen, F., Kopp, H., Lange, D., Hannemann, K., & Urlaub, M. (2019). Measuring tectonic seafloor deformation and strain-build up with acoustic direct-path ranging. *Journal of Geodynamics, 124,* 14–24. https://doi.org/10.1016/j.jog.2019.01.002

Philip, H., & Meghraoui, M. (1983). Structural analysis and interpretation of the surface deformations of the El Asnam Earthquake of October 10, 1980. *Tectonics, 2*(1), 17–49. https://doi.org/10.1029/TC002i001p00017

Pinheiro, L. M., Ivanov, M. K., Sautkin, A., Akhmanov, G., Magalhães, V. H., Volkonskaya, A., Monteiro, J. H., Somoza, L., Gardner, J., Hamouni, N., & Cunha, M. R. (2003). Mud volcanism in the Gulf of Cadiz: results from the TTR-10 cruise. *Marine Geology, 195*(1–4), 131–151. https://doi.org/10.1016/S0025-3227(02)00685-0

Pino, N. A., Piatanesi, A., Valensise, G., & Boschi, E. (2009). The 28 December 1908 Messina Straits Earthquake (M_W 7.1): A Great Earthquake throughout a Century of Seismology. *Seismological Research Letters, 80*(2), 243–259. https://doi.org/10.1785/gssrl.80.2.243

Piper, D. J. W., Shor, A. N., & Clarke, J. E. H. (1988). The 1929 Grand Banks earthquake, slump and turbidity current. In *Sedimentologic consequences of Convulsive Geological Events* (pp. 77–92). Geological Society of America. https://doi.org/10.1130/SPE229-p77

Planke, S., Norman, F., Berndt, C., Mienert, J., & Masson, D. G. (2009). Spotlight on Technology: P-Cable High-Resolution Seismic. *Oceanography, 22*(1), 85. https://doi.org/10.5670/oceanog.2009.09

Polonia, A., Romano, S., Ça atay, M. N., Capotondi, L., Gasparotto, G., Gasperini, L., Panieri, G., & Torelli, L. (2015). Are repetitive slumpings during sapropel S1 related to paleo-earthquakes? *Marine Geology, 361,* 41–52. https://doi.org/10.1016/j.margeo.2015.01.001

Polonia, A., Torelli, L., Mussoni, P., Gasperini, L., Artoni, A., & Klaeschen, D. (2011). The Calabrian Arc subduction complex in the Ionian Sea: Regional architecture, active deformation, and seismic hazard. *Tectonics, 30*(5). https://doi.org/10.1029/2010TC002821

Polonia, A., Vaiani, S. C., & de Lange, G. J. (2016). Did the A.D. 365 Crete earthquake/tsunami trigger synchronous giant turbidity currents in the Mediterranean Sea. *Geology, 44*(3), 191–194. https://doi.org/10.1130/G37486.1

Pope, E. L., Talling, P. J., & Carter, L. (2017). Which earthquakes trigger damaging submarine mass movements: Insights from a global record of submarine cable breaks? *Marine Geology, 384,* 131–146. https://doi.org/10.1016/j.margeo.2016.01.009

Popescu, I., Panin, N., Jipa, D., Lericolais, G., & Ion, G. (2014). Submarine canyons of the Black Sea basin with a focus on the Danube Canyon. In F. Briand (Ed.), *CIESM Workshop Monographs, n°47: Submarine canyon dynamics in the Mediterranean and tributary seas - An integrated geological, oceanographic and biological perspective* (pp. 103–121). CIESM Publisher. http://www.ciesm.org/online/monographs/index.htm

Pouderoux, H., Lamarche, G., & Proust, J.-N. (2012). Building an 18 000-year-long paleo-earthquake record from detailed deep-sea turbidite characterisation in Poverty Bay, New Zealand. *Natural Hazards and Earth System Sciences, 12,* 2077–2101. https://doi.org/10.5194/nhess-12-2077-2012

Prasetyo, A., Tomiczek, T., Yasuda, T., Mori, N., Mase, H., & Kennedy, A. (2016). Physical experiments of tsunami runup and force on building clusters using a hybrid tsunami generator. *Proceedings of the 6th International Conference on the Application of Physical Modelling in Coastal and Port Engineering and Science.* http://rdio.rdc.uottawa.ca/publications/coastlab16/coastlab73.pdf

Prasetyo, A., Yasuda, T., Miyashita, T., & Mori, N. (2019). Physical Modeling and Numerical Analysis of Tsunami Inundation in a Coastal City. *Frontiers in Built Environment*. https://doi.org/10.3389/fbuil.2019.00046

Pringle, W., & Yoneyama, N. (2013). The Application of a Hybrid 2D/3D Numerical Tsunami Inundation-Propagation Flow Model to the 2011 off the Pacific Coast of Tohoku Earthquake Tsunami. *Journal of Japan Society of Civil Engineers, Ser. B2 (Coastal Engineering), 69*(2), 306–310. https://doi.org/10.2208/kaigan.69.I_306

Prior, D. B., Bornhold, B. D., Coleman, J. M., & Bryant, W. R. (1982). Morphology of a submarine slide, Kitimat Arm, British Columbia. *Geology, 10*(11), 588–592. https://doi.org/10.1130/0091-7613(1982)10<588:MOASSK>2.0.CO;2

Pritchard, M. E., Allen, R. M., Becker, T. W., Behn, M. D., Brodsky, E. E., Bürgmann, R., Ebinger, C., Freymueller, J. T., Gerstenberger, M., Haines, B., Kaneko, Y., Jacobsen, S. D., Lindsey, N. J., McGuire, J. J., Page, M., Ruiz, S., Tolstoy, M., Wallace, L. M., Walter, W. R., ... Vincent, H. (2020). New Opportunities to Study Earthquake Precursors. *Seismological Research Letters, 91*(5), 2444–2447. https://doi.org/10.1785/0220200089

Ranguelov, B., & Gospodinov, D. (1994). The Seismic activity after the earthquake of 31 March, 1901 in the Shabla-Kaliakra zone. *Bulgarian Geophysical Journal, 20*(2), 49–55.

Reilinger, R., McClusky, S., Vernant, P., Lawrence, S., Ergintav, S., Cakmak, R., Ozener, H., Kadirov, F., Guliev, I., Stepanyan, R., Nadariya, M., Hahubia, G., Mahmoud, S., Sakr, K., ArRajehi, A., Paradissis, D., Al-Aydrus, A., Prilepin, M., Guseva, T., ... Karam, G. (2006). GPS constraints on continental deformation in the Africa-Arabia-Eurasia continental collision zone and implications for the dynamics of plate interactions. *JGR Solid Earth, 111*(B5). https://doi.org/10.1029/2005JB004051

Riboulot, V., Ker, S., Sultan, N., Thomas, Y., Marsset, B., Scalabrin, C., Ruffine, L., Boulart, C., & Ion, G. (2018). Freshwater lake to salt-water sea causing widespread hydrate dissociation in the Black Sea. *Nature Communications, 9.* https://doi.org/10.1038/s41467-017-02271-z

Ricco, A. (1892). Terremoti, sollevamento ed eruzione sottomarina a Pantelleria nella seconda meta dell'ottobre 1891. *Annali Dell'Ufficio Centr. Meteorol. e Geodinamico Ital. Ser. IIa Pt. 3, XI,* 7–27.

Rothwell, R. G., Thomson, J., & Kähler, G. (1998). Low-sea-level emplacement of a very large Late Pleistocene 'megaturbidite' in the western Mediterranean Sea. *Nature, 392,* 377–380. https://doi.org/10.1038/32871

Ruiz-Barajas, S., Sharma, N., Convertito, V., Zollo, A., & Benito, B. (2017). Temporal evolution of a seismic sequence induced by a gas injection in the Eastern coast of Spain. *Scientific Reports, 7.* https://doi.org/10.1038/s41598-017-02773-2

Ryan, W. B. F., & Heezen, B. C. (1965). Ionian Sea Submarine Canyons and the 1908 Messina Turbidity Current. *Geological Society of America Bulletin, 76,* 915–932. https://doi.org/10.1130/0016-7606(1965)76[915:ISSCAT]2.0.CO;2

Rygg, N., & Oset, F. (1996). The Balsfjord landslide. Landslides, Volume 1. *Proceedings of the 7th International Symposium on Landslides,* 573–577.

Sahal, A., & Lemahieu, A. (2011). The 1979 nice airport tsunami: mapping of the flood in Antibes. *Natural Hazards, 56,* 833–840. https://doi.org/10.1007/s11069-010-9594-6

Sakellariou, D., Rousakis, G., Nomikou, P., Bell, K. L. C., Carey, S., & Sigurdsson, H. (2012). Tsunami Triggering Mechanisms Associated with the 17th cent. BC Minoan Eruption of Thera Volcano, Greece. *Proceedings of the Twenty-Second (2012) International Offshore and Polar Engineering Conference.* https://d1wqtxts1xzle7.cloudfront.net/51559450/Tsunami_Triggering_Mechanisms_Associated20170130-5891-wy995n.pdf?1485808841=&response-content-disposition=inline%3B+filename%3DTsunami_triggering_mechanisms_associated.pdf&Expires=1625498050&Signature=IBdd6NU

Sakellariou, D., & Tsampouraki-Kraounaki, K. (2018). Plio-Quaternary extension and strike-slip tectonics in the Aegean. In J. C. Duarte (Ed.), *Transform Plate Boundaries and Fracture Zones*. https://doi.org/10.1016/B978-0-12-812064-4.00014-1.

Sallarès, V., Martínez-Loriente, S., Prada, M., Gràcia, E., Ranero, C. R., Gutscher, M.-A., Bartolomé, R., Gailler, A., Dañobeitia, J. J., & Zitellini, N. (2013). Seismic evidence of exhumed mantle rock basement at the Gorringe Bank and the adjacent Horseshoe and Tagus abyssal plains (SW Iberia). *Earth and Planetary Science Letters, 365*, 120–131. https://doi.org/10.1016/j.epsl.2013.01.021

Sallarès, V., & Ranero, C. R. (2019). Upper-plate rigidity determines depth-varying rupture behaviour of megathrust earthquakes. *Nature, 576*(7785), 96–101. https://doi.org/10.1038/s41586-019-1784-0

Santana-Casiano, J. M., González-Dávila, M., & Fraile-Nuez, E. (2017). The Emissions of the Tagoro Submarine Volcano (Canary Islands, Atlantic Ocean): Effects on the Physical and Chemical Properties of the Seawater. In G. Aiello (Ed.), *Volcanoes - Geological and Geophysical Setting, Theoretical Aspects and Numerical Modeling, Applications to Industry and Their Impact on the Human Health*. IntechOpen. https://doi.org/10.5772/intechopen.70422

Satake, K. (2012). Tsunamis Generated by Submarine Landslides. In Y. Yamada, K. Kawamura, K. Ikehara, Y. Ogawa, R. Urgele, Sd. Mosher, J. Chaytor, & M. Strasser (Eds.), *Submarine Mass Movements and Their Consequences: 5th International Symposium*. Springer, Dordrecht. https://doi.org/10.1007/978-94-007-2162-3_42

Satake, K., Sawai, Y., Shishikura, M., Okamura, Y., Namegaya, Y., & Yamaki, S. (2007). Tsunami source of the unusual AD 869 earthquake off Miyagi, Japan, inferred from tsunami deposits and numerical simulation of inundation. *American Geophysical Union, Fall Meeting 2007, Abstract Id. T31G-03*. https://ui.adsabs.harvard.edu/abs/2007AGUFM.T31G..03S/abstract

Schmittbuhl, J., Karabulut, H., Lengliné, O., and Bouchon, M. (2015), Seismicity distribution and locking depth along the Main Marmara Fault, Turkey, *Geochem. Geophys. Geosyst., 17,* 954– 965, doi:10.1002/2015GC006120.

Scholaert, F., Margaras, V., Pape, M., Wilson, A., & Kloecker, C. A. (2020). The blue economy: Overview and EU policy framework. In E*uropean Parliament In-depth Analysis.* European Parliamentary Research Service. https://www.europarl.europa.eu/RegData/etudes/IDAN/2020/646152/EPRS_IDA(2020)646152_EN.pdf

Sgroi, T., Di Grazia, G., & Favali, P. (2019). Volcanic Tremor of Mt. Etna (Italy) Recorded by NEMO-SN1 Seafloor Observatory: A New Perspective on Volcanic Eruptions Monitoring. *Geosciences, 9*(3). https://doi.org/10.3390/geosciences9030115

Shaw, B., Ambraseys, N. N., England, P. C., Floyd, M. A., Gorman, G. J., Higham, T. F. G., Jackson, J. A., Nocquet, J.-M., Pain, C. C., & Piggott, M. D. (2008). Eastern Mediterranean tectonics and tsunami hazard inferred from the AD 365 earthquake. *Nature Geoscience, 1*(4), 268–276. https://doi.org/10.1038/ngeo151

Sigurdsson, H., Carey, S., Alexandri, M., Vougioukalakis, G., Croff, K., Roman, C., Sakellariou, D., Anagnostou, C., Rousakis, G., Ioakim, C., Goguo, A., Ballas, D., Misaridis, T., & Nomikou, P. (2006). Marine investigations of Greece's Santorini Volcanic Field. *EOS, 87,* 337–342. https://doi.org/10.1029/2006EO340001

Sladen, A., Rivet, D., Ampuero, J. P., De Barros, L., Hello, Y., Calbris, G., & Lamare, P. (2019). Distributed sensing of earthquakes and ocean-solid Earth interactions on seafloor telecom cables. *Nature Communications, 10*. https://doi.org/10.1038/s41467-019-13793-z

Soetaert, K., van Oevelen, D., & Sommer, S. (2012). Modelling the impact of Siboglinids on the biogeochemistry of the Captain Arutyunov mud volcano (Gulf of Cadiz). *Biogeosciences, 9*(12), 5341–5352. https://doi.org/10.5194/bg-9-5341-2012

Soga, K., Alonso, E., Yerro, A., Kumar, K., & Bandara, S. (2016). Trends in large-deformation analysis of landslide mass movements with particular emphasis on the material point method. *Géotechnique, 66*(3), 248–273. https://doi.org/10.1680/jgeot.15.LM.005

Solomon, E. A., Becker, K., Kopf, A. J., & Davis, E. E. (2019). Listening Down the Pipe. *Oceanography, 32*. https://doi.org/https://www.jstor.org/stable/26604959

Solomon, E. A., Kastner, M., Morrise, D., Morrise, D., Wheat, C. G., Jannasch, H., Robertson, G., Davis, E. E., & Morris, J. D. (2009). Long-term hydrogeochemical records in the oceanic basement and forearc prism at the Costa Rica subduction zone. *Earth and Planetary Science Letters, 282*(1–4), 240–251. https://doi.org/10.1016/j.epsl.2009.03.022

Somoza, L., González, F. J., Barker, S. J., Madureira, P., Medialdea, T., de Ignacio, C., Lourenço, N., León, R., Vázquez, J.-T., & Palomino, D. (2017). Evolution of submarine eruptive activity during the 2011–2012 El Hierro event as documented by hydroacoustic images and remotely operated vehicle observations. *Geochemistry, Geophysics, Geosystems, 18*(8), 3109–3137. https://doi.org/10.1002/2016GC006733

Song, S.-R., Ku, W. Y., Chen, Y.-L., Lin, Y.-C., Liu, C.-M., Kuo, L.-W., Tsanyao, Yang, F., & Lo, H.-J. (2003). Groundwater Chemical Anomaly before and after the Chi-Chi Earthquake in Taiwan. *Terrestrial, Atmospheric and Oceanic Sciences Journal, 14*(3), 311–320. https://doi.org/10.3319/TAO.2003.14.3.311(T)

Spakman, W., Chertova, M. V., van den Berg, A., & van Hinsbergen, D. J. J. (2018). Puzzling features of western Mediterranean tectonics explained by slab dragging. *Nature Geoscience, 11,* 211–216. https://doi.org/10.1038/s41561-018-0066-z

Stacey, C. D., Hill, P. R., Talling, P. J., Enkin, R. J., Clarke, J. E. H., & Lintern, D. G. (2019). How turbidity current frequency and character varies down a fjord-delta system: Combining direct monitoring, deposits and seismic data. *Sedimentology, 66*(1), 1–31. https://doi.org/10.1111/sed.12488

Stegmann, S., Sultan, N., Kopf, A. J., Apprioual, R., & Pelleau, P. (2011). Hydrogeology and its effect on slope stability along the coastal aquifer of Nice, France. *Marine Geology, 280*(1–4), 168–181. https://doi.org/10.1016/j.margeo.2010.12.009

Sultan, N., & Garziglia, S. (2011). Geomechanical constitutive modelling of gas-hydrate-bearing sediments. *The 7th International Conference on Gas Hydrates*. https://archimer.ifremer.fr/doc/00035/14626/

Sultan, N., Garziglia, S., Bompais, X., Woerther, P., Witt, C., Kopf, A. J., & Migeon, S. (2020). Transient Groundwater Flow Through a Coastal Confined Aquifer and Its Impact on Nearshore Submarine Slope Instability. *JGR Earth Surface, 125*(9). https://doi.org/10.1029/2020JF005654

Sultan, N., Savoye, B., Jouet, G., Leynaud, D., Cochonat, P., Henry, P., Stegmann, S., & Kopf, A. J. (2010). Investigation of a possible submarine landslide at the Var delta front (Nice continental slope, southeast France). *Canadian Geotechnical Journal, 47*(4). https://doi.org/10.1139/T09-105

Suzuki, W., Aoi, S., Sekiguchi, H., & Kunugi, T. (2012). Source rupture process of the 2011 Tohoku-Oki earthquake derived from the strong-motion records. *Proceedings of the Fifteenth World Conference on Earthquake Engineering*. http://www.iitk.ac.in/nicee/wcee/article/WCEE2012_1650.pdf

Tappin, D. R. (2017). Tsunamis from submarine landslides. *Geology Today, 33*(5), 190–200. https://doi.org/10.1111/gto.12200

Tashiro, A., Kogure, M., Nagata, S., Itabashi, F., Tsuchiya, N., Hozawa, A., & Nakaya, T. (2021). Coastal exposure and residents' mental health in the affected areas by the 2011 Great East Japan Earthquake and Tsunami. *Scientific Reports, 11*(1), 16751. https://doi.org/10.1038/s41598-021-96168-z

Tepp, G., Chadwick Jr, W. W., Haney, M. M., Lyons, J. J., Dziak, R. P., Merle, S. G., Butterfield, D. A., & Young III, C. W. (2019). Hydroacoustic, Seismic, and Bathymetric Observations of the 2014 Submarine Eruption at Ahyi Seamount, Mariana Arc. *Geochemistry, Geophysics, Geosystems, 20*(7), 3608–3627. https://doi.org/10.1029/2019GC008311

Teresita, G., Nicola, M., Luca, F., & Pierfrancesco, C. (2019). Tsunami risk perception along the Tyrrhenian coasts of Southern Italy: the case of Marsili volcano. *Natural Hazards, 97,* 437–454. https://doi.org/10.1007/s11069-019-03652-x

Thomas, S., Killian, J., & Bridges, K. (2015). Influence of Macroroughness on Tsunami Loading of Coastal Structures. *Journal of Waterway, Port, Coastal and Ocean Engineering, 141*(1). https://doi.org/10.1061/(ASCE)WW.1943-5460.0000268

Tibaldi, A. (2001). Multiple sector collapses at Stromboli volcano, Italy: how they work. *Bulletin of Volcanology, 63,* 112–125. https://doi.org/10.1007/s004450100129

Tilmann, F., Howe, B. M., & Butler, R. (2017). Commercial Underwater Cable Systems Could Reduce Disaster Impact. *EOS, 98*. https://doi.org/10.1029/2017EO069575

Tinti, S., Armigliato, A., Pagnoni, G., & Zaniboni, F. (2005). Scenarios of Giant Tsunamis of Tectonic Origin in the Mediterranean. *ISET Journal of Earthquake Technology, 42*(4), 171–188. https://citeseerx.ist.psu.edu/viewdoc/download?doi=10.1.1.596.5560&rep=rep1&type=pdf

Tinti, S., Maramai, A., Armigliato, A., Graziani, L., Manucci, A., Pagnoni, G., & Zaniboni, F. (2006). Observations of physical effects from tsunamis of December 30, 2002 at Stromboli volcano, southern Italy. *Bulletin of Volcanology, 68,* 450–461. https://doi.org/10.1007/s00445-005-0021-x

Tong, X., Sandwell, D., Luttrell, K., Brooks, B., Bevis, M., Shimada, M., Foster, J., Smalley Jr., R., Parra, H., Báez Soto, J. C., Blanco, M. J., Kendrick, E., Genrich, J., & Caccamise II, D. J. (2010). The 2010 Maule, Chile earthquake: Downdip rupture limit revealed by space geodesy. *Geophysical Research Letters, 37*(24). https://doi.org/10.1029/2010GL045805

Tsabaris, C., Mallios, A., & Papathanassiou, E. (2008). Instrumentation of Gamma ray spectrometry for Underwater in-situ radon analysis: Design, Implementation and Application of an Underwater In-Situ Gamma Ray Spectrometer With a Remotely Operated Vehicle. *Sea Technology, 49*(3), 21–26.

Tsabaris, C., Patiris, D. L., & Lykousis, V. (2011). KATERINA: An *in situ* spectrometer for continuous monitoring of radon daughters in aquatic environment. *Nuclear Instruments and Methods in Physics Research Section A: Accelerators, Spectrometers, Detectors and Associated Equipment, 626–627, S,* S142–S144. https://doi.org/10.1016/j.nima.2010.06.233

Tselentis, G.-A., Stavrakakis, G. N., Sokos, E., Gkika, F., & Serpetsidaki, A. (2010). Tsunami hazard assessment in the Ionian Sea due to potential tsunamogenic sources – results from numerical simulations. *Natural Hazards and Earth System Sciences, 10,* 1021–1030. https://doi.org/10.5194/nhess-10-1021-2010

Tsunogai, U., & Wakita, H. (1995). Precursory Chemical Changes in Ground Water: Kobe Earthquake, Japan. *Science, 269*(5220), 61–63. https://doi.org/0.1126/science.269.5220.61

Uchida, N., & Bürgmann, R. (2021). A Decade of Lessons Learned from the 2011 Tohoku-Oki Earthquake. *Reviews of Geophysics, 59*(2). https://doi.org/10.1029/2020RG000713

Urgeles, R., & Camerlenghi, A. (2013). Submarine landslides of the Mediterranean Sea: Trigger mechanisms, dynamics, and frequency-magnitude distribution. *JGR Earth Surface, 118*(4), 2600–2618. https://doi.org/10.1002/2013JF002720

Urlaub, M., Petersen, F., Gross, F., Bonforte, A., Puglisi, G., Guglielmino, F., Krastel, S., Lange, D., & Kopp, H. (2018). Gravitational collapse of Mount Etna's southeastern flank. *Science Advances, 4*(10). https://doi.org/10.1126/sciadv.aat9700

USGS. (2006). Tsunami Hazards—A National Threat. In *Fact Sheet 2006–3023*. https://pubs.usgs.gov/fs/2006/3023/2006-3023.pdf

Vardy, M. E., L'Heureux, J.-S., Vanneste, M., Longva, O., Steiner, A., Forsberg, C. F., Ha.Haflidason, & Brendryen, J. (2012). Multidisciplinary investigation of a shallow near-shore landslide, Finneidfjord, Norway. *Near Surface Geophysics, 10*(4), 267–277. https://doi.org/10.3997/1873-2012022

Vendettuoli, D., Clare, M. A., Clarke, J. E. H., Vellinga, A., Hizzet, J., Hage, S., Cartigny, M. J. B., Talling, P. J., Waltham, D., Hubbard, S. M., Stacey, C. D., & Lintern, D. G. (2019). Daily bathymetric surveys document how stratigraphy is built and its extreme incompleteness in submarine channels. *Earth and Planetary Science Letters, 515,* 231–247. https://doi.org/10.1016/j.epsl.2019.03.033

Viana-Baptista, M. A., Soares, P. M., Miranda, J. M., & Luis, J. F. (2006). Tsunami Propogation along Tagus Estuary (Lisbon, Portugal) Preliminary Results. *Science of Tsunami Hazards, 24*(5), 329-338. http://tsunamisociety.org/245baptista.pdf

Vilarrasa, V., De Simone, S., Carrera, J., & Villaseñor, A. (2021). Unraveling the Causes of the Seismicity Induced by Underground Gas Storage at Castor, Spain. *Geophysical Research Letters, 48*(7). https://doi.org/10.1029/2020GL092038

Virtasalo, J. J., Schröder, J. F., Luoma, S., Majaniemi, J., Mursu, J., & Scholten, J. (2019). Submarine groundwater discharge site in the First Salpausselkä ice-marginal formation, south Finland. *Solid Earth, 10*(2), 405–423. https://doi.org/10.5194/se-10-405-2019

Voyera, M., & van Leeuwen, J. (2019). 'Social license to operate' in the Blue Economy. *Resources Policy, 62,* 102–113. https://doi.org/10.1016/j.resourpol.2019.02.020

Wallace, L. M., Araki, E., Saffer, D. M., Wang, X., Roesner, A., Kopf, A. J., Nakanishi, A., Power, W., Kobayashi, R., Kinoshita, C., Toczko, S., Kimura, T., Machida, Y., & Carr, S. (2016). Near-field observations of an offshore M_w 6.0 earthquake from an integrated seafloor and subseafloor monitoring network at the Nankai Trough, southwest Japan. *JGR Solid Earth, 121*(11), 8338–8351. https://doi.org/10.1002/2016JB013417

Walter, T. R., Haghighi, M. H., Schneider, F. M., Coppola, D., Motagh, M., Saul, J., Babeyko, A., Dahm, T., Troll, V. R., Tilmann, F., Heimann, S., Valade, S., Triyono, R., Khomarudin, R., Kartadinata, N., Laiolo, M., Massimetti, F., & Gaebler, P. (2019). Complex hazard cascade culminating in the Anak Krakatau sector collapse. *Nature Communications, 10*. https://doi.org/10.1038/s41467-019-12284-5

Wdowinski, S., Ben-Avraham, Z., Arvidsson, R., & Ekström, G. (2006). Seismotectonics of the Cyprian Arc. *Geophysical Journal International, 164*(1), 176–181. https://doi.org/10.1111/j.1365-246X.2005.02737.x

Winchester, S. (2003). *Krakatoa: The Day the World Exploded.* Viking. https://doi.org/9780141005171

Wollin, C., Bohnhoff, M., Vavry uk, V., & Martínez-Garzón, P. (2019). Stress Inversion of Regional Seismicity in the Sea of Marmara Region, Turkey. *Pure and Applied Geophysics, 176,* 1269–1291. https://doi.org/10.1007/s00024-018-1971-1

Wulf, S., Kraml, M., & Keller, J. (2008). Towards a detailed distal tephrostratigraphy in the Central Mediterranean: The last 20,000 yrs record of Lago Grande di Monticchio. *Journal of Volcanology and Geothermal Research, 177*(1), 118–132. https://doi.org/10.1016/j.jvolgeores.2007.10.009

Yakupoğlu, N., Uçarkuş, G., Eriş, K. K., Henry, P., & Çağatay, M. N. (2019). Sedimentological and geochemical evidence for seismoturbidite generation in the Kumburgaz Basin, Sea of Marmara: Implications for earthquake recurrence along the Central High Segment of the North Anatolian Fault. *Sedimentary Geology, 380,* 31–44. https://doi.org/10.1016/j.sedgeo.2018.11.002

Yalçıner, A. C., Alpar, B., Altınok, Y., Özbay, İ., & Imamura, F. (2002). Tsunamis in the Sea of Marmara: Historical documents for the past, models for the future. *Marine Geology, 190*(1–2), 445–463. https://doi.org/10.1016/S0025-3227(02)00358-4

Yamamoto, R., Kido, M., Ohta, Y., Takahashi, N., Yamamoto, Y., Pinar, A., Kalafat, D., Özener, H., & Kaneda, Y. (2019). Seafloor Geodesy Revealed Partial Creep of the North Anatolian Fault Submerged in the Sea of Marmara. *Geophysical Research Letters, 46*(3), 1268–1275. https://doi.org/10.1029/2018GL080984

Yasuda, T., Miyaue, T., Prasetyo, A., Kamo, M., Mori, N., Hiraishi, T., Mase, H., & Shimada, H. (2016). Tsunami Inundation Experiment Using Coastal City Model. *Journal of Japan Society of Civil Engineers, Ser. B2 (Coastal Engineering), 72,* 385–390. https://doi.org/10.2208/kaigan.72.I_385

Zhang, W., Randolph, M. F., Puzrin, A. M., & Wang, D. (2020). Criteria for planar shear band propagation in submarine landslides along weak layers. *Landslides, 17,* 855–876. https://doi.org/10.1007/s10346-019-01310-8

Zhu, H., & Randolph, M. F. (2010). Large Deformation Finite-Element Analysis of Submarine Landslide Interaction with Embedded Pipelines. *International Journal of Geomechanics, 10*(4). https://doi.org/10.1061/(ASCE)GM.1943-5622.0000054

Zitellini, N., Chierici, F., Sartori, R., & Torelli, L. (1999). The tectonic source of the 1755 Lisbon earthquake and tsunami. *Annali Di Geofisica, 42*(1), 49–55. https://www.earth-prints.org/bitstream/2122/1344/1/06 zitellini.pdf

Zitellini, N., Ranero, C. R., Loreto, M. F., Ligi, M., Pastore, M., D'Oriano, F., Sallarès, V., Grevemeyer, I., Moeller, S., & Prada, M. (2020). Recent inversion of the Tyrrhenian Basin. *Geology, 48*(2), 123–127. https://doi.org/10.1130/G46774.1

Glossary

Accelerometer – Tool that measures proper acceleration

Antidune – Bedform found in fluvial environments, opposing the direction of flow

Autoclave system – Device used to keep the sediment samples under the same *in situ* pressure

Biostratigraphy methods – Branch of stratigraphy that uses fossils to establish relative ages of rock

Brittle stretching – Deformation by fracturing on the scale of individual mineral grains or larger

Caldera – Large depression formed when a volcano erupts and collapses

Cyclic steps – Rhythmic bedforms associated with flow instability

Decompression melting – Rock melting when it gets closer to the surface due to pressure decrease

Degassing – Removal of dissolved gases from liquids, especially water

Deltaic sediments / deposits – Accumulation of material in deltas

Deterministic model – Model providing the same exact results for a particular set of inputs

Devolatilization process – Decomposition when volatiles are driven out from a hydrocarbon material

Diagenesis – Physical and chemical changes in sediments caused by water-rock interactions, microbial activity, and compaction after their deposition

Diatremes – Volcanic pipe formed by a gaseous explosion

Drill-hole corers – Drill specifically designed to remove a cylinder of material

Epicontinental sea – Shallow sea that covers central areas of continents during periods of high sea level

Exhumation – Exposure of a land surface that was formerly buried

Fault – Fracture or zone of fractures between two blocks of rock

Finite element analysis – computerized method for predicting how a product reacts to real-world physical effects

Gas-hydrate dissociation – Separation between the ice and gas when pressure-temperature conditions are outside the hydrate stability region

Geodesy – Science of accurately measuring and understanding Earth's geometric shape, orientation in space and gravitational field

Geodetic – Of, relating to, or determined by geodesy

Geophone – Device that converts ground movement (velocity) into voltage, recorded at a recording station

Geodynamic process – Processes by which mantle convection shapes and reshapes the Earth

Glaciogenic – Sediments with origin laid down within or under glacier ice or deposited by an ice sheet

Gravity flow – Mixture of water and sediment where the gravity acting on the sediment particles moves the fluid, in contrast to rivers, where the fluid moves the particles

Hypocenter – Point of origin of an earthquake

Lithological – Physical description of a rock or rock formation

Littoral – Relating to or situated on the shore of the sea

Magma – Hot fluid or semi-fluid material below or within the earth's crust

Material point method – Numerical technique used to simulate the behavior of solids, liquids or gases

Megaturbidite – Thick, extensive sediment deposit from an exceptionally large mass flow

Morpho-bathymetric – Related to identification and mapping of the seafloor

Morphological – Relating to the form or structure of things

Morphology – Study of the forms or structures of things

Multibeam systems – Multibeam echosounder which emit acoustic waves in a fan shape

Optically stimulated luminescence – Dating technique used to date the last time a quartz sediment was exposed to light

Orographic – Relating to mountains, especially as regards their position and form

Overpressure – Pressure caused by a shock wave over and above normal atmospheric pressure

Over-steepened flanks – Sharp inclination of the side of a construction prone to fail

Oxygen isotope methods – Determining patterns of climatic change using the ratio of the stable oxygen isotopes 18O to 16O

Paleomagnetic – Relative to the study of the record of the Earth's magnetic field

Penetrometer – Device to test the strength of a material

Petrophysical – Relative to the study of physical and chemical rock properties and their interactions with fluids

Phreatomagmatic eruption – Volcanic eruptions resulting from interaction between magma and water

Pore overpressure – Difference between the internal fluid pressures of a rock's pore space and the hydrostatic or normal pressure

Precursor – Smaller event that usually precedes a larger event

Probabilistic model – Model based on the fact that randomness plays a role in predicting future events

Propagation – Movement of a wave through a medium

Radiocarbon dating – Method for determining the age of an object containing organic material by using a radioactive isotope of carbon

Refraction – Change in direction of a wave caused by its change in speed

Retrogressive evolution – Upslope-propagating erosion wave

Sediment corer – Instrument taking undisturbed samples of the seafloor

Sedimentary successions – Vertical sequence of sedimented facies

Seismic – of, subject to, or caused by an earthquake or an earth vibration caused by something else

Seismic facies – Body of rock with specified characteristics in a seismic profile

Seismic imaging – Set of methods to obtain images of the Earth using observed seismograms as inputs

Seismic reflection profiling – Studies of the crust and upper mantle down to depths of 15 km to 100 km

Seismicity – Occurrence or frequency of earthquakes in a region

Seismogenic – Capable of generating earthquakes

Seismoturbidites – Thick, extensive sediment deposit from an exceptionally gravity flow triggered by earthquakes

Serpentinization – Processes whereby water is added into the crystal structure of the minerals

Shear zone – Structural discontinuity surface in the Earth's crust and upper mantle

Shoreline-crossing – Cross-section taken perpendicular to a given coast line contour

Slip rate – How fast the two sides of a fault are slipping relative to one another

Strain – Change in shape or size resulting from applied forces (deformation)

Stratigraphy – Study of rock layers (strata) and layering (stratification)

Subaerial – Under the air

Swath bathymetry – Method providing very high angular resolution and accuracy

Tectonic lineaments – Linear feature expressing a fault

Tephra – All the fragmental material erupted explosively from a volcano

Tephrochronological techniques – Technique that uses discrete layers of tephrato create a chronological framework

Thermoluminescence techniques – Technique using the light emitted by a mineral while heated

Tiltmeters – Sensitive inclinometer designed to measure very small changes from the vertical level

Tsunamigenic – Capable of generating tsunamis

Transient – That has a duration shorter than the recurrence interval of the process that formed it

Turbidite – Geologic deposit of a turbidity current

Turbidity currents – Rapid, downhill flow of water caused by increased density due to high amounts of sediment

Unconsolidated sediments – Sediment that is loosely arranged or unstratified (not in layers) or whose particles are not cemented together (soft rock)

Volcanic edifice – Main portion of a volcano built by volcanic deposits

Volcaniclastic – Geologic materials composed of broken fragments (clasts) of volcanic rock

Volumetric strain-meters – Instrument that detects changes in a volume filled with fluid

List of Abbreviations

AI	Artificial Intelligence
ANR	Agence Nationale de la Recherche, France
APT	Accelerator, Pressure, Temperature
AUV	Autonomous Underwater Vehicle
BCE	Before Common Era, also known as BC or Before Christ
CE	Common Era, also known as AD or Anno Domini
CNRS	Centre National de la Recherche Scientifique, France
CORK	Circulation Obviation Retrofit Kit
CPTu	Pore Pressure Sensing unit
CRED	Centre for Research on the Epidemiology of Disasters
CTD	Conductivity [=salinity], Temperature, Depth [=pressure]
DAS	Distributed Acoustic Sensing
DONET	Dense Ocean floor Network System for Earthquakes and Tsunamis
DTM	EMODnet Digital Bathymetry
EMODnet	European Marine Observation and Data Network
EMSO-ERIC	European Multidisciplinary Seafloor and Water Column Observatory
GeoEcoMar	Institutul Național de Cercetare – Dezvoltare pentru Geologie și Geoecologie Marină, Romaina
GHSZ	Gas Hydrate Stability Zone
GPS	Global Positioning System
GPS-A	Global Positioning System – Acoustic
HCMR	Hellenic Centre for Marine Research, Greece
ICG	Intergovernmental Coordination Group
ICM-CSIC	Institut de Ciències del Mar - Consejo Superior de Investigaciones Científicas, Spain
ICZM	Integrated Coastal Zone Management
IEO	Instituto Espanol de Oceanografi¬a, Spain
IFREMER	Institut Francais de Recherche pour l'Exploitation de la Mer, France
INFN	Istituto Nazionale Fisica Nucleare, Italy
INGV	Istituto Nazionale di Geofisica e Vulcanologia, Italy
IOTWMS	Indian Ocean Tsunami Warning and Mitigation System
LNEC	Laboratório Nacional de Engenharia Civil, Portugal
LNG	Liquefied Natural Gas
LTBMS	Long-Term Borehole Monitoring System
MaGIC	Marine Geohazards along the Italian Coasts
MARUM	Zentrum für Marine Umweltwissenschaften, Germany
MeBo	Seafloor robotic drilling device used by MARUM
MODAL	MOnitoring seafloor Deformation and Assessing Landslide hazards associated with fluid pressures
MoMAR	Monitoring the Mid-Atlantic Ridge
MSFD	Marine Strategy Framework Directive
MSP	Maritime Spatial Planning
MTD	Mass transport deposits

MVSS	Multi-vehicle/multi-sensor/multi-ship systems
NEAM	North-Eastern Atlantic, the Mediterranean, and connected seas
NEAMTWS	North-eastern Atlantic, Mediterranean and Connected Seas Tsunami Warning and Mitigation System
NEMO-SN1	Seafloor multidisciplinary observatory at the East of Sicily, Italy
NEPTUNE	East Pacific Time-series Underwater Networked Experiments
NOC	National Oceanography Centre, UK
OBS	Ocean-Bottom Seismometers
OECD	Organisation for Economic Co-operation and Development
OF	Optical Fibres
OGS	Istituto Nazionale di Oceanografia e di Geofisica Sperimentale, Italy
ONC	Ocean Networks Canada
OOI	Ocean Observatories Initiative
PLOCAN	Plataforma Oceánica de Canarias, Spain
PSHA	Probabilistic Seismic Hazard Assessment
PTHA	Probabilistic Tsunami Hazard Assessment
QAFI	Spanish Quaternary Faults of Iberia
ROV	Remotely Operated Vehicle
SMART	Science Monitoring and Reliable Telecommunications
SPH	Smoothed Particle Hydrodynamics
TEPCO	Tokyo Electric Power Company
TEWS	Tsunami Early detection and Warning Systems
TIPS	Temperature, Inclination and Pressure Sensors
TSUMAPS-NEAM	Probabilistic TSUnami Hazard MAPS for the NEAM Region (TSUMAPS-NEAM)
UN	United Nations
UNDRR	United Nations Office for Disaster Risk Reduction
UNISDR	Former abbreviation for the United Nations Office for Disaster Risk Reduction
USGS	United States Geological Survey
USV	Unmanned surface vehicles
VLIZ	Vlaams Instituut voor de Zee, Belgium

Annex 1: Members of the European Marine Board Working Group on Marine Geohazards

NAME	INSTITUTION	COUNTRY
WORKING GROUP CHAIRS		
Heidrun Kopp	GEOMAR Helmholtz Centre for Ocean Research Kiel	Germany
Francesco Latino Chiocci	University of Rome 'Sapienza'	Italy
CONTRIBUTING AUTHORS		
Christian Berndt	GEOMAR Helmholtz Centre for Ocean Research Kiel	Germany
Namık Çağatay	İstanbul Technical University	Turkey
Teresa Ferreira	University of the Azores	Portugal
Juana Fortes	LNEC - National Laboratory for Civil Engineering	Portugal
Eulàlia Gràcia	ICM-CSIC - Institute of Marine Sciences, CSIC	Spain
Alba González Vega	IEO - Spanish Institute of Oceanography & EMB Young Ambassador	Spain
Achim Kopf	MARUM – Center for Marine Environmental Sciences, University of Bremen	Germany
Mathilde Sørensen	University of Bergen	Norway
Nabil Sultan	IFREMER	France
Isobel Yeo	NOC - National Oceanography Centre	United Kingdom

Annex 2: External reviewers and additional contributors

NAME	INSTITUTION	COUNTRY
EXTERNAL REVIEWERS		
David Coetzee	National Emergency Management Agency	New Zealand
Sarah-Jayne McCurrach	Earthquake Commission	New Zealand
Dimitris Sakellariou	Hellenic Centre for Marine Research	Greece
ADDITIONAL CONTRIBUTORS		
Daniele Casalbore	University of Rome 'Sapienza'	Italy
David Casas	ICM-CSIC - Institute of Marine Sciences, CSIC	Spain
Gemma Ercilla	ICM-CSIC - Institute of Marine Sciences, CSIC	Spain
Paolo Tommasi	CNR-IGAG - Institute of Environmental Geology and Geoengineering, CNR	Italy

European
MARINE BOARD
Advancing Seas & Ocean Science

Cover Photo: Plume of discoloured water rising to the surface during the 2011 submarine eruption of the volcano Tagoro, in front of the town La Restinga, El Hierro Island.

Credit: Antonio Márquez - Instituto Volcanológico de Canarias (INVOLCAN)

European Marine Board IVZW
Belgian Enterprise Number: 0650.608.890

Wandelaarkaai 7 I 8400 Ostend I Belgium
Tel.: +32(0)59 34 01 63 I Fax: +32(0)59 34 01 65
E-mail: info@marineboard.eu
www.marineboard.eu